A&A 455, 303–313 (2006)
DOI: 10.1051/0004-6361:20064970

Astronomy & Astrophysics

The Nainital-Cape Survey

II. Report for pulsation in five chemically peculiar A-type stars and presentation of 140 null results*

S. Joshi[1,2], D. L. Mary[2,3], P. Martinez[4], D. W. Kurtz[5], V. Girish[6], S. Seetha[7], R. Sagar[2], and B. N. Ashoka[7]

[1] Inter-University Centre for Astronomy and Astrophysics (IUCAA), Post Bag 4, Ganeshkhind, Pune 411007, India
e-mail: santosh@iucaa.ernet.in
[2] Aryabhatta Research Institute of Observational Sciences (ARIES), Manora Peak, Nainital-263129, India
e-mail: santosh@aries.ernet.in
[3] Astronomisches Rechen-Institut am Zentrum fuer Astronomie, Moenchhofstrasse 12-14, 69120, Heidelberg, Germany
e-mail: dmary@ari.uni-heidelberg.de
[4] South African Astronomical Observatory (SAAO), PO Box 9, Observatory 7935, South Africa
e-mail: peter@saao.ac.za
[5] Centre for Astrophysics, University of Central Lancashire, Preston PR1 2HE, UK
e-mail: dwkurtz@uclan.ac.uk
[6] Tata Institute of Fundamental Research (TIFR), Homi Bhabha Road, Mumbai-400 005, India
e-mail: giri@tifr.res.in
[7] ISRO Satellite Center, Airport Road, Bangalore-560 017, India
e-mail: seetha@isac.ernet.in

Received 6 February 2006 / Accepted 25 April 2006

ABSTRACT

Aims. We search for photometric variability in chemically peculiar A type stars in the northern hemisphere.
Methods. High-speed photometric observations of Ap and Am star candidates have been carried out from ARIES (Manora Peak, Nainital) using a three-channel fast photometer attached to the ARIES 104-cm Sampurnanand telescope.
Results. This paper presents three new variables: HD 113878, HD 118660 and HD 207561. During the time span of the survey (1999 December to 2004 January) pulsations of the δ Sct type were also found for the two evolved Am stars HD 102480 and HD 98851, as reported in Joshi et al. (2002, 2003). Additionally, we present 140 null results of the survey for this time span.
Conclusions. The star HD 113878 pulsates with a period of 2.31 h, which is typical of δ Sct stars. HD 118660 exhibits multi-periodic variability with a prominent period of nearly 1 h. These periods need to be investigated and make HD 118660 a particularly interesting target for further observations. For HD 207561, a star classified as Am, a probable pulsation with a period of 6 min was found in the light curves obtained on two consecutive nights. Both HD 102480 and HD 98851 exhibit unusual alternating high and low amplitude maxima, with a period ratio of 2:1. The analysis of the null results confirms the photometric quality of the Nainital site.

Key words. stars: chemically peculiar – stars: variables: general – stars: general – stars: variables: δ Sct

1. Introduction

The Nainital-Cape Survey is a collaborative survey program to search for pulsational variability in chemically peculiar A-type stars in the northern hemisphere. It was initiated in 1997 between the Aryabhatta Research Institute of Observational Sciences (ARIES – formerly State Observatory), Nainital, India, and the South African Astronomical Observatory (SAAO), Cape Town, South Africa (Seetha et al. 2001). Details of the facilities at ARIES have been published by Sagar & Mary (2005). This paper, in which we give the current status of the survey, is the second of a series. The methods and first results of the survey were published by Martinez et al. (2001; hereafter, Paper I).

The class of A stars contains diverse stars that range from radiative photospheres at A0 to mainly convective photospheres by A9. The physics of these stars still challenges our knowledge in many respects including convection, the effects of internal rotation (Yildiz 2003; Reiners & Royer 2004), the coupling of rotation with magnetic field (Arlt 2004) and with chemical mixing (Noels et al. 2004), the origin of the magnetic field, or the mechanisms responsible for the pulsations observed in some of these stars (Kurtz 2000; Balmforth et al. 2001; Cunha 2002; Saio 2005; Cunha 2005).

The diversity in the nature of A stars makes it very difficult to draw a clear line between "normal" and "peculiar" stars. By a normal A-type star, it is generally understood that at classification dispersion the star shows none of the anomalies characteristic of other classes of stars; that when subject to a local thermodynamic equilibrium analysis, it appears to have a composition like the Sun's; and that it exhibits no variability (Wolff 1983). The problem of the resolution required to distinguish normal from peculiar stars is an old, though somewhat recurrent

* Full Table 1 and Full Figs. 9 and 10 are only available in electronic form at http://www.edpsciences.org

one. Those stars which present peculiar elemental abundances, the chemically peculiar (CP) stars, are mostly A-type stars, but range from early-B to early-F.

Their abundance anomalies are generally detected by the presence of abnormally strong and/or weak absorption lines of certain elements in their optical spectra. The peculiarity in these stars is interpreted as atmospheric under-abundance and over-abundance of different chemical elements, and is explained quite successfully by the *diffusion process* (Michaud 1970; Michaud & Proffitt 1993; Vauclair 2004). As outlined by Dworetsky (2004), the observed spectra are connected to changes in the deep interior of the stars, and diffusion cannot be regarded as only a surface phenomenon.

In the regime of CP stars, some Ap (A-peculiar) and Am (A-metallic line) stars in the spectral range A-F, lying within or near to the δ Sct instability strip, show p-mode photometric variability in the period range of 5.65 min to 8 h. Those Ap stars which exhibit non-radial, low-degree, high-overtone acoustic pulsations with observed periods between 5.65–21 min are known as rapidly oscillating Ap (roAp) stars (Kurtz 1982, 1990; Kurtz & Martinez 2000). Those variables with variability periods of 18.12 min (HD 34282, Amado et al. 2004) to about 8 h are known as δ Sct stars (see Breger 2000 for a review of these stars). The majority of δ Sct stars are non-radial, low-order, low-degree, pressure (p) mode pulsators. Both roAp and δ Sct-like CP stars are of interest for the present survey.

A total of 35 members of the class of roAp stars have been discovered so far. One of them, HD 12098, was discovered in the framework of the Nainital-Cape survey; see Paper I and Girish et al. (2001). These stars exhibit strong global magnetic fields. Recent results show that the distribution of the number of stars versus $\langle H \rangle$ is close to a negative exponential with very few stars having more intense fields than 8 kG (Dworetsky 2004). The second largest magnetic field in an Ap star (24.5 kG) was discovered recently in HD 154708 (Hubrig et al. 2005); this star is also a newly-discovered roAp star (Kurtz et al., in preparation). The predominant structure of the field is dipolar, although deviations from the dipolar case have been discovered by Leroy et al. (1995) and modelled by Bagnulo et al. (1999).

The Ap stars exhibit chemical abundance anomalies, particularly overabundances of Rare-Earth elements. Since the discovery that chemical peculiarity and pulsation can coexist in some magnetic CP stars (see Kurtz 1982), many attempts have been made to understand the geometry and driving mechanisms of the corresponding pulsations. The pulsation axis is thought to be aligned with the magnetic axis, and is consequently oblique to the rotation axis: the *oblique pulsator model*. See Kurtz (1982, 2000), Takata & Shibahashi (1995), Saio & Gautschy (2004) and Saio (2005) for discussion of the oblique pulsator model, and also see Bigot & Dziembowski (2002) who find that the axis of pulsation is not necessarily aligned with the magnetic axis in the case of relatively weak magnetic fields, $H_s \leq 1$ kG, when centrifugal effects from rotation may dominate.

In order to explain the driving mechanism of the short-period, high-overtone modes of roAp stars, many works have turned to the κ mechanism. This mechanism acts for δ Sct stars in the He II ionization zone (Chevalier 1971) and leads to long periods corresponding to fundamental/low-overtone modes; as such, it is not able to explain directly the short-period pulsations of roAp stars. Several works have investigated the respective influence of the magnetic field on helium settling and on convection efficacy (Dolez & Gough 1982), stellar wind likely to activate the κ mechanism in the He I ionization zone (Dolez et al. 1988), the possible role played by the ionisation of Si IV (Matthews 1988), the κ mechanism acting in the H I ionization zone (Dziembowski & Goode 1996), or mechanisms based on the possible existence of chromospheres (Gautschy et al. 1998). Apart from the κ mechanism, some works have investigated other possible causes for driving the pulsations, such as the Lorentz force (Dziembowski & Goode 1985), overstable convective modes (Shibahashi 1983; Cox 1984), or stochastic excitation (Houdek et al. 1999). The current understanding is that the κ mechanism acting in the region of the first ionization of hydrogen is probably the driving mechanism of pulsations in roAp stars, acknowledging the facts that in this case oscillations are aligned with the magnetic axis, that this model leads to frequencies as high as those observed in roAp stars, and that the diffusion-induced helium gradient of this model may lead to particular asteroseismic signatures[1] as observable in some roAp stars. Using these ideas, Balmforth et al. (2001) have proposed a model for the excitation mechanism in roAp stars where the effect of the magnetic field is to freeze the convection at the poles. On the basis of this model, Cunha (2002) calculated the theoretical boundaries of the instability strip in the Hertzsprung-Russell (H-R) diagram, and provided many theoretical insights on the pulsations of these stars. Saio (2005) calculates that high-overtone p modes are excited by the κ mechanism for H I, and that low-overtone p modes – those typical of δ Sct stars – are not excited in the presence of a magnetic field. These results are consistent with the short periods of the roAp stars and the lack of δ Sct pulsations found in *confirmed* magnetic stars.

So far, many Ap stars seen within the instability strip have not been observed to pulsate despite having similar properties to known roAp stars. These stars, where pulsations are not observed, are commonly called the non-oscillating Ap (noAp) stars. Many attempts have been made to determine systematic differences between roAp and noAp stars (see the discussions in Hubrig et al. 2000 and Cunha 2002). Hubrig et al. (2000) discovered that no roAp star is known to be a spectroscopic binary. Also, in the similar colour range to roAp stars, the noAp stars seem to be more evolved on average than the roAp stars (North et al. 1997), although this may be a selection effect (Elkin et al. 2005). This apparent distinction in the evolutionary stages between roAp and noAp stars is supported theoretically by Cunha (2002), who showed that a magnetic field is less likely to suppress convection in more evolved stars, and that the growth rate of unstable modes decreases as these stars evolve, so that evolved stars are stabilized more easily. This brief review shows how theory and observations are complementary to our understanding of the physics of these stars.

As far as the δ Sct stars are concerned, these are in general chemically normal stars, either because the pulsations disrupt the element separation due to the diffusion process, or because diffusion stabilizes the star. It was long thought for these reasons that metallicism and pulsations were mutually exclusive. In the late 1970s, theoretical models predicted however that pulsations could occur in *evolved* Am stars: when these stars evolve, the He II ionization is shifted more deeply into the star, where there is sufficient residual He to drive pulsations (Cox et al. 1979). Such cases of ρ Pup stars[2] are now not unusual. Extreme

[1] I.e. modulation of frequencies due to partial reflection of the sound wave where the He gradient occurs, e.g. in HD 60435 (Vauclair & Théado 2004).

[2] The group of ρ *Puppis* (formerly δ *Delphini*) stars are luminous, cool, evolved stars that may exhibit low-overtone pulsation characteristic of δ Sct variability (Kurtz 1976; Turcotte et al. 2000).

cases of co-existence of metallicism and long-period pulsations have been found in the evolved Am star HD 40765 (Kurtz et al. 1995) and in the strongly peculiar star HD 188136 (Kurtz 1980; Wegner 1981). The present paper briefly discusses the existence of two other evolved, long period Am pulsators, HD 98851 and HD 102480, also discovered during this survey and published Joshi et al. (2003).

Cunha (2002) predicted that longer period oscillations (20–25 min) in magnetic roAp stars should exist in the more evolved stars. The works of Turcotte (2000) and Turcotte et al. (2000) also support this theory. Periods longer than about 16 min remained for a long time not observed in the known roAp stars, which are concentrated in the lower (fainter) part of the theoretical instability strip; in fact, δ Sct type of pulsations were thought to be completely suppressed in roAp stars (Kurtz & Martinez 2000). Recent works still support this view, and show theoretically that both low-order adiabatic (Saio & Gautschy 2004) and non-adiabatic (Saio 2005) oscillations are damped by the magnetic field. Recently, however, Elkin et al. (2005) discovered pulsations in an evolved and luminous Ap star HD 116114, with a pulsation period of 21 min – the longest period among the known roAp stars. This in turn may support the theory that longer periods do exist in luminous stars, and that the current observational distinction between the roAp and noAp stars are due to an observational bias toward fainter stars. Also, HD 21190 was reported by Koen et al. (2001) to be both a very evolved Ap and a δ Sct star. The classification of this star is F2III SrEuSi:, which indicates a possible magnetic nature. Since some works (e.g. Saio 2005) showed theoretically that the presence of a magnetic field stabilizes the star against low-overtone δ Sct pulsation, the case of HD 21190 is particularly interesting. Beyond this particular star, the search of low-overtone δ Sct pulsations in magnetic Ap star is very important for our understanding of magnetism and pulsations.

We note here that for the detection of pulsation, the method of spectroscopic studies of radial velocity variations from time series can be more efficient than the photometric studies, as illustrated by the cases of HD 116114 (Elkin et al. 2005), HD 154708 (Kurtz et al., in preparation) and β CrB (Hatzes & Mkrtichian 2004). See also the review of Kurtz (2005) on this topic.

For main sequence stars, the coexistence of spectral peculiarity and pulsations for a long time remained doubtful. Kurtz (1978, 1984) first found low-amplitude (a few mmag) δ Sct pulsation in the marginal Am stars HR 4594, HR 8210 and HR 3321. Kurtz (1989) further reported the discovery of the classical Am star HD 1097 as a δ Sct star, thereby showing that both classical and evolved Am stars can pulsate. Two more classical Am pulsators were discovered in the framework of the present survey: HD 13038 and HD 13079; see Paper I.

The more detailed the analysis of pulsations in CP stars, the more complicated the picture. HD 188136 is, for instance, a very peculiar, multiperiodic δ Sct star with 50-mmag peak-to-peak variations (Kurtz 1980). The extreme peculiarity of this star is surprisingly not mixed away by the large amplitude pulsations. It is classified as a δ Del (ρ Pup) star, but the Rare Earth abundances in this star suggest the possible presence of a strong magnetic field (Wegner 1981) – which, if true, would mean that magnetic fields do not always prevent δ Sct type of pulsations.

In some stars the δ Sct pulsations may exhibit both p modes and g modes (e.g. HD 50018; Zhiping 2000). Henry & Fekel (2005) have shown that HD 8801 appears to be an Am star that is also both a δ Sct star and a g-mode γ Doradus star (see Henry & Fekel 2003 for a review of γ Dor stars).

In many respects, the information that we have on pulsations and metallicity is therefore a puzzle. What we observe (and what the theoretical models can at least partially explain) is that evolved Am stars – i.e. ρ Pup, or δ Del stars – can pulsate (i.e., the κ-mechanism in He II can drive the pulsation in evolved stars, and low-amplitude pulsations may not mix away the peculiarities); that marginal Am stars can be low-amplitude δ Sct stars (a sufficient amount of He remains to drive low-amplitude oscillations) and that strong magnetic fields and high-overtone pulsation can, and actually do, coexist in the roAp stars.

Among the things still to be ascertained are the mechanisms making some classical Am stars δ Sct pulsators (in particular why large amplitude pulsations do not mix away the peculiarities), how δ Sct pulsations may occur in the presence of strong magnetic fields, and how frequent is the occurrence of long period pulsations in evolved roAp stars. As in the past, much insight into these questions will most probably come from observational discoveries.

Since the early 1980s, the South African working group has devoted a lot of time to detect mmag variations in Ap and Am stars. They discovered more than twenty new roAp stars (Martinez & Kurtz 1995) and published an extensive list of null results (Martinez & Kurtz 1994). Of the 31 roAp stars known in 1997, only 3 were in the northern sky hemisphere. This situation gave birth to a number of surveys in the northern hemisphere to find new members of this group (Heller & Kramer 1998; Nelson & Kreidl 1993; Dorokhova & Dorokhov 1998; Handler et al. 1999). The Nainital-Cape Survey is one of them, and as such one of its major motivations is to search new roAp stars in the northern hemisphere. Regarding the discussion above, this kind of survey presents numerous other potential benefits: basically, they represent the primary materials to determine statistically the physical properties of the complicated classes of stars described above, and to constrain more precisely the theoretical models. More precisely, the instrumental setting of the present survey for acquiring high-precision, fast photometric observations (see Sect. 2.2) is particularly well suited to search for long periods (above $\approx$20 min) in magnetic Ap stars (cf. Turcotte et al. 2000; Cunha 2002; Saio 2005) to search for low-overtone δ Sct pulsations in (either cool or evolved) A-F peculiar stars, and to search for the coexistence of p- and g-modes pulsations in Am stars. The selection of the candidates was traditionally oriented towards cool objects (Martinez & Kurtz 1994) but we include in our list evolved stars as well (see Sect. 2.1).

The rest of the paper is organized as follows: Sect. 2 summarizes the strategy for the selection of the candidates, the observations and the data analysis procedure. Section 3 presents five variables discovered during this Survey. The null results are presented and analysed in Sect. 4. The last section summarizes our results.

2. Selection of the candidates, observations and data reduction

2.1. Selection of the candidates

In order to increase the chances of discovering variability in Ap and Am stars, the strategy adopted for the current survey was to select candidates presenting Strömgren photometric indices similar to those of the known variable Ap and Am stars (see Paper I). The range of the indices was also slightly extended with respect to Paper I to take in the evolved stars that might be peculiar. The primary source of candidates for the survey was from Strömgren photometry of A and F-type stars in the Simbad

Table 1. Sample of stars classified as null results during the Nainital-Cape survey. The unprewhitened and prewhitened spectra of these stars are depicted in Fig. 9 and Fig. 10, respectively. The columns list: HD number, right ascension α_{2000}, declination δ_{2000}, visual magnitude V, spectral type, spectral indices $b-y$, m_1, c_1, β, δm_1, δc_1, peculiarity parameter Δp (Masana et al. 1998), Julian dates (2 450 000+) on which the star was observed, and the duration of observation (Δt) in hours. The full table is available in the electronic material attached to this paper.

HD	α_{2000}	δ_{2000}	V	Spectral type	$b-y$	m_1	c_1	β	δm_1	δc_1	Δp	JD	Δt h
154	00 06 24	34 36 25	8.93	F0	0.223	0.230	0.746	2.782	–0.033	0.002	2.892	1503	1.54
416	00 08 51	37 12 56	8.91	A5	0.194	0.211	0.746	2.803	–0.008	-0.040	2.064	2174	2.30
573	00 10 13	25 31 36	8.90	F0III	0.208	0.253	0.783	2.780	–0.057	0.043	3.497	1832	0.96
												2174	1.31
1607	00 20 27	22 28 47	8.67	F0	0.254	0.222	0.638	2.723	–0.044	0.029	2.544	2235	1.70
2123	00 26 02	67 50 46	9.60	F5	–	–	–	–	–	–	–	2223	1.30
2471	00 28 40	37 18 15	8.15	A5	0.084	0.251	0.900	2.892	–0.075	–0.058	2.449	1499	2.05
2523	00 29 08	11 19 12	8.08	F0	0.219	0.208	0.655	2.733	–0.028	0.016	1.675	2215	2.06
												2223	1.97
												2283	0.79
4564	00 48 00	36 12 17	8.05	A5	0.150	0.228	0.802	2.824	–0.022	–0.024	2.290	2214	2.12
7901	01 20 36	67 14 02	8.44	A3	0.212	0.209	0.720	2.750	–0.024	0.040	1.670	2240	1.05
9550	01 34 24	38 50 44	8.29	A3	0.199	0.213	0.740	2.762	–0.024	0.036	1.765	1827	1.14
9843	01 36 41	35 36 59	8.22	F8	0.286	0.179	0.735	2.706	–0.006	0.187	0.908	1917	1.65
												1919	1.37
												1923	1.44

data base (Hauck & Mermilliod 1998). The following range of Strömgren photometric indices was used to select candidates: $0.46 \leq c_1 \leq 0.88$; $0.19 \leq m_1 \leq 0.33$; $2.69 \leq \beta \leq 2.88$; $0.08 \leq b-y \leq 0.31$; $-0.12 \leq \delta m_1 \leq 0.02$ and $\delta c_1 \leq 0.04$, where c_1 is the Balmer discontinuity parameter, an indicator of luminosity; m_1 is the line-blanketing parameter, an indicator of metallicity; β is the H_β line strength index, reasonably free from reddening, an indicator of temperature in the range from around A3 to F2; $b-y$ is also an indicator of temperature, but is affected by reddening. A more negative value of δm_1 indicates a stronger metallicity; a negative δc_1 index is an indicator of peculiarity. For the more evolved, more luminous stars δc_1 may be positive, even for strongly peculiar stars, since c_1 increases with luminosity.

Another indicator for peculiarity is the "Δp parameter" as defined by Masana et al. (1998). According to these authors, 50% of the late region CP stars (roughly A2 and later) should present a Δp greater than $\Delta p_0 = 2$ mag, and only 17% of normal stars should present a Δp greater than 2 mag (see Eq. (5) of their paper; for hotter stars Eq. (4) should be used, and interpreted with $\Delta p_0 = 1.25$ mag). Most of our stars have Δp scattered around 2 mag, and $\Delta p > 2$ mag for 60 stars (see Table 1). The mean and the median of the distribution of the Δp are respectively 2.08 mag and 1.99 mag, indicating strong peculiarity for those stars. The combination of the spectral types, Strömgren photometric and Δp indices demonstrates chemical peculiarity in almost all of the stars we have studied. Some normal stars and some hotter stars have been included to extend the range of our search, and for comparison.

2.2. Observations and data reduction

For the Nainital-Cape Survey, high-speed photometric observations of Ap and Am star candidates are carried out from ARIES (Manora Peak, Nainital) using a three-channel fast photometer attached to the ARIES 104-cm Sampurnanand telescope (Sagar 1999; Ashoka et al. 2000). Most of the selected program stars are between 6 and 10 mag. It is therefore very difficult in general to find a nearby comparison star of similar magnitude and colour as those of the program star. Hence, most of the time we use the photometer in two-channel mode (one channel measuring the target star plus sky background and a second channel measuring sky only). The time-series photometric observations consist of continuous 10-s integrations obtained through a Johnson B filter. This filter is expected to yield the highest amplitude variations and to maximize the number of counts. An aperture of $30''$ is used to minimize flux variations caused by seeing fluctuations and guiding errors. The observing protocol is simple. We acquire time-series photometric observations of the candidate stars for 1 to 3 h in order to be able to reveal both roAp and δ Sct pulsations on photometric nights. As a single null result is insufficient to exclude a candidate from being variable, several runs are recorded for some of the same target stars (see Sect. 4).

The data reduction process comprises the following steps: (a) Visual inspection of the light curve to identify and remove all obvious bad data points; (b) correction for coincident counting losses; (c) subtraction of the interpolated sky background; and (d) correction for the mean atmospheric extinction ($\langle \kappa_B \rangle = 0.26$ for Nainital; the best extinction coefficient is calculated for each observing run). After applying these corrections, the times of the mid-points of the observations are converted into heliocentric Julian dates (HJD) with an accuracy of 10^{-5} day ($\approx$1 s). The reduced data comprise a time-series of the HJD and B magnitudes with respect to the mean of the run. These data are then analyzed using an algorithm based on the Discrete Fourier Transform (DFT) for unequally spaced data (Deeming 1975; Kurtz 1985). The DFT of the time series produces an amplitude spectrum of the light curve. Since we seldom can observe a comparison star, there is always some degree of low-frequency sky transparency variations (see Sect. 4) mixed with the possible low-frequency stellar variations. The sky transparency variations are well-separated in frequency space from possible roAp pulsation frequencies.

3. Pulsating variables discovered during this survey

The pulsating variables discovered since the last survey report in Paper I are discussed below. The results about the first two stars below have been already published: we only summarize here the main results and discuss them.

3.1. HD 98851

HD 98851 (α_{2000} = 11 22 51.17; δ_{2000} = +31 49 41.1; m_B = 7.72; m_V = 7.41) is a star of spectral type F2. The Strömgren photometric indices for this star are: $b - y = 0.199$, $m_1 = 0.222$, $c_1 = 0.766$ (Hauck & Mermilliod 1998). There is no published value of the β index. Using low resolution spectroscopy, Joshi et al. (2003) found that this is a cool star of effective temperature 7000 K. The calibration of Crawford (1975) for F-type stars gives $\delta m_1 = -0.051$ and $\delta c_1 = 0.236$. The δm_1 index is well within the range of Strömgren photometric indices for the known roAp stars; δc_1 indicates that the star is evolved. Abt (1984) classified this star as a marginal Am star, with Ca II K line, H I Balmer lines and metallic lines (respectively, K/H/M) of the types F1/F1 IV/F3.

Joshi et al. (2000) found δ Scuti pulsation with three main frequencies, $f_1 = 0.20$ mHz, $f_2 = 0.10$ mHz and $f_3 = 0.02$ mHz. Alternating high and low amplitude cycles visible in the light curves indicate a nearly sub-harmonic period ratio of 2:1, a phenomenon not commonly observed in other Am or δ Sct stars (Joshi et al. 2003). Zhou (2001) also observed this star photometrically from the Xinglong Station of the National Astronomical Observatory, China, using a three-channel fast photometer attached to a 85-cm Cassegrain telescope, and reported similar types of light curves with the same periodicity.

3.2. HD 102480

The star HD 102480 (α_{2000} = 11 47 52.88; δ_{2000} = +53 00 54.5; m_B = 8.78, m_V = 8.45) is of spectral type F1. Its Strömgren photometric indices are $b - y = 0.211$, $m_1 = 0.204$, $c_1 = 0.732$ (Hauck & Mermilliod 1998). The Strömgren metallicity and luminosity indices are $\delta m_1 = -0.034$ and $\delta c_1 = 0.292$. The effective temperature is 6750 K derived using low-resolution spectroscopy (Joshi et al. 2003). The K/H/M lines are also those of a marginal Am star: Am(F2/F4/F4) (Abt 1984). The Strömgren photometric indices in combination with effective temperature indicate that this is a cool, evolved marginal Am star.

The photometric variability of this star was discovered from ARIES by Joshi et al. (2002). Combining data sets closely spaced in time, the amplitude spectra show that HD 102480 pulsates with three frequencies: $f_1 = 0.107$ mHz, $f_2 = 0.156$ mHz and $f_3 = 0.198$ mHz (Joshi et al. 2003). As with HD 98851, the light curves present alternating high and low amplitude variations with a period ratio close to 2:1.

The light curves of HD 98851 and HD 102480 are similar to those of the luminous yellow supergiant pulsating variables RV Tauri stars, which show alternating deep (primary) and shallow (secondary) minima, with a periods in the range 30–150 d and a brightness range of up to four magnitudes. This group of stars is composed of binaries with circumstellar or circumbinary disks which interchange material with the photosphere. It is thought that the underlying variability in RV Tauri stars arises from pulsations, with the alternating light curve arising from a 2:1 resonance between the fundamental and first overtone modes. The unusual nearly harmonic period ratios, alternating high and low maxima, and Am spectral types of HD 98851 and HD 102480 make these stars particularly interesting objects for further observational and theoretical studies.

3.3. HD 113878

HD 113878 (α_{2000} = 13 06 00.74; δ_{2000} = +48 01 41.3; m_B = 8.59, m_V = 8.24) is an early F-type star, with the following

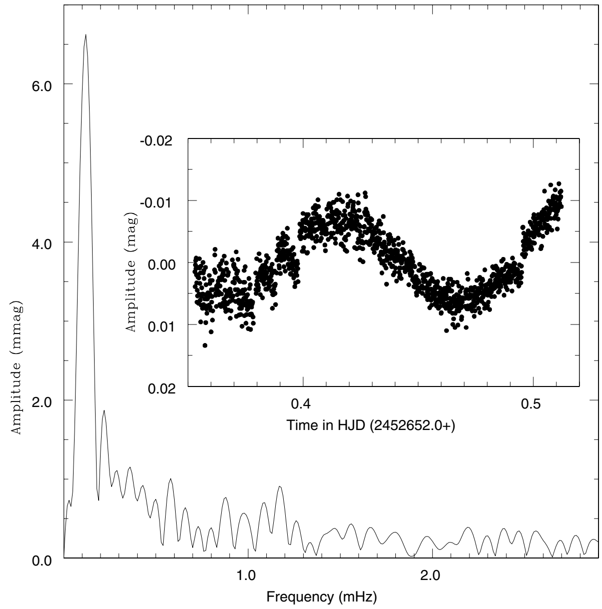

Fig. 1. Johnson B light curve (inset) and corresponding amplitude spectrum of HD 113878 obtained on HJD 2452652.

Strömgren photometric indices: $b - y = 0.219$, $m_1 = 0.257$, $c_1 = 0.729$, $\beta = 2.745$ (Hauck & Mermilliod 1998), giving $\delta m_1 = -0.037$ and $\delta c_1 = 0.069$. From Abt (1984), the spectral type of this star is F1/F3V/F3 indicating that HD 113878 is a marginal Am star.

We have discovered low-amplitude pulsations in HD 113878 (Fig. 1). From the analysis of the light curves obtained on different nights, the star has a clear variability period of 2.31 h ($f_1 = 0.12$ mHz), which is typical of δ Sct stars. To investigate possible additional pulsational frequencies, we observed this star for a total of 8 photometric nights. Unfortunately, the large time gaps between the runs made the identification of the additional frequencies particularly difficult because of frequency aliases in the Fourier spectra. In order to study this star in more detail, densely sampled time-series data are required.

Very interestingly, Abt (1984) showed that the stars HD 98851, HD 102480, HD 113878 and HD 104202 are similar in the sense that they do not show the classical difference of more than 0.5 spectral class between the K line types and the metallic lines. These four stars are, however, classified as Am stars by their strong Sr II lines, weak λ4226 Ca I line, and by Strömgren δm_1 indices supporting their peculiarity. Among these stars, HD 98851, HD 102480 and HD 113878 turned out to be photometric variables. HD 98851 and HD 102480 also exhibit interesting light curves with alternating high- and low-amplitude maxima. If the star HD 104202 turns out to exhibit variability as well, then these objects may provide a useful insight on the relationship of chemical peculiarity to variability.

3.4. HD 118660

HD 118660 (α_{2000} = 13 38 07.89; δ_{2000} = +14 18 06.9; m_B = 6.746; m_V = 6.500) is a bright star of spectral type A8V (Abt & Morrell 1995). Its Strömgren photometric indices are $b - y = 0.150$, $m_1 = 0.214$, $c_1 = 0.794$ and $\beta = 2.778$ (Hauck & Mermilliod 1998), giving $\delta m_1 = -0.018$ and $\delta c_1 = 0.054$, indicating that the star is metallic and evolved.

Time-series data (Fig. 2) have revealed that this star is a multi-periodic δ Scuti variable pulsating with a principal period

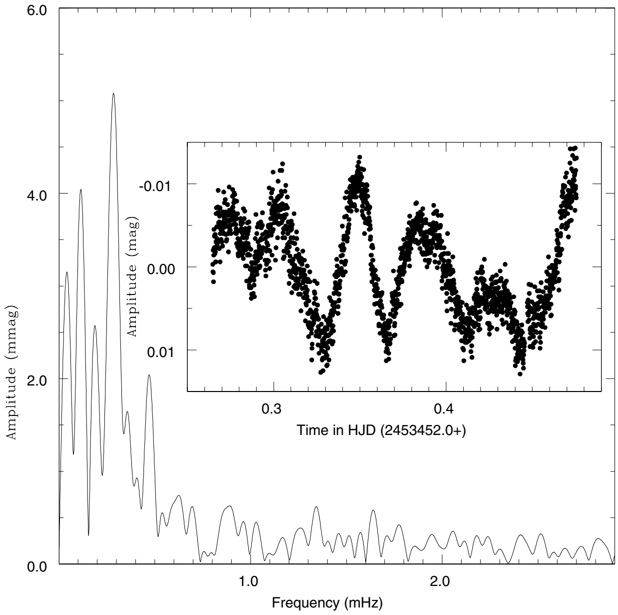

Fig. 2. Johnson B light curve (inset) and amplitude spectrum of HD 118660 obtained on HJD 2453452.

of about 1 h. Another prominent period of 2.52 h is also apparent. Preliminary analyses indicate that many other periods may also be present in the data, though we could not investigate them further so far. More time-series data are consequently required. At a declination of about 14°, HD 118660 is a good target for a multi-site campaign with 0.5-m to 1.0-m class telescopes situated in both northern and southern hemispheres.

3.5. HD 207561

HD 207561 (α_{2000} = 21 48 16.05; δ_{2000} = +54 23 14.6; m_B = 8.09; m_V = 7.85) is an F0III star with Strömgren indices of $b - y$ = 0.142, m_1 = 0.220, c_1 = 0.820 and β = 2.825, giving metallicity and luminosity indices of $\delta m_1 = -0.014$ and $\delta c_1 = -0.040$. These indices are typical for roAp stars, but this star is classified as an Am star (Cowley & Cowley 1965; Bertaud & Floquet 1974; Nicolet 1982).

We have discovered 6-min oscillations in the light curve of this star on two consecutive nights, as shown in Figs. 3 and 4. For this first two nights, the variability is evident. Figure 5 shows the amplitude spectra for the light curves on these three nights where a peak at 2.75 mHz (P = 6.1 min) is clear with excellent signal-to-noise ratio on both nights. Both the light curves and amplitude spectra are typical of the roAp stars. In our experience studying these stars for more than 20 years, we have never seen a spurious signal as clear as this for any star. Furthermore, in the next section we show the null results from our survey where no signal stands out like this one. This shows that our instrumentation and sky conditions do not produce false peaks such a high frequency as we see in Fig. 5.

Thus it seems that HD 207561 is a newly discovered roAp star. However, we have been unable to reproduce the results shown in Figs. 3 and 5 over two following seasons. We have observed this star for a total of 43.5 h on 17 nights over three observing seasons. On some nights there is no signal at all to high precision, as we show in Fig. 4 and in the bottom panel of Fig. 5. On other nights we have seen possibly significant peaks, but at lower frequencies than the one detected in Figs. 3 and 5.

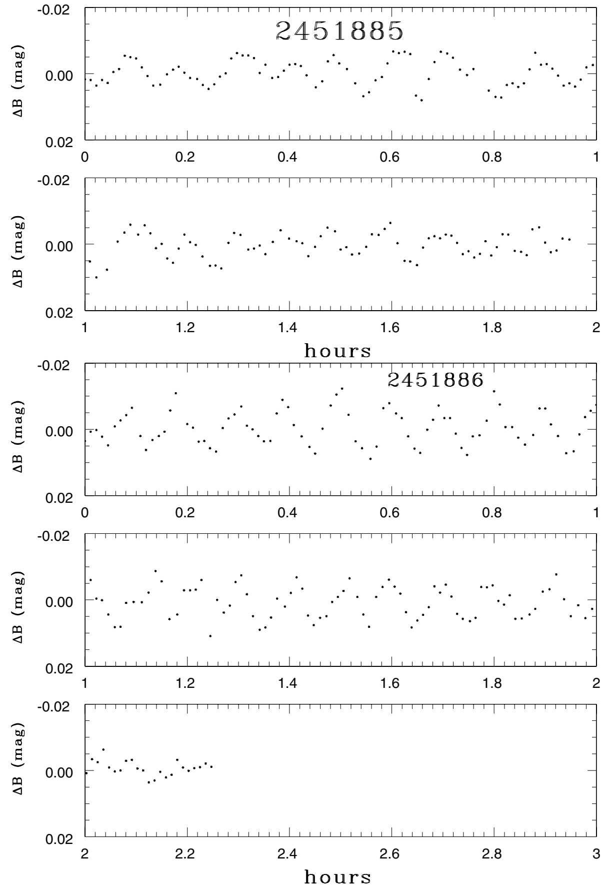

Fig. 3. Johnson B light curves of HD 207561 obtained on two consecutive nights. These curves clearly show the 6-min oscillations.

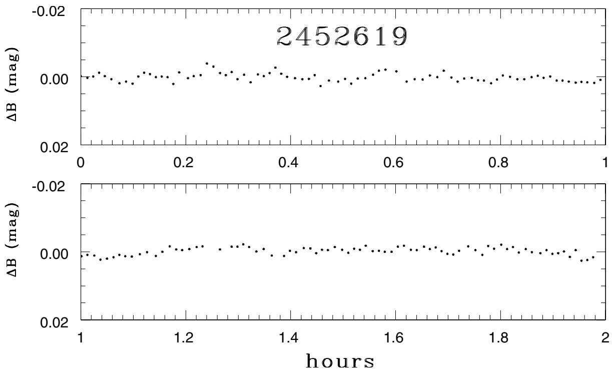

Fig. 4. Johnson B light curves of HD 207561 obtained on a third night from a different season. This curve shows a clear lack of signal at high precision. In all the light curves, the data have been merged to 40-s integrations and low-frequency sky transparency variations have been prewhitened at frequencies below 0.5 mHz.

While roAp stars are oblique pulsators, so their observed amplitude varies with rotation and can decrease to zero, or rise to many mmag from night-to-night, most of them have stable frequency spectra. Exceptions to this is HD 60435 (Matthews et al. 1987) where the mode lifetimes appear to be shorter than one week, and HD 217522 which had a new frequency at 2.02 mHz in 1989 in addition to the 1.2 mHz peak known from 1982 (Kreidl et al. 1991). We have not previously seen the apparent behaviour that the light curves and amplitude spectra for the 17 nights of observations of HD 207561 show, so

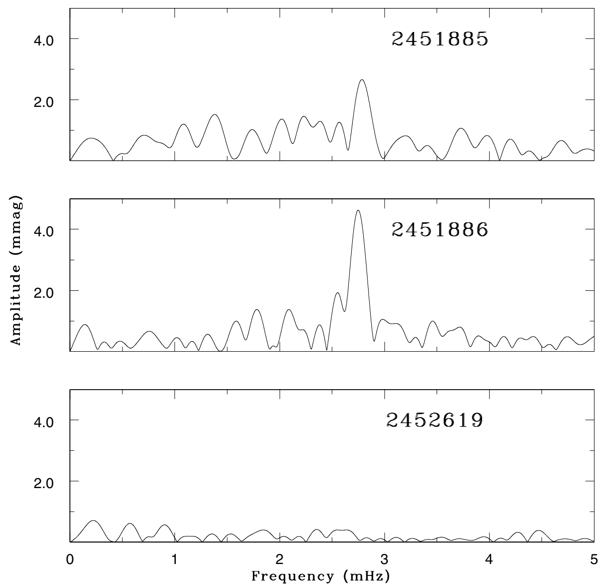

Fig. 5. Amplitude spectra of the light curves shown in Figs. 3 and 4 (HJDs are mentioned in each panel). The peaks at 2.75 mHz in the top two panels have high signal-to-noise ratio. We have never seen a case where signals as strong as this, and at this high frequency, have been instrumental or atmospheric in origin. We therefore consider them to be real, but have not been able to confirm them on 15 other nights of observation. Note, however, that roAp stars can be amplitude variable due to rotation and multiperiodicity. See the text for further discussion.

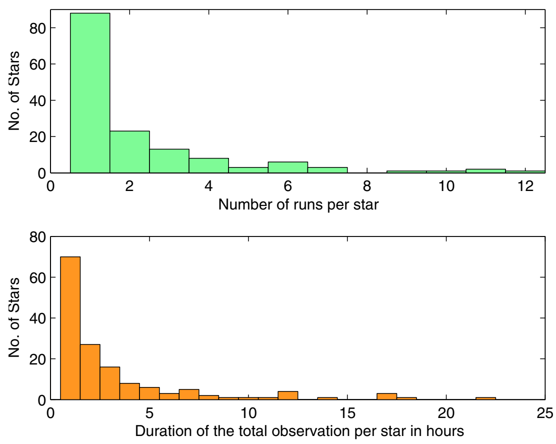

Fig. 6. Statistics of the runs for the Nainital-Cape Survey. *Top*: distribution of the number of runs per star. Clearly, most of the stars have been observed only once. A few of them, where some variability was suspected, were observed many times. *Bottom*: distribution of the total time dedicated to observe one star (in hours). Most of the stars have been observed less than 2 h. The median value is 1.6 h and the mean 3.2 h.

we do not claim with certainty that it is an roAp star, although we strongly suspect this from the evidence shown.

From the Strömgren indices given above, HD 207561 is clearly a chemically peculiar star – either Am or Ap. These can be confused with each other at classification dispersions, so the Am classification of the star needs to be re-examined in light of the possible pulsation. A definitive spectral type is needed, as is a search for the presence of a magnetic field.

If the 6-min pulsations in HD 207561 can be confirmed, this star will be interesting to study for its amplitude variability to determine if it is due to short mode lifetimes or rotation. We expect that it will be found to be an Ap star; if it should be an Am star, then the short period is unique and demands extensive further study. Unfortunately, this star is poorly placed for observing from ARIES. It is only observable during October to December from this site because the monsoon precludes observing it earlier than October. The best signal-to-noise ratio for the observations is obtained when the sky is stable and the object is near the meridian. The sky transparency usually becomes stable only two to three hours after the sunset at Nainital. But by that time, HD 207561 is two to three hours west of the meridian. This makes it difficult to obtain long observing runs of this star from Nainital. Consequently, observations of HD 207561 from other astronomical sites would be very useful to confirm the above results.

4. Null results

As we shall see, the detection of small amplitude variations (a few mmag, or less) in roAp stars, as well as low-amplitude δ Sct pulsators, is challenging. Detection of mmag pulsations can, however, be accomplished with good conditions from a single site (down to about 0.3 mmag for the highest noise peaks, or a precision of about 0.1 mmag in 1 h of observing; see Martinez & Kurtz 1994), provided that scintillation noise is sufficiently low, and that variations in the sky transparency are sufficiently slow[3]. Since the stars of our survey are brighter than $m_V = 10$, sky transparency variations and scintillation noise are the limiting factors in detecting the small amplitude pulsations we are searching for.

We present here null results from our survey for 140 stars. The observations cover a time range from 1999 January to 2004 December. They are presented in both tabular and graphic form, and analyzed below. Table 1, Figs. 9 and 10 show examples of the results for a few stars; the complete table and figures are available in electronic form with this paper.

The fourteen columns of Table 1 list respectively, for each star: HD number, right ascension α_{2000}, declination δ_{2000}, visual magnitude V, spectral type, spectral indices $b-y$, m_1, c_1, β, δm_1, δc_1, peculiar parameter Δp (Masana et al. 1998), Julian dates on which the star was observed, and time of each observing run in hours. Figure 9 shows examples of spectra corrected for extinction, but filtered for low-frequency noise that we consider to be mostly, or completely caused by sky transparency variations. Figure 10 presents prewhitened spectra that have been filtered for low-frequency noise. The prewhitening strategy was to remove the low-frequency peaks in the range 0–0.5 mHz, if those were higher than peaks above 0.5 mHz. Because of this procedure, the amplitude threshold above which low frequency peaks were removed varies from star to star. In this sense, the spectra corrected only for extinction form a more homogeneous set of data, since the data reduction process is the same for all stars. On the other hand, the corresponding spectra often present a large low frequency peak, in the sidelobes of which stellar peaks may be buried. We decided to present the two sets of data because they are complementary, and both are required for a proper analysis of the observations.

By observing the amplitude spectra of Fig. 9, one can notice that the average level of the peaks is in general higher in the low frequency region, and decreases towards higher frequencies. This higher level is mainly caused by residual sky transparency variations. Above the low-frequency region, the spectrum

[3] For comparison, Kurtz et al. (2005) achieved 14-μmag photometric precision for the roAp star HR 1217 with a three-week multi-site campaign using the Whole Earth Telescope.

flattens to a level which corresponds to the scintillation noise. This tells us that the detection of a peak in the low-frequency region is more difficult than at higher frequencies because the noise level is higher. Hence, detecting δ Sct pulsations (longer than about 0.5 h) is difficult, unless they have very large amplitude. This is the reason why long pulsation periods are difficult to detect with our high-speed technique, and might explain why such pulsations are actually not detected in evolved roAp stars. In the prewhitened spectra (Fig. 10), note that the tallest peaks are not found in the [0−0.5] mHz frequency region, because prewhitening has removed the largest low frequency contributions. Prewhitening is aimed at removing the major part of the sky transparency variations, but this process also removes any pulsations which may be hidden at low frequency.

In this regard, the null results mean that no peak in any region of the spectrum was sufficiently high with respect to the surrounding noise level to be considered as the signature of a pulsating star. One may be tempted to extrapolate that for any particular star which belongs to these null results, there is at any given frequency no pulsation higher than the noise level reported in the corresponding spectrum. This is true for the particular epochs at which the star was observed, but it may *not* be the case at other epochs. Rotational amplitude modulation and beating between frequencies may result in pulsations not being visible at a particular time (see, e.g., Martinez & Kurtz 1994 and Handler 2004 for further discussions of these phenomena). It is therefore likely that some of these 140 stars are actually pulsating. Many of the stars have been observed only once or a very few times (see full electronic figure and the table). Hence, many of the corresponding results are inconclusive rather than negative, and observers should not be discouraged from observing these stars further.

For stars with multiple observing runs, if a null result is found every time the star is observed, no variability or variability with an amplitude below the noise level are strongly favoured conclusions. For those stars where variability could not be detected several times, this result is interesting, showing that there are stars lying inside the classical instability strip that do not show any variability at high precision. This knowledge is essential to our understanding of what distinguishes the pulsating CP stars from similar non-pulsating CP stars, and helps us to identify or refine the parameters which distinguish constant from variable CP stars.

For those stars that may in the future be found to be pulsating, even though classified as null results here, the present spectra provide a useful reference about the time and the sensitivity for which pulsations were not apparent. This was, for example, the case for HD 116114, which was observed in two photometric searches for new roAp stars (Nelson & Kreidl 1993; Martinez & Kurtz 1994). No photometric variability was found in either survey, and the star was considered to be a noAp star. However, Elkin et al. (2005) later discovered in HD 116114 radial velocity variations with a period near 21 min.

We shall go a bit further in the analysis of our null results, and turn to their detection limits. Assessing a criterion to derive a detection limit, with the purpose that this limit is both general and significant is difficult (see Mary 2005, and references therein for the problem of asteroseismic light curve analysis, and Mary 2006 for the particular problem of the detection limits in fast photometry). The reasons are that the level of the sky transparency variation, that of the scintillation noise, and the frequency regions where either of these noise sources dominates varies from night to night, and sometimes during a given night, as well. For each particular run, one can assess the detection

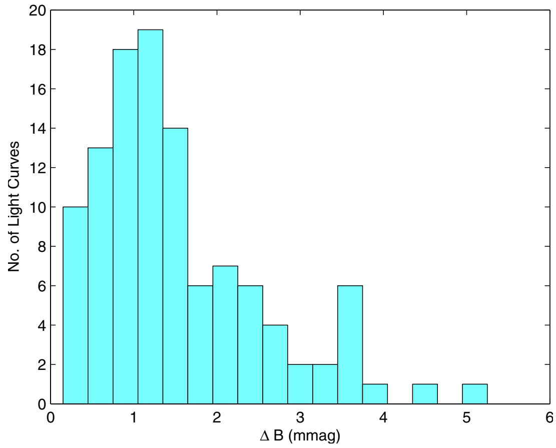

Fig. 7. Distribution of the detection limits (as the tallest peak in the spectrum) in the Nainital-Cape Survey.

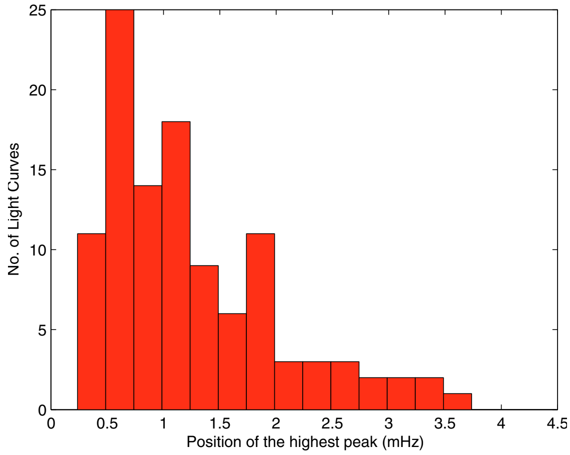

Fig. 8. Distribution of the positions of the tallest peaks in the prewhitened light curves.

limit by considering the shape of the spectrum, the noise level in the flat frequency region, and the tallest peak of the spectrum. This tallest peak can be considered as an upper value of the detection limit for a particular observation. For each prewhitened light curve of our null results, we selected the tallest peak; the distribution of these detection limits is displayed in Fig. 7.

In most cases, the tallest peak has an amplitude in the range 0.5−1.5 mmag. For this distribution, the mean and median values are respectively 1.5 and 1.3 mmag; 1.5 mmag, which is less than the largest amplitude of many known roAp stars. On the other hand, the number of roAp stars having small amplitude pulsations is expected to increase dramatically below 1.5 mmag, so that efforts towards pushing down this limit would most probably lead to the discovery of many new variables. This may be accomplished by increasing the duration of the observing runs for each star. If we now turn to the frequency at which the tallest peak occurs, we obtain the distribution of Fig. 8.

Again, it can be observed that the prewhitening procedure has removed the peaks at very low frequency. Usually, the highest peak is found in the low frequency region of 0.5−2 mHz; the median value is 1.0 mHz and the mean 1.3 mHz. The occurrence of the tallest peak at these frequencies is due to residual sky transparency variations, but probably also to undetected δ Sct and roAp stars. Above about 2 mHz, the distribution tends to flatten. It is not clear whether the bump around 1.9 mHz in the typical range for roAp star frequencies is caused by noise, or is

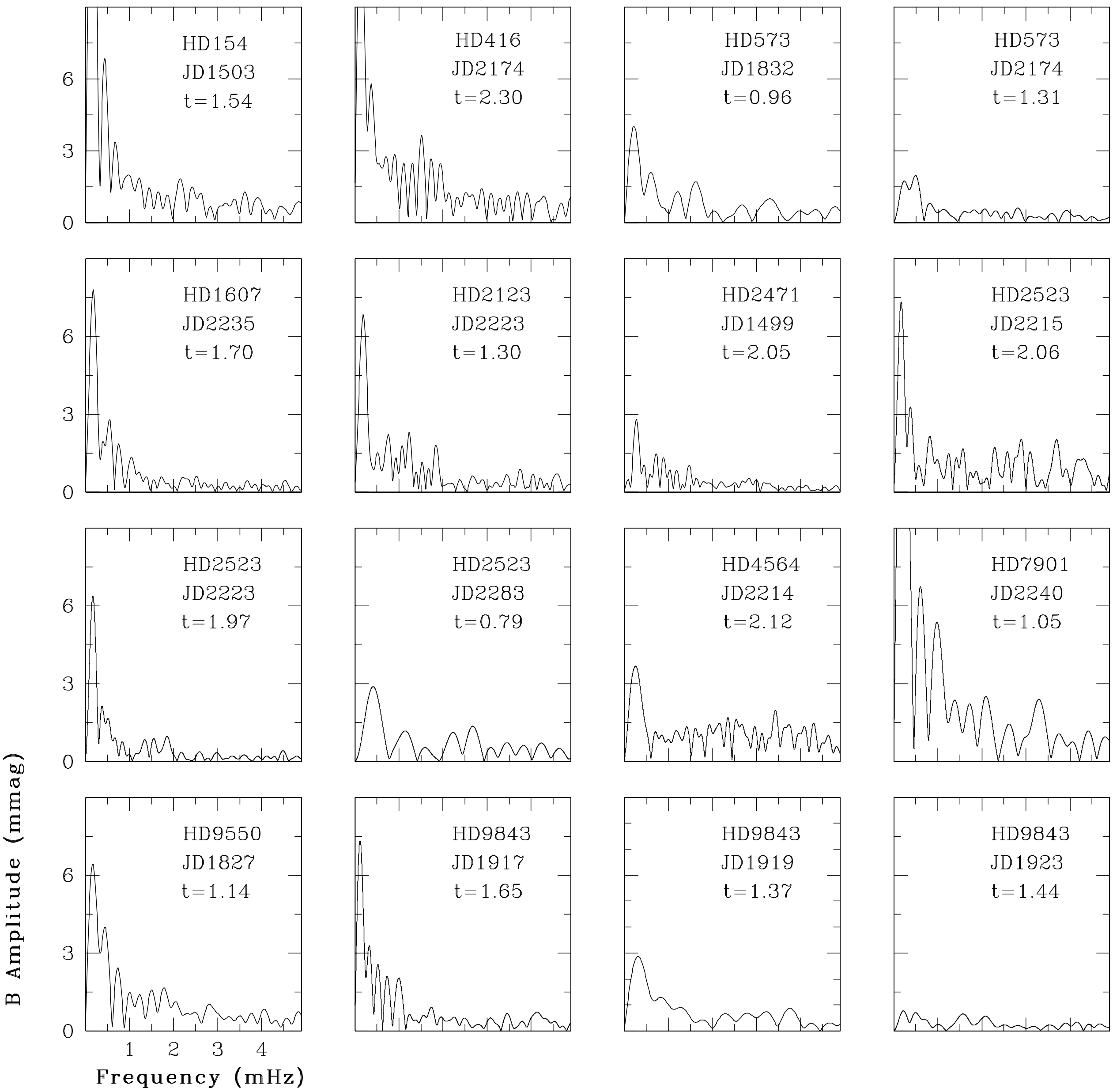

Fig. 9. Null results from the Nainital-Cape Survey: Examples of amplitude spectra for eleven sample stars corrected only for extinction, and in some cases for some very long-term sky transparency variations. Each panel contains the Fourier transform of an individual light curve, covering a frequency range of 0 to 5 mHz, and an amplitude range of 0 to 9 mmag. The name of the object, date of the observation in Julian date (JD 2 450 000+) and duration of the observations in hours (h), are mentioned in each panel. The rest of these amplitude spectra are available electronically.

indicative of more pulsators in the sample. It could also be indicative of a low-level instrumentally-induced frequency, such as a telescope drive oscillation, affecting the data of many stars.

The above results are very similar to those obtained at the SAAO site and discussed by Martinez & Kurtz 1994 (see in particular their Figs. 1 and 2 for a comparison of Fig. 7 and Fig. 8). These analyses show in particular that Manora Peak (Nainital) is a good photometric site.

We shall make a few comments regarding the possible improvements of our null results. As far as scintillation noise is concerned on the one hand, its level can be reduced by increasing the size of the telescope and by observing at a lower airmass (Young 1967; Dravins et al. 1998). These two factors will be improved in the future since ARIES is building a 1.3-m telescope 50 km further away in the mountains, and at a higher altitude (Devasthal site, 2420 m instead of 1951 m at Manora Peak). There is also a project to build a 3-m telescope. For the studies of this kind of variables, such a telescope will be useful for photometry indeed, but also mostly for spectroscopy. The benefits of spectroscopic studies for asteroseismology are huge; see, for instance, the review of Kurtz (2005) on this topic, and the cases of HD 116114 (Elkin 2005), HD 154708 (Kurtz et al., in preparation) and β CrB (Hatzes & Mkrtichian 2004). As for reducing sky transparency variations on the other hand, it would be possible to improve the detection in the low frequency range by increasing the duration of the runs, but this would be at the price of investigating a reduced number of candidates – a compromise to be dealt with in this kind of survey.

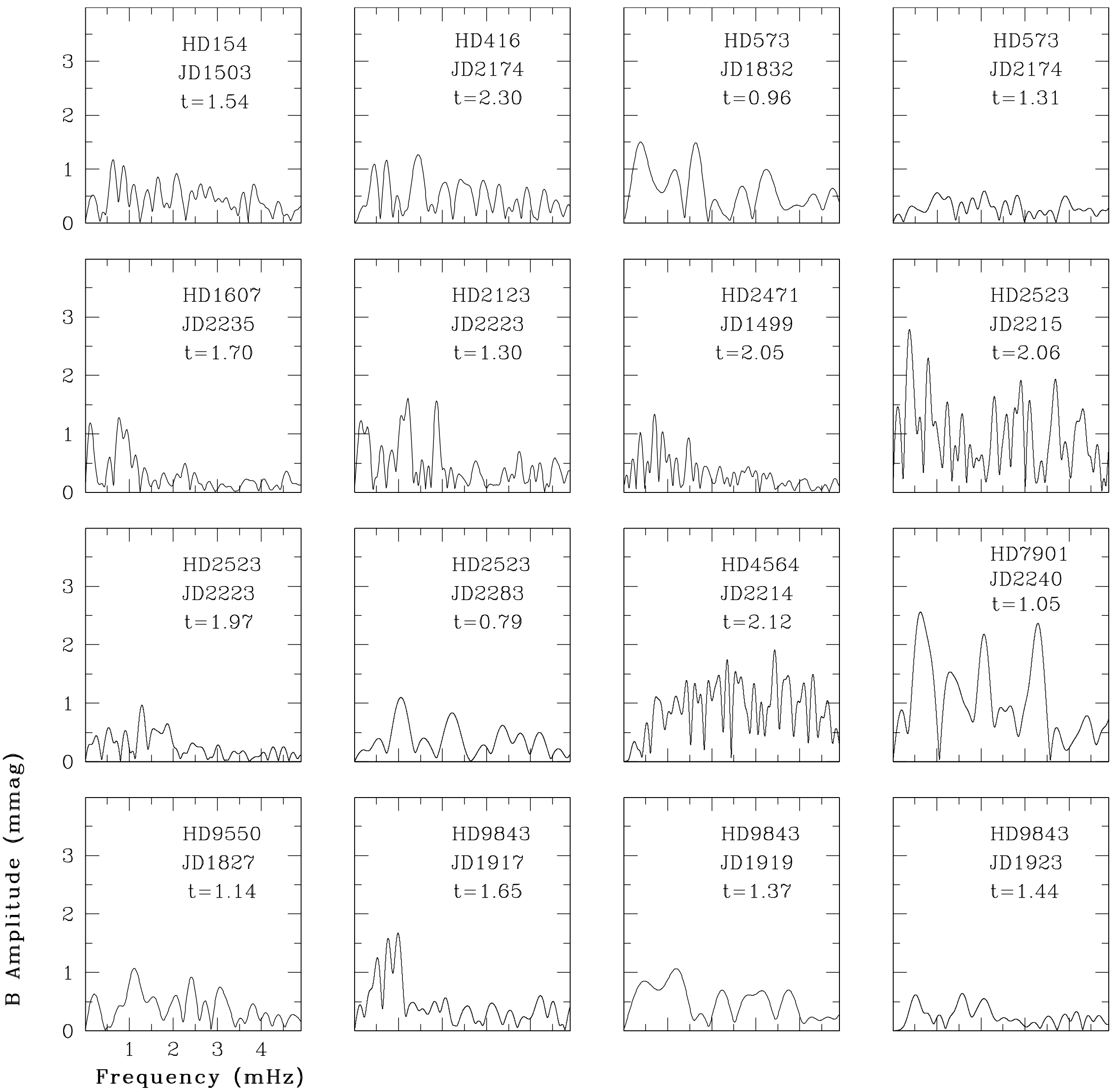

Fig. 10. Null results from the Nainital-Cape Survey: Examples of prewhitened amplitude spectra for eleven sample stars. Each panel contains the Fourier transform of an individual light curve, covering a frequency range of 0 to 5 mHz, and an amplitude range of 0 to 4 mmag. The name of the object, date of the observation in Julian date (JD 2 450 000+) and the length duration in hours (h), are mentioned in each panel. The rest of the amplitude spectra are available electronically.

5. Conclusions

We presented in this paper results obtained from the Nainital-Cape Survey from the years 2000 to 2004. We reported the pulsation discovered in several stars with CP spectral classifications during this time range; we also presented and analyzed our null results.

Pulsations of the δ Sct type were discovered in the evolved Am stars HD 98851 (main frequencies: 0.20 mHz and 0.10 mHz) and HD 102480 (main frequencies: 0.09 mHz and 0.19 mHz). Very interestingly, both stars exhibit unusual and alternating high and low amplitude maxima, with a period ratio of 2:1. The star HD 113878 pulsates with a period of 2.31 h, which is also typical for δ Sct stars. The three stars HD 98851, HD 102480 and HD 113878 form part of a group of four stars described by Abt (1984) and are similar in the sense that they do not show the classical difference of more than 0.5 spectral class between the K line types and the metallic lines. These four stars are, however, classified as Am stars by their strong Sr II lines, weak λ4226 Ca I line, and other indications of their general abnormality. The other star in this group is HD 104202. If that star turns out to be variable as well, these objects can provide interesting insights on the relationship of chemical composition and pulsations. The star HD 118660 seems to exhibit multi-periodic variability with a prominent period of nearly 1 h. Further observations are required to determine the additional periods. This bright star is a good target for a multi-site campaign using small telescopes. Finally, in HD 207561, classified as an Am star, an intriguing pulsation period of 6 min was clearly detected in the light curves obtained on two consecutive nights. It does not seem that this oscillation is caused by instrumental noise, but this result should be taken with care. The importance of the question of the coexistence of pulsations, chemical peculiarity and magnetic field calls for further photometric, spectroscopic, and magnetic studies of this star.

The Nainital-Cape survey is an on-going project. As the survey progresses, new results are obtained regularly. In order to improve our strategy for the current and future observations, more luminous peculiar stars were recently included in our list. The peculiarity criterion defined by Masana et al. (1998) is a useful tool in this direction. Up to now, the results obtained from the survey (reported in Paper I and here) have brought new and important information regarding the general properties of variable Ap and Am stars. These results will contribute to, and stimulate other investigations of these fascinating objects.

Acknowledgements. S.J. acknowledges the help from *INDU* for reading the manuscript rigorously. This work was carried out under the Indo-South African Science and Technology Cooperation Program as a joint project titled "Nainital-Cape Survey for roAp stars", funded by Departments of Science and Technology of the Indian and South African governments.

References

Abt, H. A. 1984, ApJ, 285, 247
Abt, H. A., & Morrell, N. I. 1995, ApJS, 99, 135
Amado, P., et al. 2004, in The A-Star Puzzle, ed. J. Zverko, W. W. Weiss, J. Žižňovský, S. J. Adelman, & W. W. Weiss (Cambridge University Press), IAU Symp., 224, 863
Arlt, R. 2004, in The A-Star Puzzle, ed. J. Zverko, W. W. Weiss, J. Žižňovský, S. J. Adelman, & W. W. Weiss (Cambridge University Press), IAU Symp., 224, 103
Ashoka, B. N., Seetha, S., Raj, E., et al. 2000, BASI, 28, 251
Bagnulo, S., Landolfi, M., & Landi degl'Innocenti, M. 1999, A&A, 343, 865
Balmforth, N. J., Cunha, M. S., Dolez, N., Gough D. O., & Vauclair, S. 2001, MNRAS, 323, 362
Bertaud, C., & Floquet, M. 1974, A&AS, 1974, 16, 71
Bigot, L., & Dziembowski, W. A. 2002, A&A, 391, 235
Breger, M. 2000, in Delta-Scuti and Related Stars, ed. M. Breger, & H. Montgomery (San Francisco: ASP), ASP Conf. Ser., 210, 3
Chevalier, C. 1971, A&A, 14, 24
Cowley, A. P., & Cowley, C. R. 1965, PASP, 77, 184
Cox, J. P. 1984, ApJ, 280, 220
Cox, A. N., King, D. S., & Hodson, S. W. 1979, ApJ, 231, 798
Crawford, D. L. 1975, AJ, 80, 955
Cunha, M. S. 2002, MNRAS, 333, 47
Cunha, M. S. 2005, JApA, 26, 213
Deeming, T. J. 1975, Ap&SS, 36, 137
Dorokhova, T. N., & Dorokhov, N. I. 1998, in Proceedings of the 26th meeting of the European Working Group on CP stars, ed. P. North, A. Schnell, & J. Žižňovský, Contributions of the Astronomical Observatory Skalnaté Pleso, Slovak Academy of Sciences, 27, 338
Dolez, N., & Gough, D. O. 1982, in Pulsations in Classical & Cataclys. Var. stars, Knudsen, 248
Dolez, N., Gough, D. O., & Vauclair, S. 1988, in Advances in Helio- and Asteroseismology, ed. J. Christensen-Dalsgaard, & S. Frandsen, IAU Symp., 123, 291
Dravins, D., Lindegren, L., Mezey, E., & Young, A. T. 1998, PASP, 110, 1118
Dworetsky, M. M. 2004, in The A-Star Puzzle, ed. J. Zverko, W. W. Weiss, J. Žižňovský, S. J. Adelman, & W. W. Weiss (Cambridge University Press), IAU Symp., 224, 499
Dziembowski, W. A., & Goode, P. R. 1985, ApJ, 296, L27
Dziembowski, W. A., & Goode, P. R. 1996, ApJ, 458, 338
Elkin, V. G., Riley, J. D., Cunha, M. S., Kurtz, D. W., & Mathys, G. 2005, MNRAS, 358, 665
ESA 1997, The Hipparcos and Tycho Catalogue, European Space Agency, SP 1239, ESA Publications, Division, ESTEC, Noordwijk, The Netherlands
Gautschy, A., Saio, H., & Harzenmoser, H. 1998, MNRAS, 301, 31
Girish, V., Seetha, S., Martinez, P., et al. 2001, A&A, 380, 142
Hauck, B., & Mermilliod, M. 1998, A&AS, 129, 431
Handler, G. 2004, Commun. Asteroseismol., 145, 71
Handler, G., & Paunzen, E. 1999, A&AS, 135, 57
Hatzes, A. P., & Mkrtichian, D. E. 2004, MNRAS, 351, 2
Heller, C. H., & Kramer, K. S. 1988, PASP, 100, 583
Henry, G. W., & Fekel, F. C. 2003, AJ, 126, 3058
Henry, G. W., & Fekel, F. C. 2005, AJ, 129, 2026
Houdek, G., Balmforth, N. J., Christensen-Dalsgaard, J., & Gough, D. O. 1999, A&A, 351, 582
Hubrig, S., Nesvacil, N., Schöller, M., et al. 2005, A&A, 440, 37
Hubrig, S., Kharchenko, N., Mathys, G., & North, P. 2000, A&A, 335, 1031
Joshi, S., Girish, V., Martinez, P., et al. 2000, IBVS, 4900
Joshi, S., Girish, V., Sagar, R., Martinez, P., & Seetha, S. 2002, Commun. Asteroseismol., 142, 50
Joshi, S., Girish, V., Sagar, R., et al. 2003, MNRAS, 344, 431
Koen, C., Kurtz, D. W., Gray, R. O., et al. 2001, MNRAS, 326, 387
Kreidl, T. J., Kurtz, D. W., Bus, S. J., et al. 1991, MNRAS, 250, 477
Kurtz, D. W. 1976, ApJS, 32, 651
Kurtz, D. W. 1978, ApJ, 221, 869
Kurtz, D. W. 1980, MNRAS, 193, 61
Kurtz, D. W. 1982, MNRAS, 200, 807
Kurtz, D. W. 1984, MNRAS, 206, 253
Kurtz, D. W. 1985, MNRAS, 213, 773
Kurtz, D. W. 1989, MNRAS, 238, 1077
Kurtz, D. W. 1990, ARA&A, 28, 607
Kurtz, D. W. 2000, in Delta-Scuti and Related Stars, ed. M. Breger, & H. Montgomery (San Francisco: ASP), ASP Conf. Ser., 210, 287
Kurtz, D. W. 2005, JApA, 26, 123
Kurtz, D. W., Garrison, R. F., Koen, C., Hofmann, G. F., & Viranna, N. B. 1995, MNRAS, 276, 199
Kurtz, D. W., & Martinez, P. 2000, Baltic Astron., 9, 253
Kurtz, D. W., Cameron, C., Cunha, M. S., et al. 2005, MNRAS, 358, 651
Leroy, J. L., Landolfi, M., Landi degl'Innocenti, M., Landi degl'Innocenti, E., Bagnulo, S., & Laporte, P. 1995, A&A, 301, 797
Martinez, P., & Kurtz, D. W. 1994, MNRAS, 271, 129
Martinez, P., & Kurtz, D. W. 1995, Ap&SS, 230, 29
Martinez, P., Kurtz, D., Ashoka, B. N., et al. 2001, A&A, 371, 1048 (Paper I)
Mary, D. L. 2005, JApA, 26, 283
Mary, D. L. 2006, A&A, 452, 715
Masana, E., Jordi, C., Maitzen, H. M., & Torra, J. 1998, A&AS, 128, 265
Matthews, J. M., Wehlau, W. H., & Kurtz, D. W. 1987, ApJ, 313, 782
Matthews, J. M. 1988, MNRAS, 235, 7P
Michaud, G. 1970, ApJ, 160, 641
Michaud, G., & Proffitt, C. R. 1993, in Inside the stars, ed. W. W. Weiss, & A. Baglin (San Francisco: ASP), ASP Conf. Ser., 40, 246
Nelson, M. J., & Kreidl, T. J. 1993, AJ, 105, 1903
Nicolet, B. 1982, A&AS, 48, 485
Noels, A., Montalbán, J., & Maceroni, C. 2004, The A-Star Puzzle, ed. J. Zverko, W. W. Weiss, J. Žižňovský, S. J. Adelman, & W. W. Weiss (Cambridge University Press), IAU Symp., 224, 47
North, et al. 1997, in Proceedings of the ESA Symposium, Hipparcos – Venice 97, Venice, Italy, ESA SP-402 (July 1997), p. 239
Reiners, A., & Royer, F. 2004, A&A, 415, 325
Sagar, R. 1999, Current Science, Vol. 77, No. 5, p. 643
Sagar, R., & Mary, D. L. 2005, JApA, 26, 339
Saio, H. 2005, MNRAS, 360, 1022
Saio, H., & Gautschy, A. 2004, MNRAS, 350, 485
Seetha, S., Chaubey, U. S., Girish, V., et al. 2001, BASI, 29, 309
Shibahashi, H. 1983, ApJ, 275, L5
Takata, M., & Shibahashi, Hiromoto 1995, PASJ, 27, 219
Turcotte, S. 2000, in Delta-Scuti and Related Stars, ed. M. Breger, & H. Montgomery (San Francisco: ASP), ASP Conf. Ser., 210, 468
Turcotte, S., Richer, J., Michaud, G., & Christensen-Dalsgaard, J. 2000, A&A, 360, 603
Vauclair, S. 2004, in Variable Stars in the Local Group, ed. D. W. Kurtz, & K. R. Pollard (San Francisco: ASP), ASP Conf. Ser., 310, 413
Vauclair, S., & Théado, S. 2004, A&A, 425, 179
Wegner, G. 1981, ApJ, 247, 969
Wolff, S. C. 1983, The A-Type Stars: Problems and Perspectives, Monograph series on nonthermal phenomena in stellar atmospheres Nasa Special Publication, 463
Yildiz, M. 2003, A&A, 409, 689
Young, A. T. 1967, AJ, 72, 747
Zhiping, Li 2000, A&A, 362, 595
Zhou, Ai-Ying 2001, Commun. Asteroseismol., 140, 59

Online Material

Table 1. Stars classified as null results during the Nainital-Cape survey. A sample of the unprewhitened and prewhitened spectra of these stars are depicted in Fig. 9 and 10 of the paper, respectively. All the spectra are archived electronically. The columns list: HD number, right ascension α_{2000}, declination δ_{2000}, visual magnitude V, spectral type, spectral indices $b-y$, m_1, c_1, β, δm_1, δc_1, peculiarity parameter Δp (Masana et al. 1998), Julian dates (2450000+) on which the star was observed, and the duration of observation (Δt) in hours.

HD	α_{2000}	δ_{2000}	V	Spectral Type	$b-y$	m_1	c_1	β	δm_1	δc_1	Δp	JD	Δt hr
154	00 06 24	34 36 25	8.93	F0	0.223	0.230	0.746	2.782	-0.033	0.002	2.892	1503	1.54
416	00 08 51	37 12 56	8.91	A5	0.194	0.211	0.746	2.803	-0.008	-0.040	2.064	2174	2.30
573	00 10 13	25 31 36	8.90	F0III	0.208	0.253	0.783	2.780	-0.057	0.043	3.497	1832	0.96
												2174	1.31
1607	00 20 27	22 28 47	8.67	F0	0.254	0.222	0.638	2.723	-0.044	0.029	2.544	2235	1.70
2123	00 26 02	67 50 46	9.60	F5	–	–	–	–	–	–	–	2223	1.30
2471	00 28 40	37 18 15	8.15	A5	0.084	0.251	0.900	2.892	-0.075	-0.058	2.449	1499	2.05
2523	00 29 08	11 19 12	8.08	F0	0.219	0.208	0.655	2.733	-0.028	0.016	1.675	2215	2.06
												2223	1.97
												2283	0.79
4564	00 48 00	36 12 17	8.05	A5	0.150	0.228	0.802	2.824	-0.022	-0.024	2.290	2214	2.12
7901	01 20 36	67 14 02	8.44	A3	0.212	0.209	0.720	2.750	-0.024	0.040	1.670	2240	1.05
9550	01 34 24	38 50 44	8.29	A3	0.199	0.213	0.740	2.762	-0.024	0.036	1.765	1827	1.14
9843	01 36 41	35 36 59	8.22	F8	0.286	0.179	0.735	2.706	-0.006	0.187	0.908	1917	1.65
												1919	1.37
												1923	1.44
11215	01 51 40	54 56 37	7.93	A2m	0.145	0.239	0.921	2.803	-0.036	0.135	2.197	1833	1.01
11318	01 52 29	49 47 58	7.94	A3	0.240	0.362	0.388	2.813	-0.157	-0.418	9.219	1498	3.03
												1499	2.04
												2174	1.60
												2176	2.61
11948	01 58 50	55 34 54	7.84	A5	0.115	0.242	0.879	2.873	-0.040	-0.037	2.514	2209	1.48
												2225	1.51
12519	02 03 29	26 32 14	8.46	A5	0.238	0.290	0.552	2.802	-0.087	-0.232	5.985	1500	1.55
13929	02 17 34	58 01 14	7.49	Am	0.134	0.237	0.840	2.826	-0.030	0.011	2.386	2211	4.04
												2212	2.43
14522	02 21 19	28 04 16	8.78	A2	0.141	0.229	0.913	2.901	-0.071	-0.066	2.190	2225	1.40
15023	02 27 29	58 58 12	8.30	F2II	0.178	0.221	0.736	2.790	-0.021	-0.024	2.151	1831	0.53
16127	02 36 22	35 32 10	9.38	A0	0.057	0.190	1.068	2.865	0.014	0.168	1.174	2281	2.13
16956	02 43 41	21 08 51	7.79	A2mp	0.104	0.277	0.822	2.851	-0.071	-0.050	3.779	1502	2.01
												1503	1.98
17317	02 47 28	21 20 44	8.62	Am	0.230	0.226	0.780	2.750	-0.041	0.100	2.390	1501	1.05
												1825	1.32
												2300	1.16
17431	02 49 18	45 15 37	8.50	A3	0.218	0.258	0.672	2.769	-0.066	-0.046	3.921	1827	1.41
												1830	1.45
												2239	3.19
												2250	2.37
19342	03 09 21	58 45 25	8.00	Am	0.310	0.198	0.772	2.733	-0.018	0.133	2.062	1832	0.91
20919	03 24 19	49 13 16	9.00	A8	0.207	0.178	0.765	2.775	0.016	0.035	0.610	1834	0.85
21213	03 26 03	20 14 44	8.70	A5	0.218	0.221	0.741	2.758	-0.034	0.045	2.237	1826	1.28
												1830	0.85
												1834	0.84
21527	03 30 19	48 29 58	8.89	A7I	–	–	–	–	–	–	–	1926	0.85
23734	03 48 10	21 19 45	7.97	A5	0.125	0.211	0.820	2.808	-0.007	0.024	1.175	2283	1.83
25515	04 05 36	50 45 35	8.70	F3III	0.262	0.177	0.745	2.706	-0.004	0.197	0.540	1832	0.78
26894	04 19 12	63 57 29	7.97	F0	0.118	0.228	0.847	2.847	-0.021	-0.017	1.993	1565	1.79
												1566	2.07
												1567	1.30
												1596	2.01
												1600	1.58
												1825	2.13
												1826	0.92
												1827	1.52
												1828	1.58
												1830	0.84

HD	α_{2000}	δ_{2000}	V	Spectral Type	$b-y$	m_1	c_1	β	δm_1	δc_1	Δp	JD	Δt hr
27086	04 18 22	37 34 38	8.47	F0	0.217	0.190	0.920	2.833	0.017	0.080	1.408	1551	0.93
												1950	0.93
												2191	2.40
												2209	0.86
												2287	4.49
												2295	2.07
27380	04 23 44	65 59 28	9.16	G5	–	–	–	–				1566	1.73
29717	04 40 58	02 30 21	8.09	F0	0.239	0.223	0.760	2.769	-0.031	0.042	2.630	2300	1.12
30110	04 48 12	59 14 27	7.48	Fm	0.192	0.202	0.729	2.760	-0.014	0.029	1.268	1568	1.01
												1571	3.23
												1572	5.02
												1591	1.26
												1594	2.53
												1919	0.59
												1948	1.51
32444	05 06 21	55 07 15	8.51	A3	0.362	0.233	0.753	2.769	-0.041	0.035	4.411	2212	1.41
												2223	2.92
32608	05 06 01	35 56 12	6.50	A5V	0.094	0.202	0.908	2.838	0.006	0.061	0.542	2238	3.33
32633	05 06 08	33 55 09	7.07	B9p	-0.012	0.132	0.534	2.725	-0.029	0.108	5.062	2296	1.04
												2305	2.01
33619	05 13 24	41 18 54	8.65	A5	0.186	0.211	0.745	2.784	-0.014	-0.003	1.775	1503	1.29
												1923	0.74
												2225	1.15
37009	05 38 12	50 31 58	8.06	F0	0.216	0.196	0.732	2.736	-0.015	0.084	1.046	1830	0.89
												1833	1.15
												1834	1.89
												1835	2.06
												1857	2.25
												1883	1.18
												1919	0.55
37154	05 39 57	57 08 14	8.81	F0	0.215	0.279	0.654	2.769	-0.087	-0.064	4.727	2285	1.17
												2297	0.97
38143	05 44 22	18 31 37	8.41	A2	0.208	0.205	0.698	2.786	-0.007	-0.054	1.919	1567	1.33
38180	05 45 10	28 15 10	8.43	A5	0.212	0.250	0.776	2.782	-0.053	0.032	3.465	1599	0.84
38271	05 44 43	03 11 38	8.58	A2	0.102	0.255	0.895	2.858	-0.050	0.009	2.789	2300	0.61
39390	05 56 03	59 01 44	8.53	Fm	0.199	0.183	0.701	2.723	-0.005	0.092	0.300	1917	0.73
												1943	1.02
41786	06 08 02	21 17 43	7.29	F0	0.193	0.275	0.690	2.782	-0.078	-0.054	4.393	1500	1.37
												1917	0.64
43478	06 17 51	32 30 16	7.50	A3	0.259	0.240	0.663	2.721	-0.063	0.060	3.213	1511	1.94
43623	06 19 07	39 46 28	9.23	F0	0.199	0.231	0.732	2.791	-0.031	-0.030	2.788	2212	2.49
43682	06 18 11	15 57 09	8.43	Am	0.195	0.190	0.736	2.776	1.007	0.004	1.008	1923	0.62
												1976	1.59
												1977	2.52
44714	06 23 29	05 36 09	8.63	A5	0.146	0.209	0.801	2.846	-0.002	-0.061	1.679	1564	0.91
46297	06 34 02	33 31 40	8.56	A2	0.015	0.272	0.849	2.874	-0.071	-0.069	2.599	1598	1.38
												2250	1.74
47606	06 42 52	56 41 35	7.32	A5	0.130	0.209	0.997	2.804	-0.005	0.209	0.728	1923	0.75
48409	06 45 46	49 04 51	8.40	A3	0.213	0.308	0.517	2.838	-0.100	-0.330	6.779	1498	0.79
												1500	3.49
48933	06 45 57	01 15 10	8.79	A2	0.090	0.181	1.010	2.839	0.027	0.161	1.825	2295	1.44
50186	06 53 06	25 18 41	7.40	Am	0.157	0.261	0.716	2.766	-0.071	0.004	3.219	1923	1.45
51496	07 00 57	56 51 13	9.83	F5	–	–	–	–	–	–	–	1883	1.03
51596	06 58 03	00 22 09	7.50	A2	0.180	0.209	0.670	2.768	-0.018	-0.046	1.618	1502	3.12
												1504	1.83
												1883	0.80
												1943	1.43
55997	07 15 57	16 44 29	9.09	A5III	0.200	0.224	0.683	2.762	-0.035	0.021	2.320	1566	0.78

HD	α_{2000}	δ_{2000}	V	Spectral Type	$b-y$	m_1	c_1	β	δm_1	δc_1	Δp	JD	Δt hr
56148	07 19 48	61 35 31	9.00	F0	0.204	0.178	0.628	2.722	-0.001	0.022	0.316	1567	1.41
												1591	0.96
												1592	1.28
56684	07 19 14	26 59 59	8.31	F0	0.193	0.180	0.673	2.719	-0.003	0.077	0.143	1620	1.00
57955	07 23 48	06 56 46	7.65	A2	0.201	0.290	0.636	2.763	-0.101	-0.070	4.961	1534	1.09
58431	07 25 53	06 42 49	7.84	F0	0.190	0.193	0.683	2.750	-0.008	0.003	0.893	1621	1.52
												1622	1.09
58452	07 27 21	37 36 31	8.76	A3	0.173	0.247	0.704	2.820	-0.041	-0.116	3.453	1500	1.87
60210	07 33 29	00 16 10	9.03	A2	–	–	–	–	–	–	–	1623	0.64
61659	07 42 36	46 29 29	8.65	Am	0.182	0.237	0.797	2.806	-0.033	0.005	2.839	1917	0.56
62140	07 46 28	62 49 53	6.47	F0	0.143	0.265	0.735	2.854	-0.059	-0.143	3.965	2223	1.26
68140	08 12 04	25 10 50	8.74	F0	0.143	0.254	0.772	2.809	-0.050	-0.026	3.132	1568	0.93
												1572	0.86
69476	08 18 15	29 04 46	8.26	A3	0.239	0.232	0.633	2.718	-0.056	0.041	2.722	1511	1.90
69521	08 18 39	31 48 34	8.77	A3	0.032	0.195	0.651	2.868	0.008	-0.255	0.278	1564	0.98
70318	08 21 54	17 36 05	8.20	A3	0.203	0.233	0.707	2.761	-0.045	0.005	2.633	1598	1.11
												1620	0.80
71866	08 31 10	40 13 29	6.71	A0	0.014	0.264	0.823	2.845	-0.057	-0.037	2.236	2238	1.25
72459	08 35 13	50 22 52	8.53	A5V	0.095	0.211	1.036	2.863	-0.007	0.140	0.742	1933	0.71
72792	08 37 26	55 59 11	7.63	F0	0.217	0.231	0.714	2.738	-0.050	0.060	2.451	1502	0.74
												1919	0.99
73045	08 36 48	18 52 59	8.62	Am	0.211	0.199	0.759	2.775	-0.005	0.029	1.469	1943	0.71
73174	08 37 37	19 43 58	7.76	Am	0.089	0.243	0.954	2.858	-0.038	0.068	2.057	1923	0.72
73574	08 39 42	20 05 10	7.75	A5V	0.127	0.207	0.871	2.799	-0.004	0.093	0.843	1566	1.33
73800	08 40 28	07 08 38	8.58	F0	0.218	0.178	0.608	2.718	-0.002	0.016	0.481	1566	2.30
												1567	0.93
75592	08 52 14	37 56 33	9.32	F0	0.180	0.214	0.725	2.751	-0.029	0.043	1.501	2339	1.88
75664	08 51 23	02 13 16	8.65	A5	0.159	0.232	0.740	2.787	-0.034	-0.014	2.316	1534	1.42
												1563	1.17
												1564	0.84
												1567	1.15
76310	08 55 59	21 41 33	8.54	Am	0.168	0.211	0.770	2.775	-0.017	0.040	1.419	1568	0.96
												1571	0.86
												1572	1.25
												1591	1.06
												1943	1.93
76444	08 57 07	29 12 58	9.11	F0	0.176	0.191	0.752	2.745	-0.008	0.082	0.455	1598	1.55
												1599	1.25
												1620	0.76
77081	09 00 20	03 31 48	8.94	A3	0.187	0.239	0.724	2.804	-0.035	-0.064	3.111	1533	1.27
78140	09 07 23	28 07 13	9.09	F0	0.171	0.225	0.734	2.779	-0.029	-0.004	2.109	2246	0.63
78214	09 06 54	-02 19 00	9.82	F8	–	–	–	–	–	–	–	1948	1.59
78388	09 09 52	49 49 57	7.61	FIII	0.231	0.172	0.710	2.709	0.002	0.153	0.101	1917	0.55
												1948	2.28
												1950	1.49
												1983	1.44
												2296	2.62
												2297	3.62
												2305	1.86
79798	09 18 42	60 53 12	8.61	A2	0.155	0.188	0.814	2.778	0.007	0.078	0.333	2239	0.86
81029	09 23 15	03 30 04	7.30	F0	0.200	0.199	0.727	2.737	-0.018	0.076	1.001	1943	0.75
81722	09 33 49	77 41 34	8.31	G5	0.616	0.342	0.430	–				1919	0.76
83920	09 42 47	43 03 15	8.68	A7	0.179	0.221	0.707	2.750	-0.036	0.027	1.785	1917	0.58
85216	09 50 53	19 19 25	8.39	A3	0.180	0.218	0.760	2.777	-0.023	0.026	1.865	1923	0.71
86167	09 57 27	29 10 19	8.39	A5	0.190	0.225	0.682	2.754	-0.039	-0.006	2.159	1923	0.65

HD	α_{2000}	δ_{2000}	V	Spectral Type	$b-y$	m_1	c_1	β	δm_1	δc_1	Δp	JD	Δt hr
90011	10 23 27	02 15 13	8.69	F0	0.216	0.252	0.746	2.753	-0.066	0.060	3.330	1923	0.74
92764	10 43 25	44 57 01	9.01	A7V	0.116	0.210	0.859	2.816	-0.005	0.047	1.026	1917	0.55
												1950	1.29
												1976	1.71
												1977	2.03
												2297	1.34
93075	10 45 59	56 55 14	7.12	A8V	0.173	0.207	0.718	2.786	-0.009	-0.034	1.557	1999	3.96
												2009	1.25
93991	10 52 01	55 21 17	8.09	F0	0.165	0.252	0.826	2.787	-0.054	0.072	2.958	1919	0.96
94779	10 57 17	46 55 09	8.68	Am	0.083	0.213	0.991	2.823	-0.007	0.166	0.542	1923	0.76
98710	11 21 51	34 51 37	8.74	Am	0.147	0.203	0.815	2.796	-0.001	0.043	1.007	1923	0.64
98880	11 22 52	44 49 28	8.04	A5	0.233	0.233	0.644	2.719	-0.056	0.048	2.677	1917	0.64
												1948	2.01
99831	11 29 22	42 05 31	8.90	Am	0.186	0.220	0.720	2.750	-0.035	0.040	1.797	1919	0.59
100215	11 32 13	38 55 34	7.99	Am	0.205	0.175	0.679	2.733	0.005	0.040	0.207	1923	0.60
100654	11 35 12	35 24 20	8.68	F5	0.217	0.248	0.676	2.739	-0.066	0.019	3.193	1943	0.80
101953	11 44 07	29 34 48	8.04	Am	0.169	0.185	0.732	2.754	0.001	0.044	0.289	1943	0.72
102102	11 45 16	43 12 37	8.09	F0	0.174	0.236	0.765	2.794	-0.035	-0.003	2.657	1923	0.60
103498	11 55 11	46 28 11	6.99	A1	0.003	0.196	1.010	2.858	0.009	0.124	2.263	1563	0.80
												1564	0.38
												1659	0.85
104202	12 00 09	70 39 06	8.44	A	0.144	0.236	0.769	–	–	–	–	2280	0.96
												2282	1.37
												2295	1.27
104817	12 04 13	01 27 44	7.69	Am	0.115	0.205	0.873	2.843	0.003	0.017	1.002	1923	0.77
104957	12 05 06	30 49 59	8.87	Am	0.170	0.178	0.746	2.760	0.010	0.046	0.068	1917	0.65
105680	12 09 59	22 38 23	8.06	Am	0.188	0.220	0.714	2.763	-0.031	0.008	1.976	1943	0.77
107513	12 21 26	24 59 49	7.38	Am	0.172	0.176	0.738	2.753	0.010	0.052	4.276	1948	3.31
												1950	2.36
												2297	1.06
												2305	0.92
109306	12 33 36	28 04 53	8.60	F3V	0.238	0.223	0.683	2.717	-0.047	0.095	2.249	1923	0.61
												2283	0.72
109782	12 37 11	21 11 54	7.71	F3V	0.243	0.228	0.683	2.724	-0.050	0.071	2.559	1983	1.64
115606	13 18 02	13 00 00	8.57	A2	0.165	0.296	0.631	2.846	-0.089	-0.231	5.581	1566	1.19
												1567	2.28
115708	13 18 37	26 21 56	7.83	A2p	0.164	0.192	0.747	2.788	0.007	-0.009	0.843	1977	3.05
115722	13 18 25	35 57 14	9.55	Am	0.208	0.199	0.665	2.756	-0.012	-0.027	1.430	2034	1.09
116635	13 24 26	30 33 14	9.63	F2	0.092	0.199	0.934	2.890	-0.019	-0.019	0.487	2034	0.99
117044	13 27 30	13 54 49	8.19	F0	0.209	0.211	0.674	2.749	-0.026	-0.004	1.803	1950	1.74
119563	13 43 39	21 05 44	8.81	A5	0.215	0.217	0.763	2.737	-0.036	0.112	1.778	1943	0.89
124883	14 15 26	27 44 02	7.30	A2	–	–	–	–	–	–	–	1619	1.28
												1622	0.97
												1627	3.14
134305	15 08 44	12 29 19	7.24	A7p	–	–	–	–	–	–	–	1660	1.17
												2043	1.62
135297	15 14 21	00 22 10	7.94	A0p	-0.010	0.182	0.969	2.855	-0.055	0.102	2.365	1619	0.97
												1620	1.04
												1650	1.32
139319	15 33 48	63 54 00	7.43	A5	0.193	0.186	0.836	2.770	0.006	0.116	0.547	2035	0.99
139478	15 36 00	52 04 11	6.70	F4	0.207	0.169	0.666	2.739	0.013	0.009	0.090	2034	0.97
144999	16 07 38	28 59 43	7.70	A3	–	–	–	–	–	–	–	1620	1.00
												1622	0.97
												1623	0.79
												1650	1.69
												1659	2.04
151070	16 44 10	23 31 01	7.03	F5	0.351	0.203	0.697	2.688	-0.032	0.208	2.522	2035	1.01
153897	17 01 09	27 11 50	6.57	F5	0.274	0.154	0.457	2.6762	0.016	0.002	0.261	2036	0.94

HD	α_{2000}	δ_{2000}	V	Spectral Type	$b-y$	m_1	c_1	β	δm_1	δc_1	Δp	JD	Δt hr
162705	17 51 47	15 00 24	7.53	F0	0.218	0.219	0.766	2.765	-0.029	0.056	2.184	2034	0.97
166894	18 10 54	38 57 40	7.80	A2	0.066	0.187	1.090	2.879	0.013	0.162	0.681	2036	1.17
168605	18 19 50	19 10 17	8.19	A0p	0.037	0.101	1.089	2.828	0.106	0.257	–	1659	1.66
												1660	1.01
177332	19 04 10	03 19 50	6.72	A5	0.071	0.204	1.088	2.857	0.001	0.204	0.070	2034	0.92
191742	20 09 47	42 32 28	8.16	A7	0.114	0.232	0.960	2.884	-0.040	0.021	1.946	1825	1.51
												1826	1.31
192224	20 12 08	41 21 01	8.86	Ap	–	–	–	–	–	–	–	1830	1.18
200177	21 00 06	48 40 46	7.34	B9p	-0.017	0.200	0.845	2.873	-0.069	-0.063	3.075	1829	1.00
												2209	1.00
203819	21 22 43	54 13 50	7.87	A0p	0.013	0.153	1.086	2.890	0.027	0.133	–	2190	1.64
203922	21 24 12	35 01 35	8.52	A2	–	–	–	–	–	–	–	1824	1.54
204038	21 25 00	33 41 16	8.38	F1V	0.291	0.158	0.668	2.691	0.013	0.170	0.211	1831	0.99
206977	21 44 54	36 11 26	9.01	A5	0.109	0.191	1.016	2.886	-0.003	0.072	0.202	1829	1.38
												1830	0.57
207564	21 49 42	10 42 41	9.50	F8	–	–	–	–	–	–	–	2215	3.33
208525	21 55 24	51 00 13	9.06	A2	–	–	–	–	–	–	–	1826	1.43
210433	22 08 35	59 17 22	7.15	A0	–	–	–	2.846	–	–	–	1827	1.55
221072	23 28 18	63 23 27	8.32	F5	0.302	0.211	0.698	2.702	-0.039	0.162	2.360	1830	1.02
223247	23 47 46	28 24 26	8.13	F0	0.182	0.217	0.773	2.772	-0.024	0.049	1.765	1832	1.01
												1833	1.18
228112	20 10 29	41 09 28	9.03	Ap	–	–	–	–	–	–	–	1827	1.29

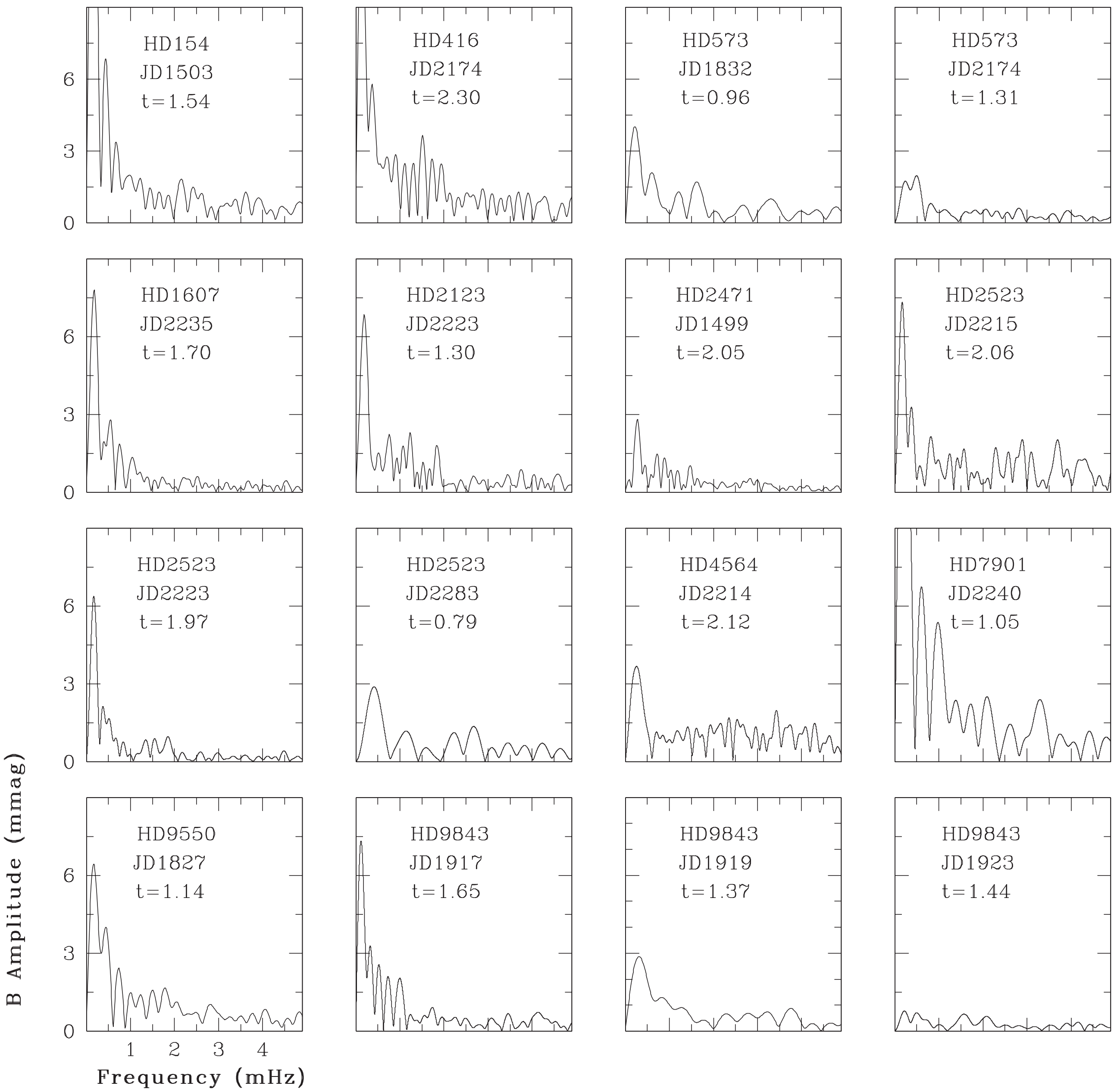
HD154
JD1503
t=1.54
HD416
JD2174
t=2.30
HD573
JD1832
t=0.96
HD573
JD2174
t=1.31
HD1607
JD2235
t=1.70
HD2123
JD2223
t=1.30
HD2471
JD1499
t=2.05
HD2523
JD2215
t=2.06
HD2523
JD2223
t=1.97
HD2523
JD2283
t=0.79
HD4564
JD2214
t=2.12
HD7901
JD2240
t=1.05
HD9550
JD1827
t=1.14
HD9843
JD1917
t=1.65
HD9843
JD1919
t=1.37
HD9843
JD1923
t=1.44
B Amplitude (mmag)
Frequency (mHz)
0
3
6
1
2
3
4

Fig. 9.

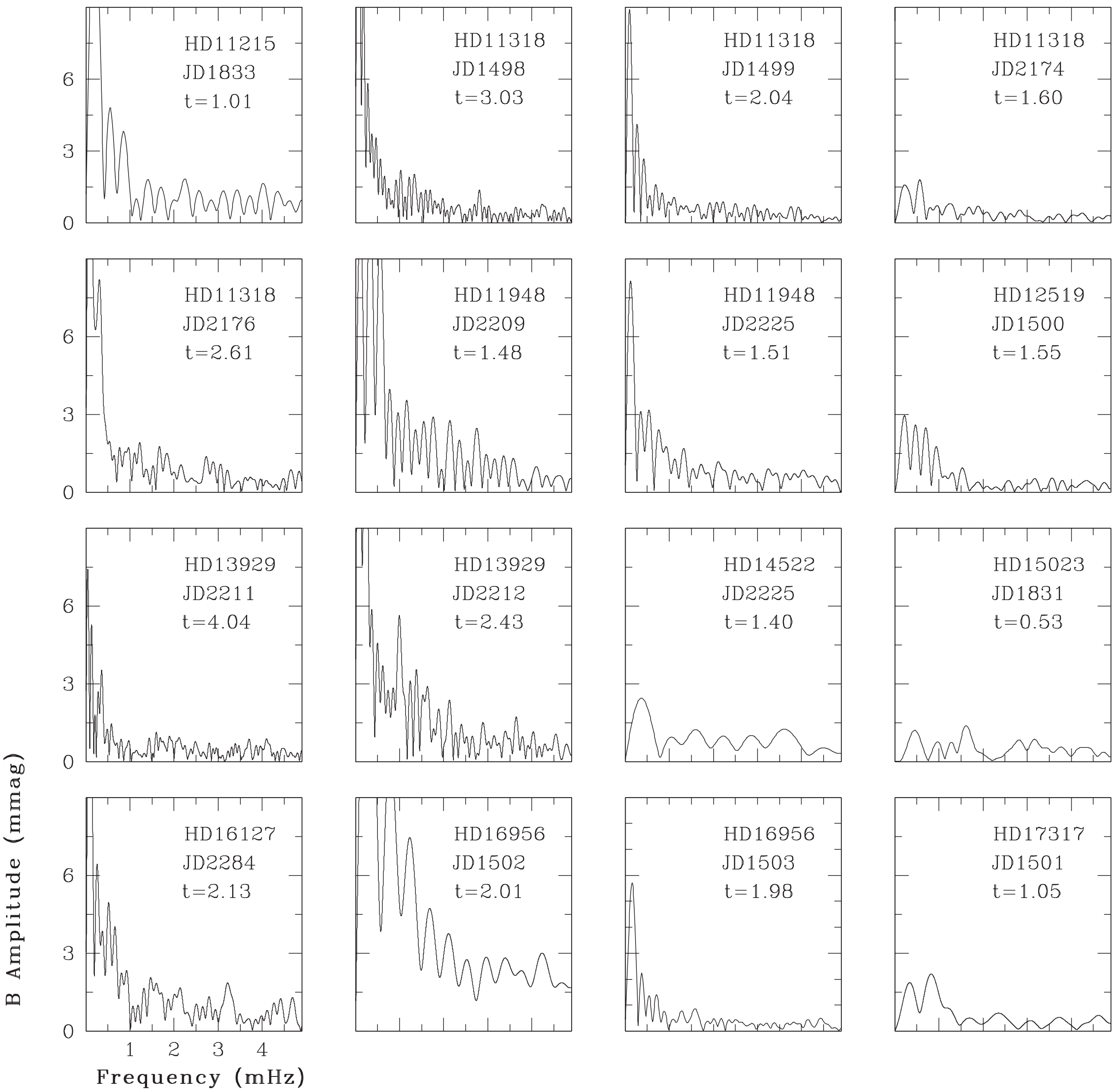
HD11215
JD1833
t=1.01
HD11318
JD1498
t=3.03
HD11318
JD1499
t=2.04
HD11318
JD2174
t=1.60
HD11318
JD2176
t=2.61
HD11948
JD2209
t=1.48
HD11948
JD2225
t=1.51
HD12519
JD1500
t=1.55
HD13929
JD2211
t=4.04
HD13929
JD2212
t=2.43
HD14522
JD2225
t=1.40
HD15023
JD1831
t=0.53
HD16127
JD2284
t=2.13
HD16956
JD1502
t=2.01
HD16956
JD1503
t=1.98
HD17317
JD1501
t=1.05
B Amplitude (mmag)
0
3
6
1
2
3
4
Frequency (mHz)

Fig. 9.

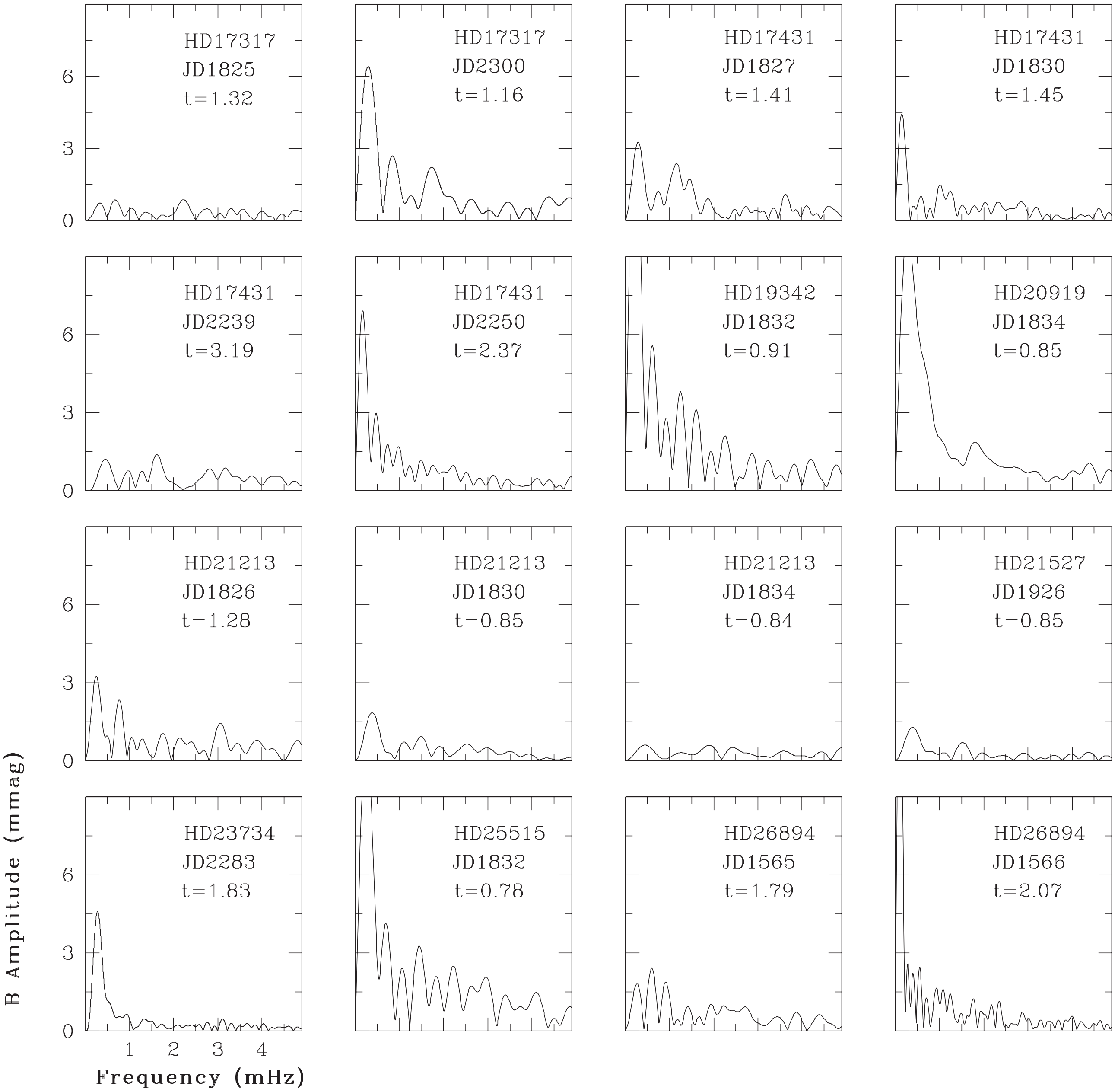
HD17317
JD1825
t=1.32
HD17317
JD2300
t=1.16
HD17431
JD1827
t=1.41
HD17431
JD1830
t=1.45
HD17431
JD2239
t=3.19
HD17431
JD2250
t=2.37
HD19342
JD1832
t=0.91
HD20919
JD1834
t=0.85
HD21213
JD1826
t=1.28
HD21213
JD1830
t=0.85
HD21213
JD1834
t=0.84
HD21527
JD1926
t=0.85
HD23734
JD2283
t=1.83
HD25515
JD1832
t=0.78
HD26894
JD1565
t=1.79
HD26894
JD1566
t=2.07
B Amplitude (mmag)
0
3
6
1
2
3
4
Frequency (mHz)

Fig. 9.

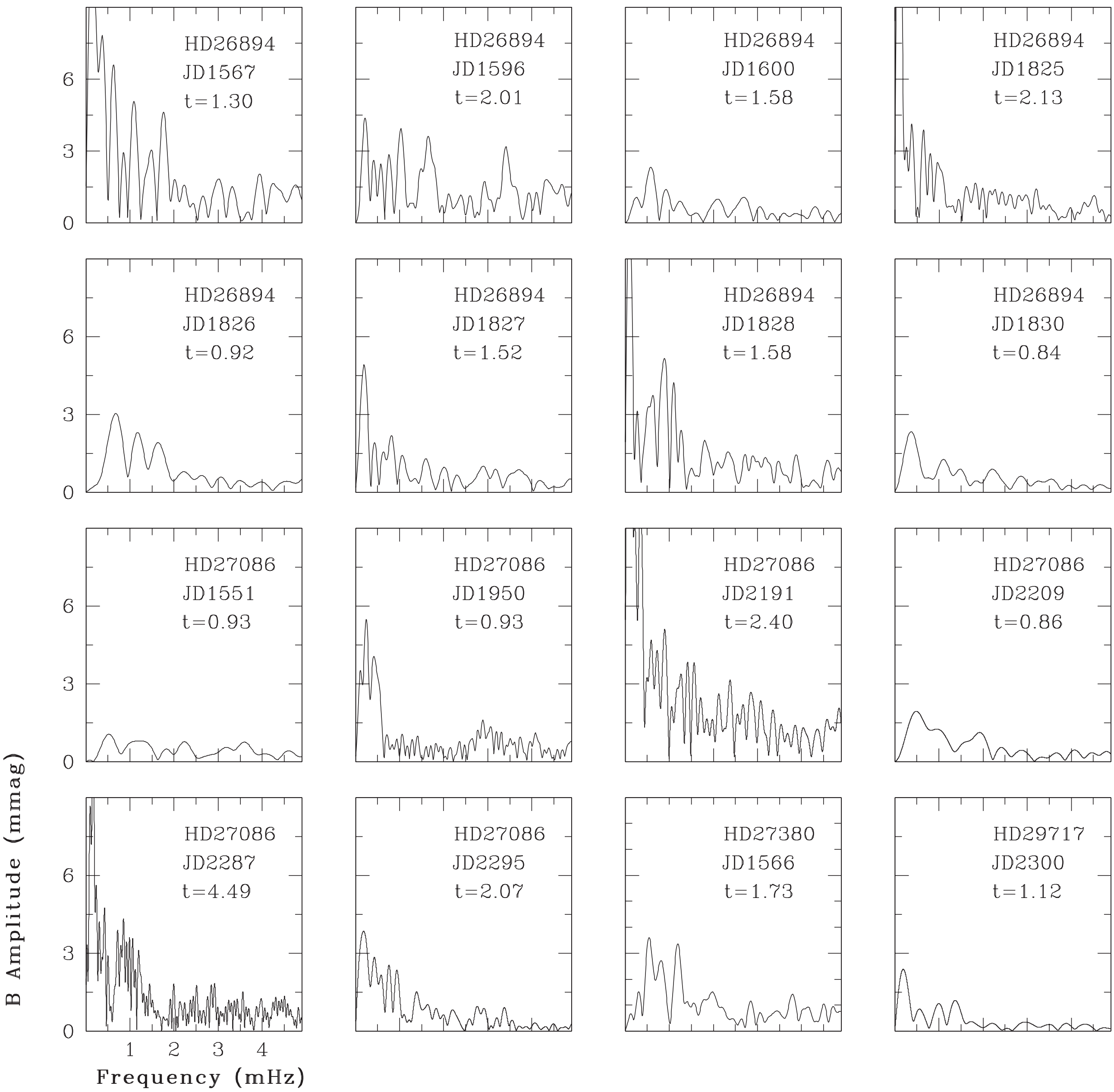
HD26894
JD1567
t=1.30
HD26894
JD1596
t=2.01
HD26894
JD1600
t=1.58
HD26894
JD1825
t=2.13
HD26894
JD1826
t=0.92
HD26894
JD1827
t=1.52
HD26894
JD1828
t=1.58
HD26894
JD1830
t=0.84
HD27086
JD1551
t=0.93
HD27086
JD1950
t=0.93
HD27086
JD2191
t=2.40
HD27086
JD2209
t=0.86
HD27086
JD2287
t=4.49
HD27086
JD2295
t=2.07
HD27380
JD1566
t=1.73
HD29717
JD2300
t=1.12
B Amplitude (mmag)
Frequency (mHz)
0
3
6
1
2
3
4

Fig. 9.

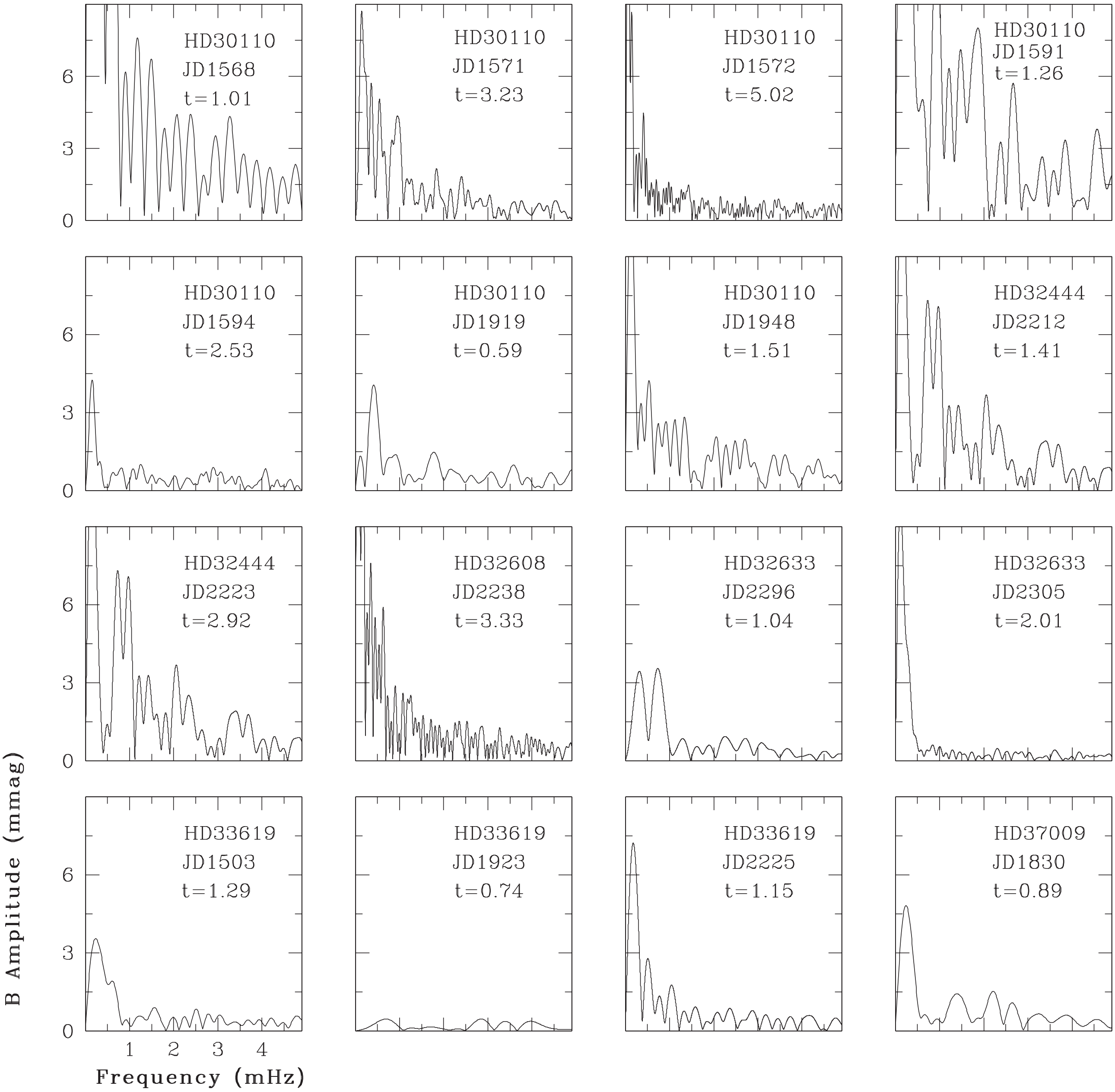
HD30110
JD1568
t=1.01
HD30110
JD1571
t=3.23
HD30110
JD1572
t=5.02
HD30110
JD1591
t=1.26
HD30110
JD1594
t=2.53
HD30110
JD1919
t=0.59
HD30110
JD1948
t=1.51
HD32444
JD2212
t=1.41
HD32444
JD2223
t=2.92
HD32608
JD2238
t=3.33
HD32633
JD2296
t=1.04
HD32633
JD2305
t=2.01
HD33619
JD1503
t=1.29
HD33619
JD1923
t=0.74
HD33619
JD2225
t=1.15
HD37009
JD1830
t=0.89
B Amplitude (mmag)
0
3
6
1
2
3
4
Frequency (mHz)

Fig. 9.

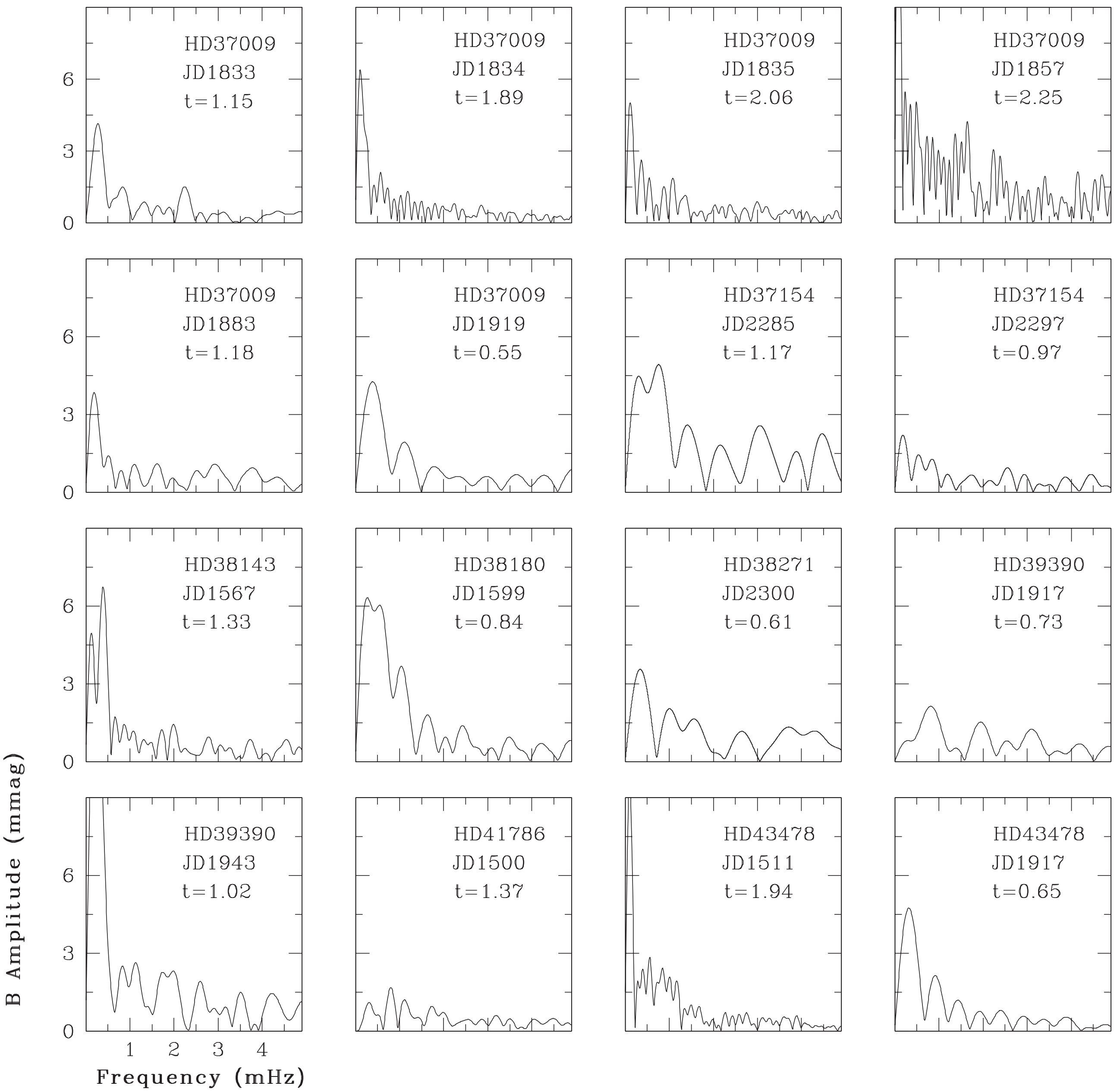
HD37009
JD1833
t=1.15
HD37009
JD1834
t=1.89
HD37009
JD1835
t=2.06
HD37009
JD1857
t=2.25
HD37009
JD1883
t=1.18
HD37009
JD1919
t=0.55
HD37154
JD2285
t=1.17
HD37154
JD2297
t=0.97
HD38143
JD1567
t=1.33
HD38180
JD1599
t=0.84
HD38271
JD2300
t=0.61
HD39390
JD1917
t=0.73
HD39390
JD1943
t=1.02
HD41786
JD1500
t=1.37
HD43478
JD1511
t=1.94
HD43478
JD1917
t=0.65
B Amplitude (mmag)
Frequency (mHz)
0
3
6
1
2
3
4

Fig. 9.

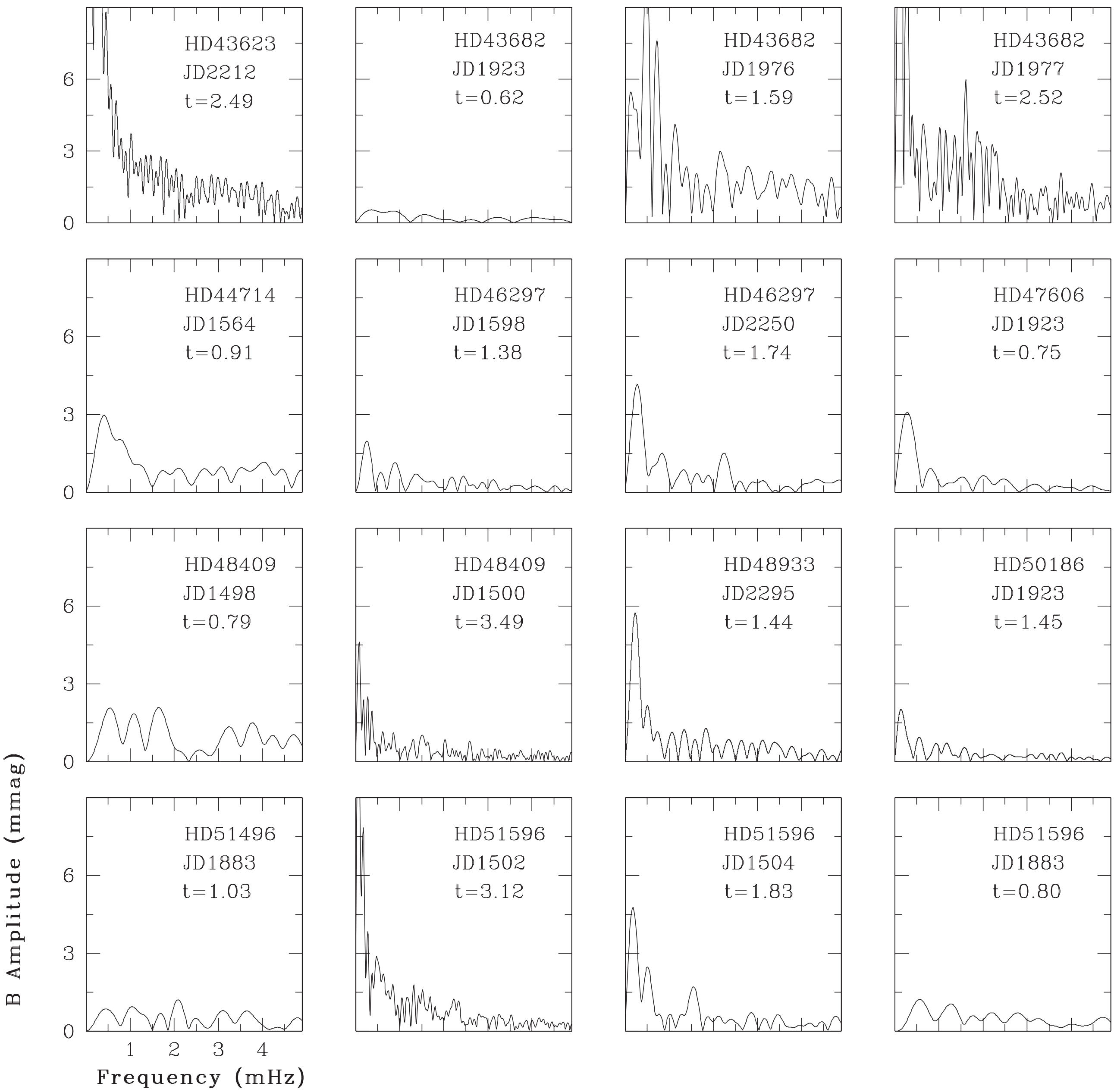
HD43623
JD2212
t=2.49
HD43682
JD1923
t=0.62
HD43682
JD1976
t=1.59
HD43682
JD1977
t=2.52
HD44714
JD1564
t=0.91
HD46297
JD1598
t=1.38
HD46297
JD2250
t=1.74
HD47606
JD1923
t=0.75
HD48409
JD1498
t=0.79
HD48409
JD1500
t=3.49
HD48933
JD2295
t=1.44
HD50186
JD1923
t=1.45
HD51496
JD1883
t=1.03
HD51596
JD1502
t=3.12
HD51596
JD1504
t=1.83
HD51596
JD1883
t=0.80
B Amplitude (mmag)
Frequency (mHz)

Fig. 9.

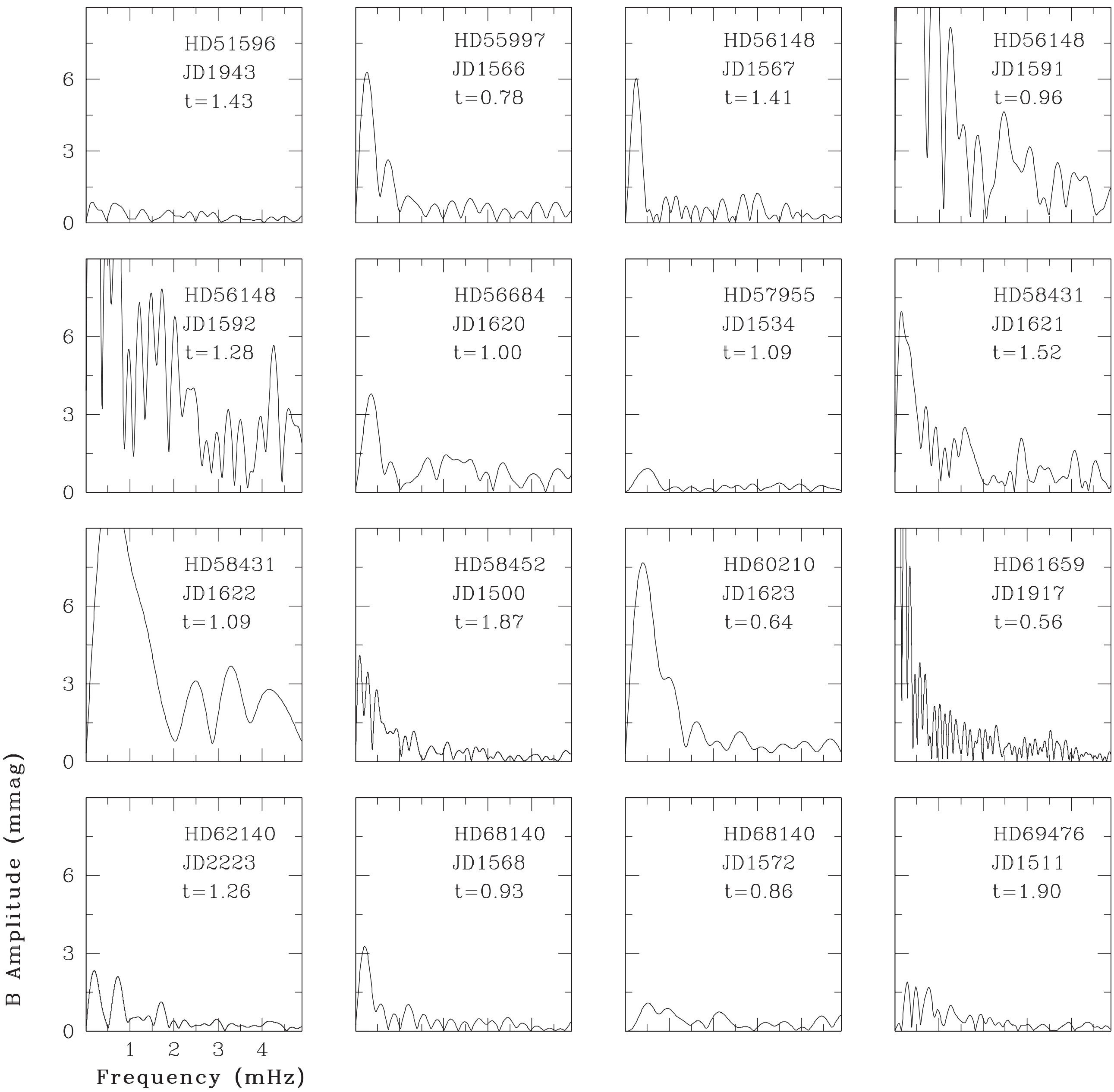

HD51596
JD1943
t=1.43
HD55997
JD1566
t=0.78
HD56148
JD1567
t=1.41
HD56148
JD1591
t=0.96
HD56148
JD1592
t=1.28
HD56684
JD1620
t=1.00
HD57955
JD1534
t=1.09
HD58431
JD1621
t=1.52
HD58431
JD1622
t=1.09
HD58452
JD1500
t=1.87
HD60210
JD1623
t=0.64
HD61659
JD1917
t=0.56
HD62140
JD2223
t=1.26
HD68140
JD1568
t=0.93
HD68140
JD1572
t=0.86
HD69476
JD1511
t=1.90
B Amplitude (mmag)
Frequency (mHz)

Fig. 9.

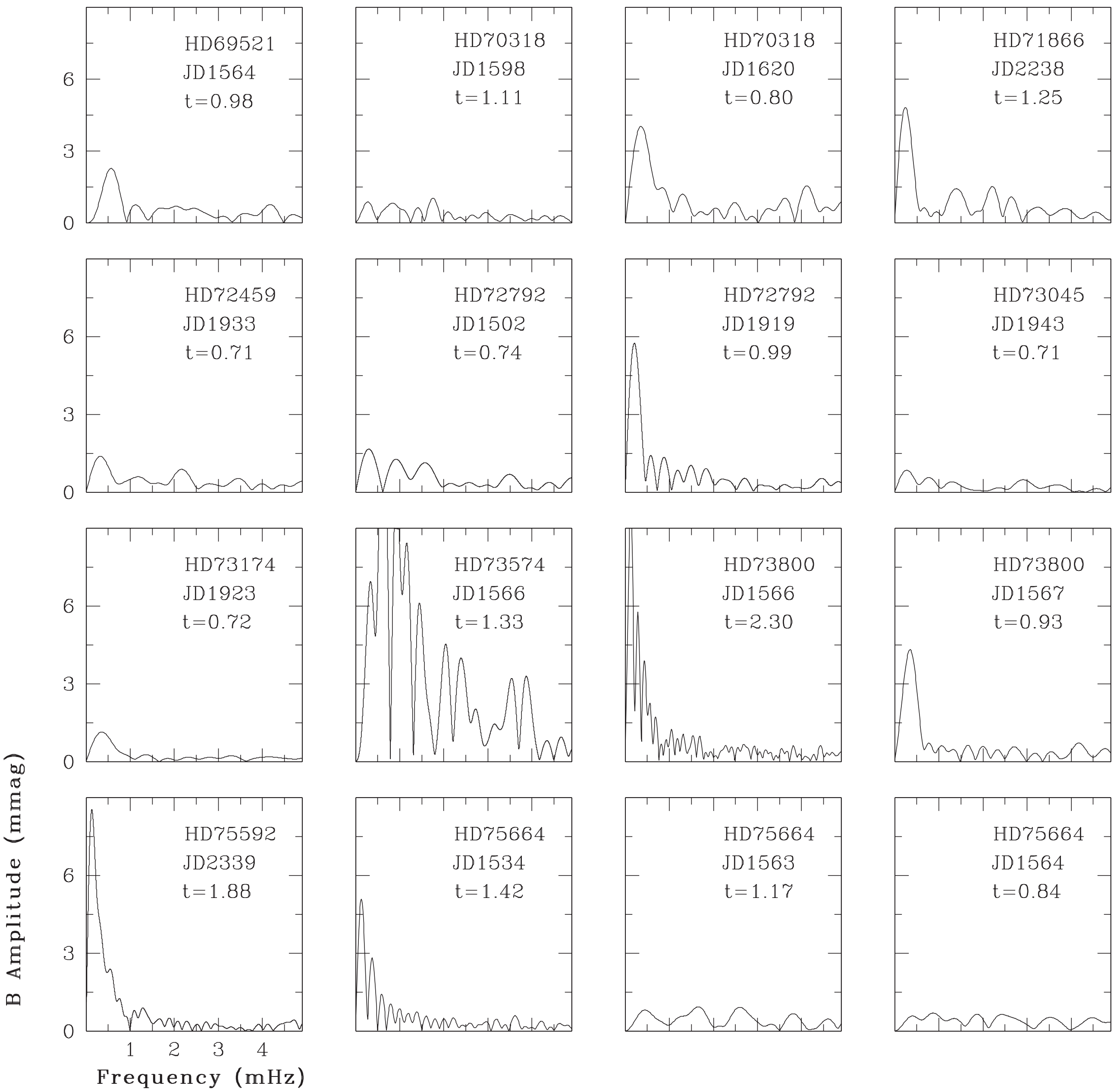
HD69521
JD1564
t=0.98
HD70318
JD1598
t=1.11
HD70318
JD1620
t=0.80
HD71866
JD2238
t=1.25
HD72459
JD1933
t=0.71
HD72792
JD1502
t=0.74
HD72792
JD1919
t=0.99
HD73045
JD1943
t=0.71
HD73174
JD1923
t=0.72
HD73574
JD1566
t=1.33
HD73800
JD1566
t=2.30
HD73800
JD1567
t=0.93
HD75592
JD2339
t=1.88
HD75664
JD1534
t=1.42
HD75664
JD1563
t=1.17
HD75664
JD1564
t=0.84
B Amplitude (mmag)
0
3
6
1
2
3
4
Frequency (mHz)

Fig. 9.

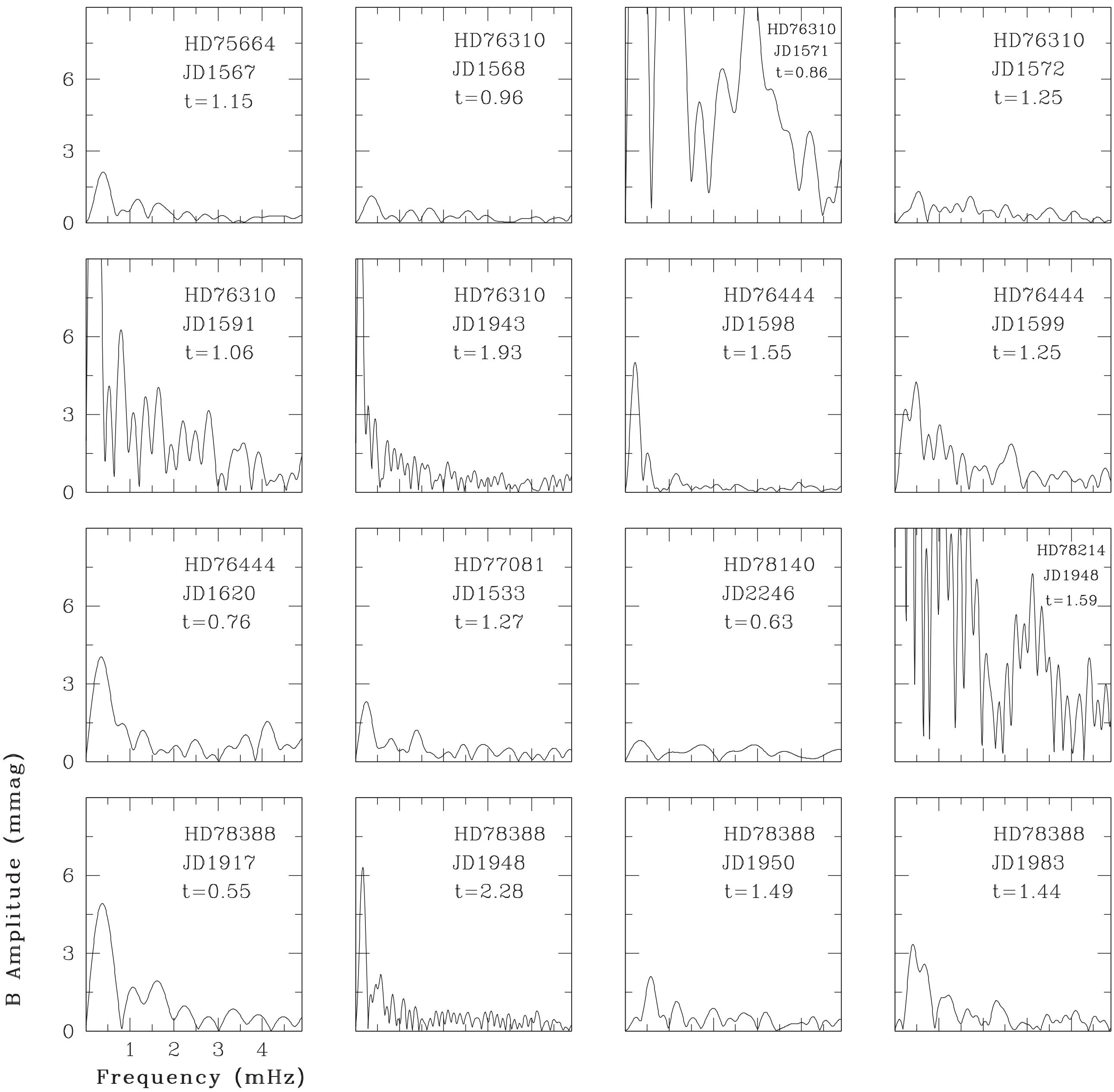

HD75664
JD1567
t=1.15
HD76310
JD1568
t=0.96
HD76310
JD1571
t=0.86
HD76310
JD1572
t=1.25
HD76310
JD1591
t=1.06
HD76310
JD1943
t=1.93
HD76444
JD1598
t=1.55
HD76444
JD1599
t=1.25
HD76444
JD1620
t=0.76
HD77081
JD1533
t=1.27
HD78140
JD2246
t=0.63
HD78214
JD1948
t=1.59
HD78388
JD1917
t=0.55
HD78388
JD1948
t=2.28
HD78388
JD1950
t=1.49
HD78388
JD1983
t=1.44
B Amplitude (mmag)
Frequency (mHz)
0
3
6
1
2
3
4

Fig. 9.

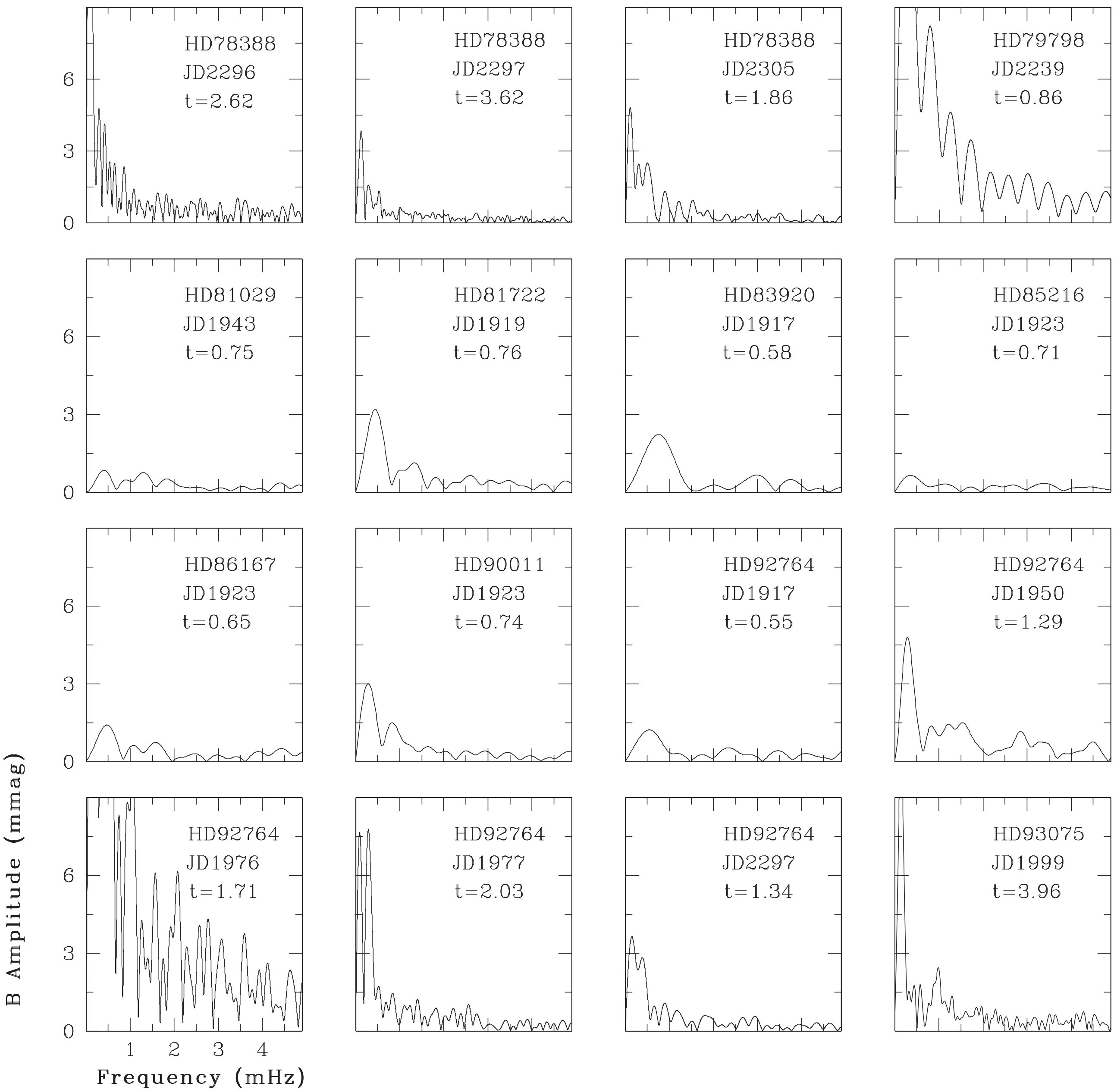
HD78388
JD2296
t=2.62
HD78388
JD2297
t=3.62
HD78388
JD2305
t=1.86
HD79798
JD2239
t=0.86
HD81029
JD1943
t=0.75
HD81722
JD1919
t=0.76
HD83920
JD1917
t=0.58
HD85216
JD1923
t=0.71
HD86167
JD1923
t=0.65
HD90011
JD1923
t=0.74
HD92764
JD1917
t=0.55
HD92764
JD1950
t=1.29
HD92764
JD1976
t=1.71
HD92764
JD1977
t=2.03
HD92764
JD2297
t=1.34
HD93075
JD1999
t=3.96
B Amplitude (mmag)
Frequency (mHz)
0
3
6
1
2
3
4

Fig. 9.

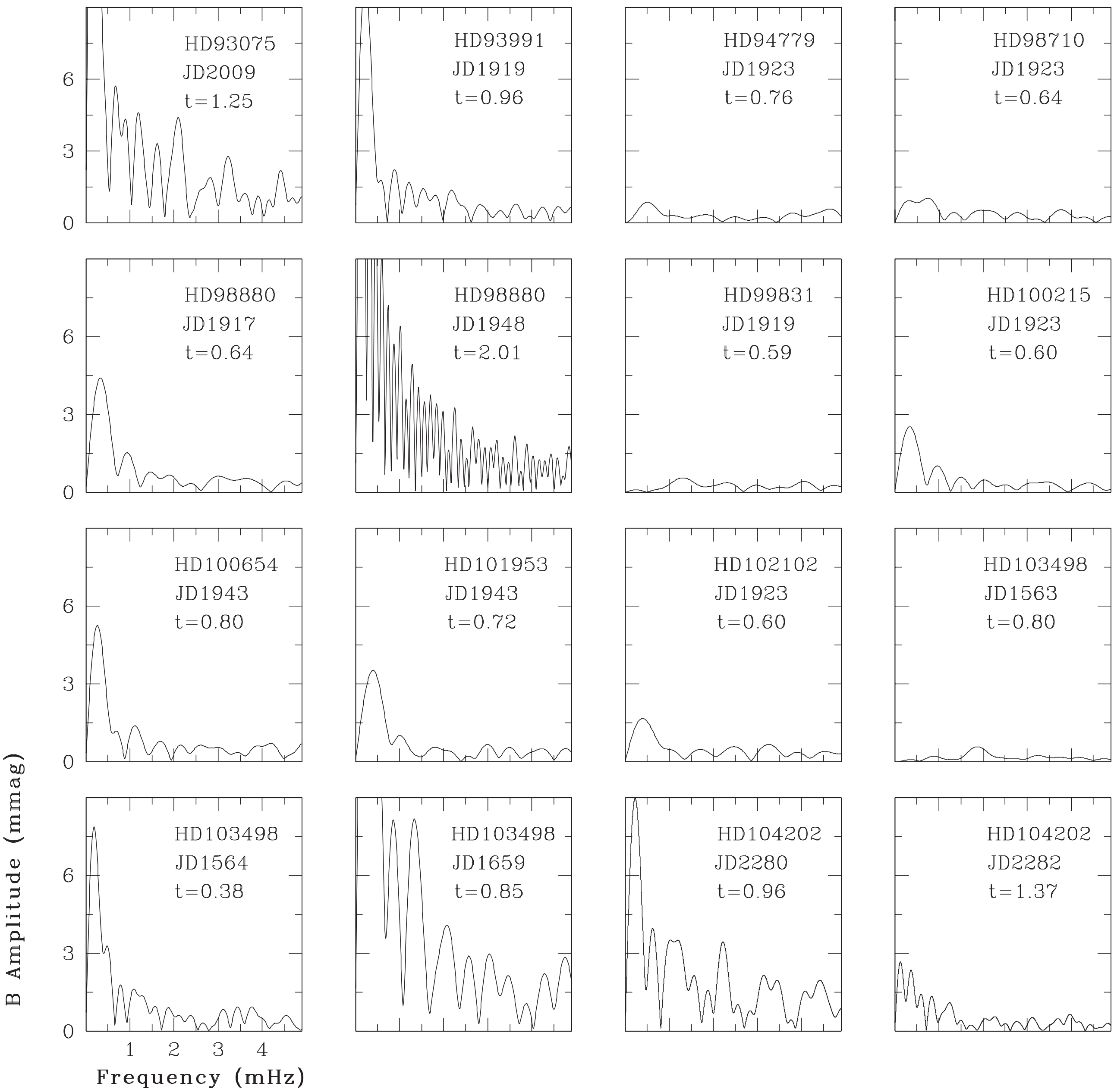

HD93075
JD2009
t=1.25
HD93991
JD1919
t=0.96
HD94779
JD1923
t=0.76
HD98710
JD1923
t=0.64
HD98880
JD1917
t=0.64
HD98880
JD1948
t=2.01
HD99831
JD1919
t=0.59
HD100215
JD1923
t=0.60
HD100654
JD1943
t=0.80
HD101953
JD1943
t=0.72
HD102102
JD1923
t=0.60
HD103498
JD1563
t=0.80
HD103498
JD1564
t=0.38
HD103498
JD1659
t=0.85
HD104202
JD2280
t=0.96
HD104202
JD2282
t=1.37
B Amplitude (mmag)
0
3
6
1
2
3
4
Frequency (mHz)

Fig. 9.

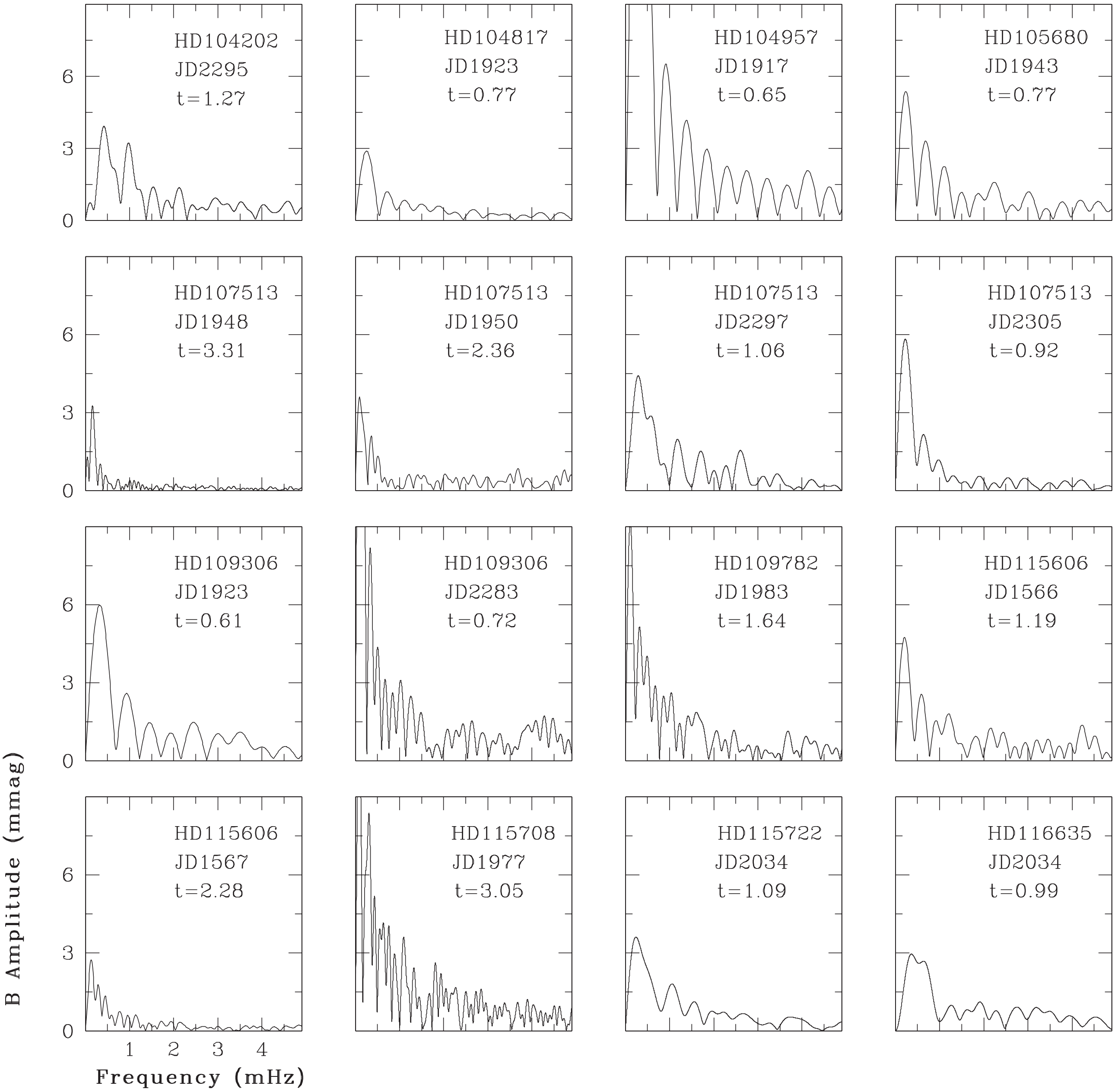
HD104202
JD2295
t=1.27
HD104817
JD1923
t=0.77
HD104957
JD1917
t=0.65
HD105680
JD1943
t=0.77
HD107513
JD1948
t=3.31
HD107513
JD1950
t=2.36
HD107513
JD2297
t=1.06
HD107513
JD2305
t=0.92
HD109306
JD1923
t=0.61
HD109306
JD2283
t=0.72
HD109782
JD1983
t=1.64
HD115606
JD1566
t=1.19
HD115606
JD1567
t=2.28
HD115708
JD1977
t=3.05
HD115722
JD2034
t=1.09
HD116635
JD2034
t=0.99
B Amplitude (mmag)
Frequency (mHz)
0
3
6
1
2
3
4

Fig. 9.

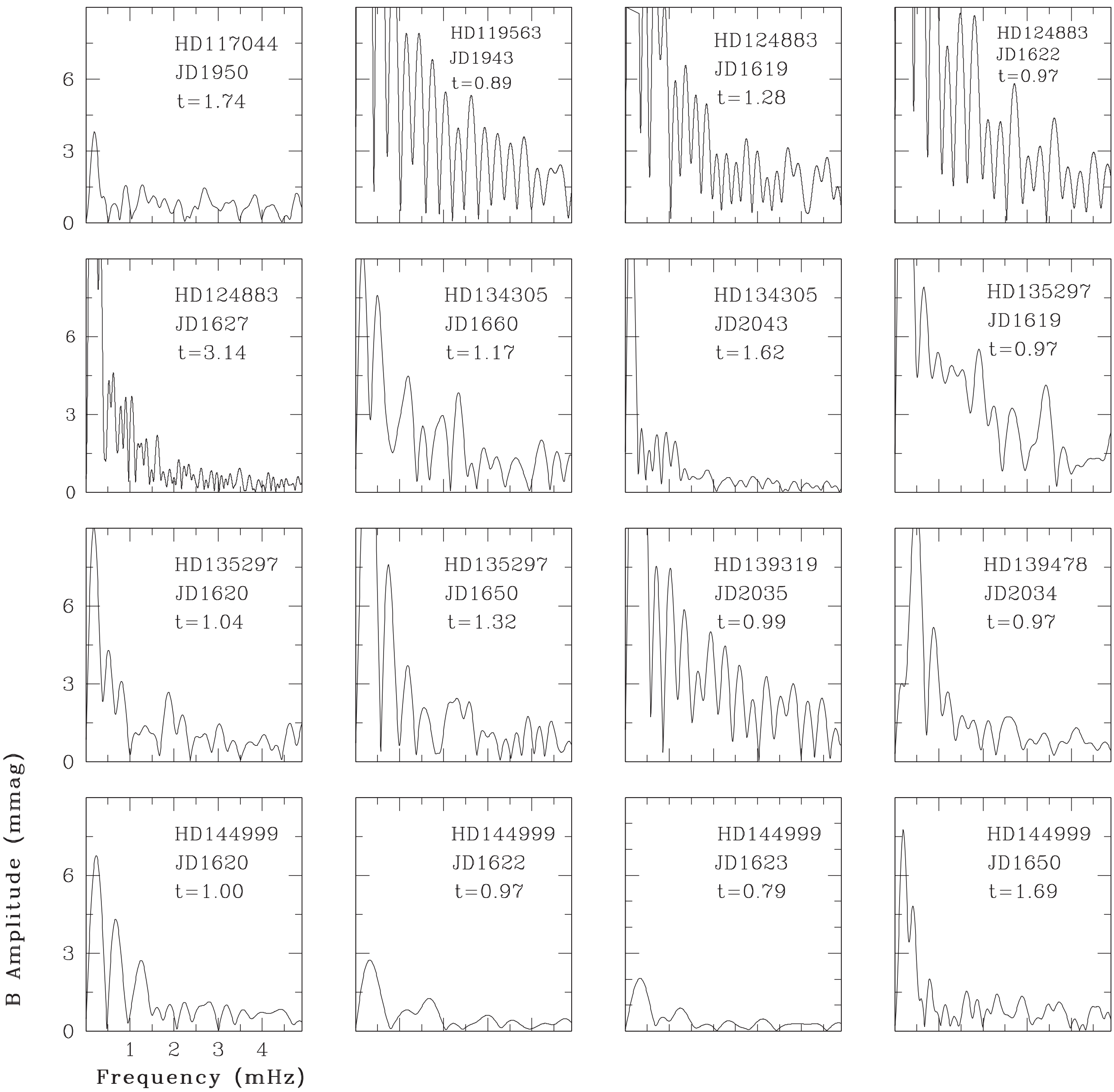
HD117044
JD1950
t=1.74
HD119563
JD1943
t=0.89
HD124883
JD1619
t=1.28
HD124883
JD1622
t=0.97
HD124883
JD1627
t=3.14
HD134305
JD1660
t=1.17
HD134305
JD2043
t=1.62
HD135297
JD1619
t=0.97
HD135297
JD1620
t=1.04
HD135297
JD1650
t=1.32
HD139319
JD2035
t=0.99
HD139478
JD2034
t=0.97
HD144999
JD1620
t=1.00
HD144999
JD1622
t=0.97
HD144999
JD1623
t=0.79
HD144999
JD1650
t=1.69
B Amplitude (mmag)
Frequency (mHz)
0
3
6
1
2
3
4

Fig. 9.

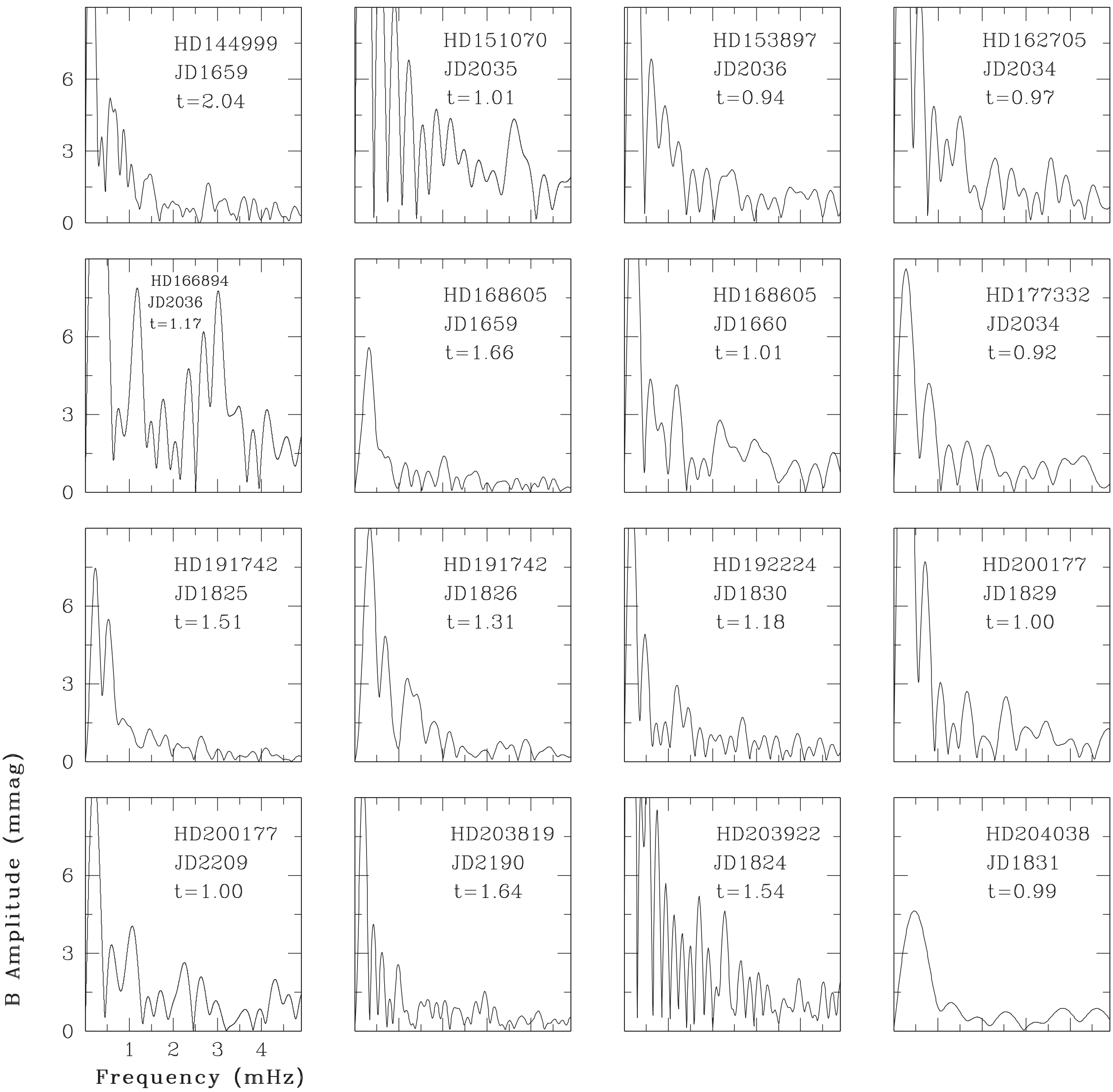

HD144999
JD1659
t=2.04
HD151070
JD2035
t=1.01
HD153897
JD2036
t=0.94
HD162705
JD2034
t=0.97
HD166894
JD2036
t=1.17
HD168605
JD1659
t=1.66
HD168605
JD1660
t=1.01
HD177332
JD2034
t=0.92
HD191742
JD1825
t=1.51
HD191742
JD1826
t=1.31
HD192224
JD1830
t=1.18
HD200177
JD1829
t=1.00
HD200177
JD2209
t=1.00
HD203819
JD2190
t=1.64
HD203922
JD1824
t=1.54
HD204038
JD1831
t=0.99
B Amplitude (mmag)
0
3
6
1
2
3
4
Frequency (mHz)

Fig. 9.

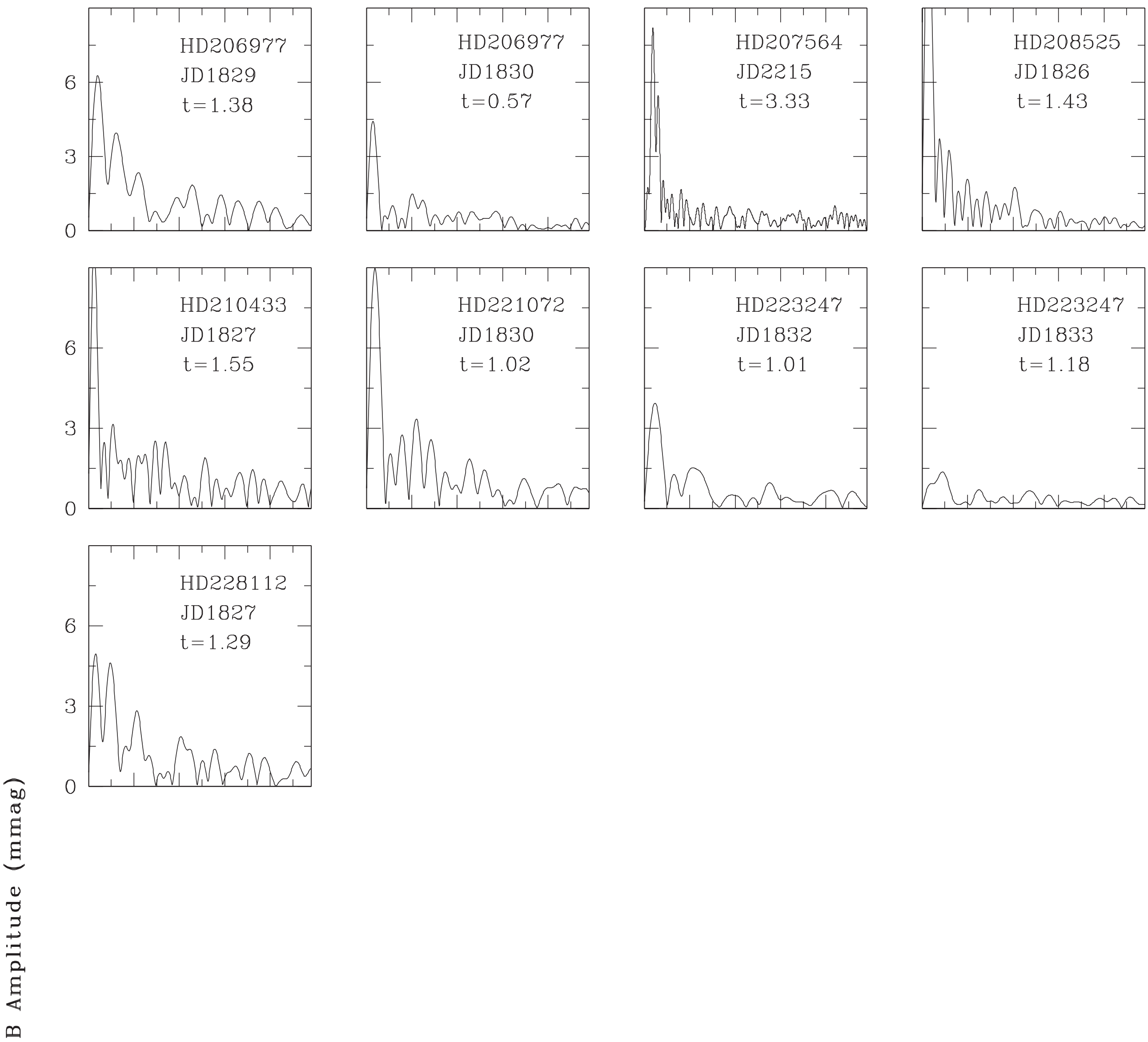
HD206977
JD1829
t=1.38
HD206977
JD1830
t=0.57
HD207564
JD2215
t=3.33
HD208525
JD1826
t=1.43
HD210433
JD1827
t=1.55
HD221072
JD1830
t=1.02
HD223247
JD1832
t=1.01
HD223247
JD1833
t=1.18
HD228112
JD1827
t=1.29
0
3
6
B Amplitude (mmag)

Fig. 9.

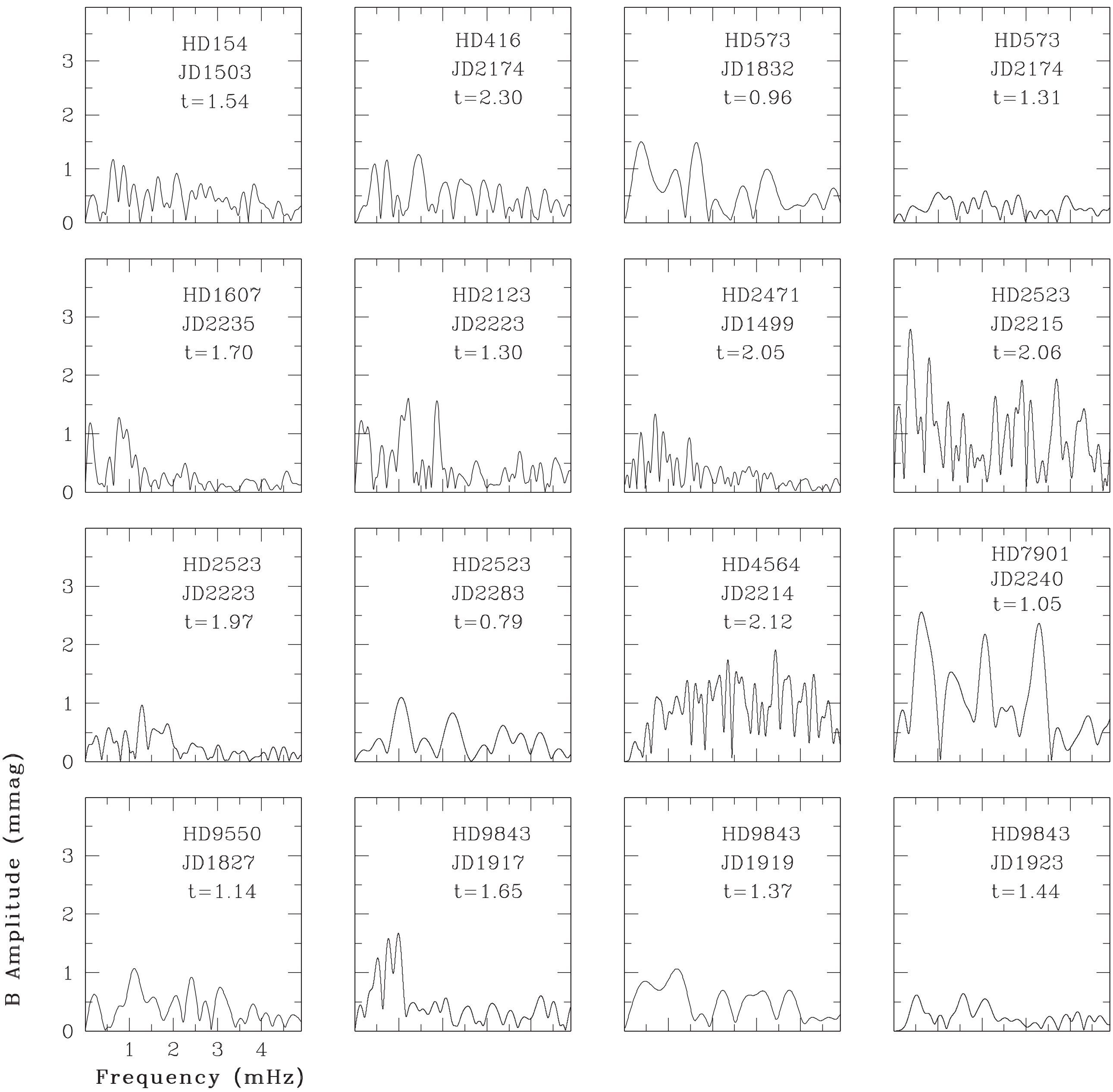
HD154
JD1503
t=1.54
HD416
JD2174
t=2.30
HD573
JD1832
t=0.96
HD573
JD2174
t=1.31
HD1607
JD2235
t=1.70
HD2123
JD2223
t=1.30
HD2471
JD1499
t=2.05
HD2523
JD2215
t=2.06
HD2523
JD2223
t=1.97
HD2523
JD2283
t=0.79
HD4564
JD2214
t=2.12
HD7901
JD2240
t=1.05
HD9550
JD1827
t=1.14
HD9843
JD1917
t=1.65
HD9843
JD1919
t=1.37
HD9843
JD1923
t=1.44
B Amplitude (mmag)
Frequency (mHz)
0
1
2
3
4

Fig. 10.

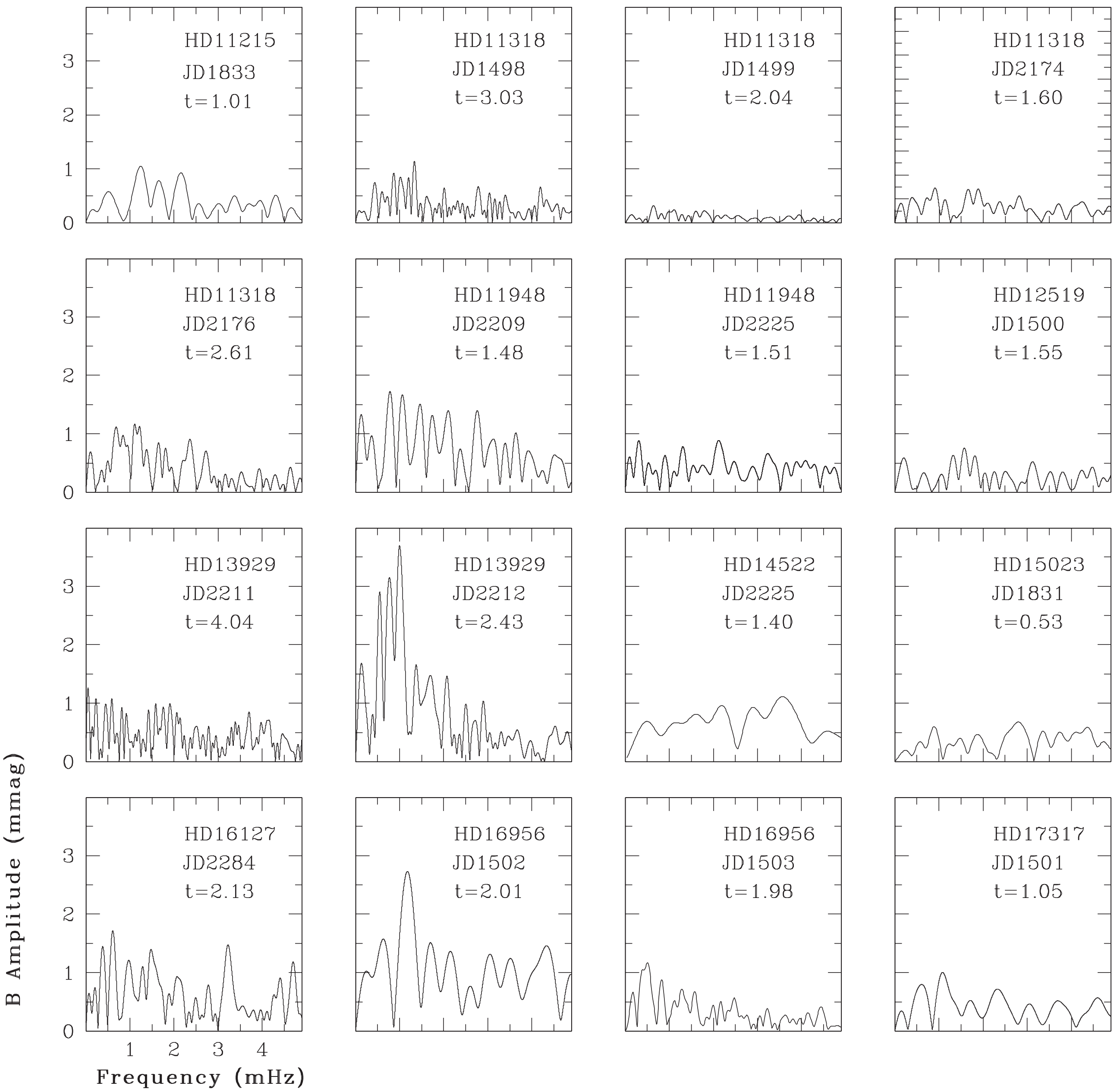
HD11215
JD1833
t=1.01
HD11318
JD1498
t=3.03
HD11318
JD1499
t=2.04
HD11318
JD2174
t=1.60
HD11318
JD2176
t=2.61
HD11948
JD2209
t=1.48
HD11948
JD2225
t=1.51
HD12519
JD1500
t=1.55
HD13929
JD2211
t=4.04
HD13929
JD2212
t=2.43
HD14522
JD2225
t=1.40
HD15023
JD1831
t=0.53
HD16127
JD2284
t=2.13
HD16956
JD1502
t=2.01
HD16956
JD1503
t=1.98
HD17317
JD1501
t=1.05
B Amplitude (mmag)
Frequency (mHz)
0
1
2
3
4

Fig. 10.

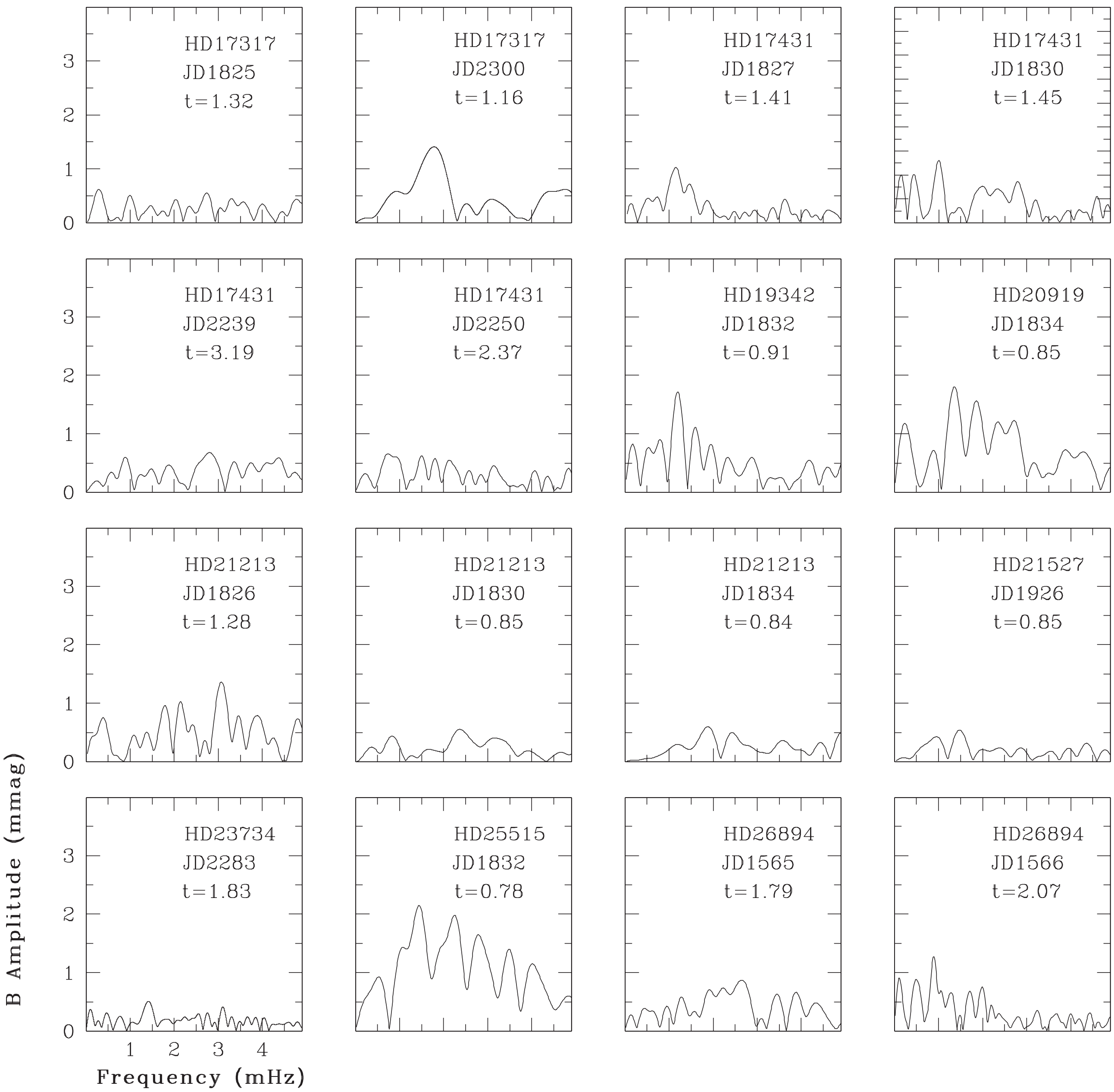
HD17317
JD1825
t=1.32
HD17317
JD2300
t=1.16
HD17431
JD1827
t=1.41
HD17431
JD1830
t=1.45
HD17431
JD2239
t=3.19
HD17431
JD2250
t=2.37
HD19342
JD1832
t=0.91
HD20919
JD1834
t=0.85
HD21213
JD1826
t=1.28
HD21213
JD1830
t=0.85
HD21213
JD1834
t=0.84
HD21527
JD1926
t=0.85
HD23734
JD2283
t=1.83
HD25515
JD1832
t=0.78
HD26894
JD1565
t=1.79
HD26894
JD1566
t=2.07
B Amplitude (mmag)
Frequency (mHz)
0
1
2
3
4

Fig. 10.

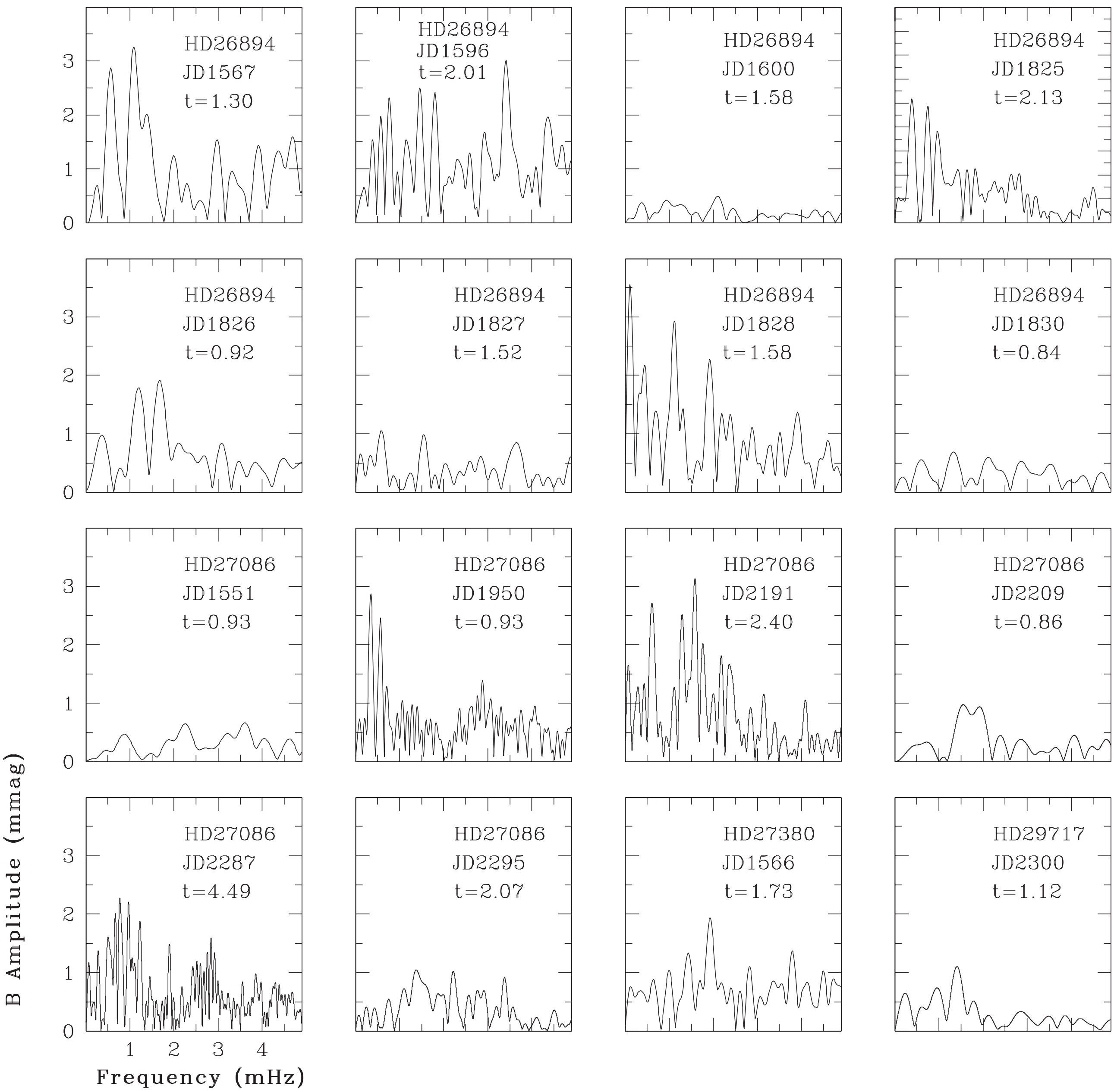
HD26894
JD1567
t=1.30
HD26894
JD1596
t=2.01
HD26894
JD1600
t=1.58
HD26894
JD1825
t=2.13
HD26894
JD1826
t=0.92
HD26894
JD1827
t=1.52
HD26894
JD1828
t=1.58
HD26894
JD1830
t=0.84
HD27086
JD1551
t=0.93
HD27086
JD1950
t=0.93
HD27086
JD2191
t=2.40
HD27086
JD2209
t=0.86
HD27086
JD2287
t=4.49
HD27086
JD2295
t=2.07
HD27380
JD1566
t=1.73
HD29717
JD2300
t=1.12
B Amplitude (mmag)
Frequency (mHz)

Fig. 10.

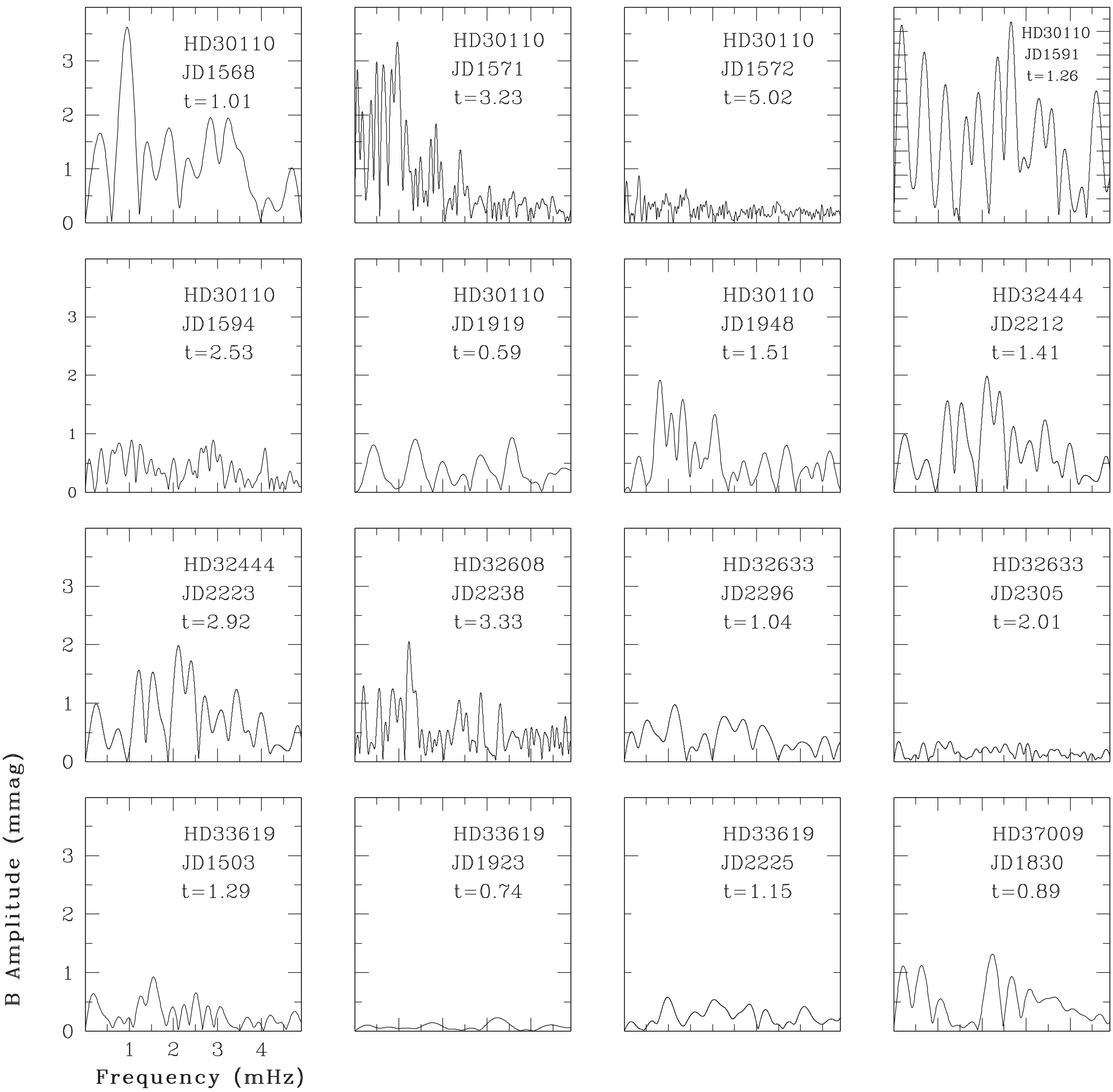
HD30110
JD1568
t=1.01
HD30110
JD1571
t=3.23
HD30110
JD1572
t=5.02
HD30110
JD1591
t=1.26
HD30110
JD1594
t=2.53
HD30110
JD1919
t=0.59
HD30110
JD1948
t=1.51
HD32444
JD2212
t=1.41
HD32444
JD2223
t=2.92
HD32608
JD2238
t=3.33
HD32633
JD2296
t=1.04
HD32633
JD2305
t=2.01
HD33619
JD1503
t=1.29
HD33619
JD1923
t=0.74
HD33619
JD2225
t=1.15
HD37009
JD1830
t=0.89
B Amplitude (mmag)
Frequency (mHz)

Fig. 10.

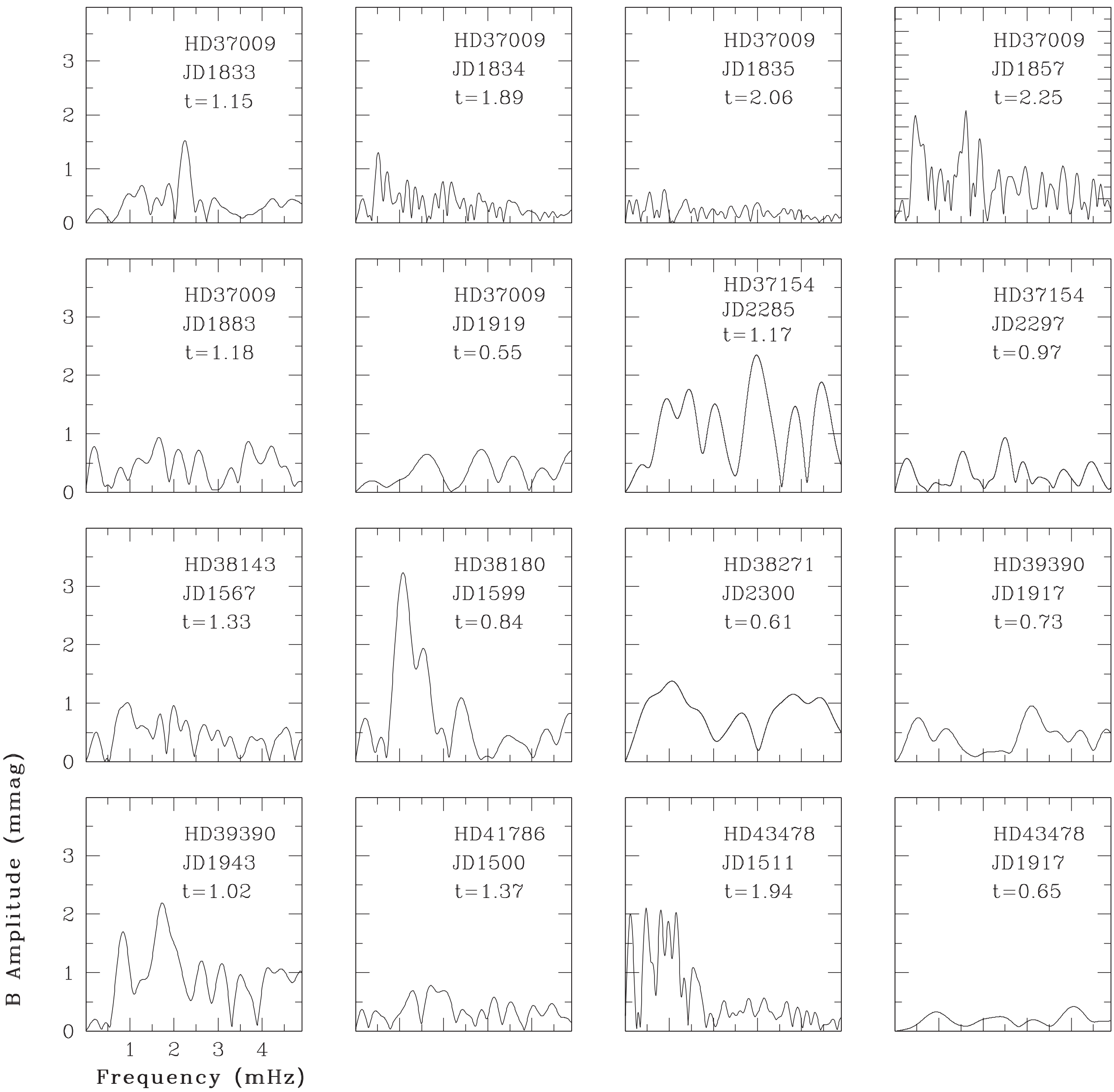
HD37009
JD1833
t=1.15
HD37009
JD1834
t=1.89
HD37009
JD1835
t=2.06
HD37009
JD1857
t=2.25
HD37009
JD1883
t=1.18
HD37009
JD1919
t=0.55
HD37154
JD2285
t=1.17
HD37154
JD2297
t=0.97
HD38143
JD1567
t=1.33
HD38180
JD1599
t=0.84
HD38271
JD2300
t=0.61
HD39390
JD1917
t=0.73
HD39390
JD1943
t=1.02
HD41786
JD1500
t=1.37
HD43478
JD1511
t=1.94
HD43478
JD1917
t=0.65
B Amplitude (mmag)
Frequency (mHz)
0
1
2
3
1
2
3
4

Fig. 10.

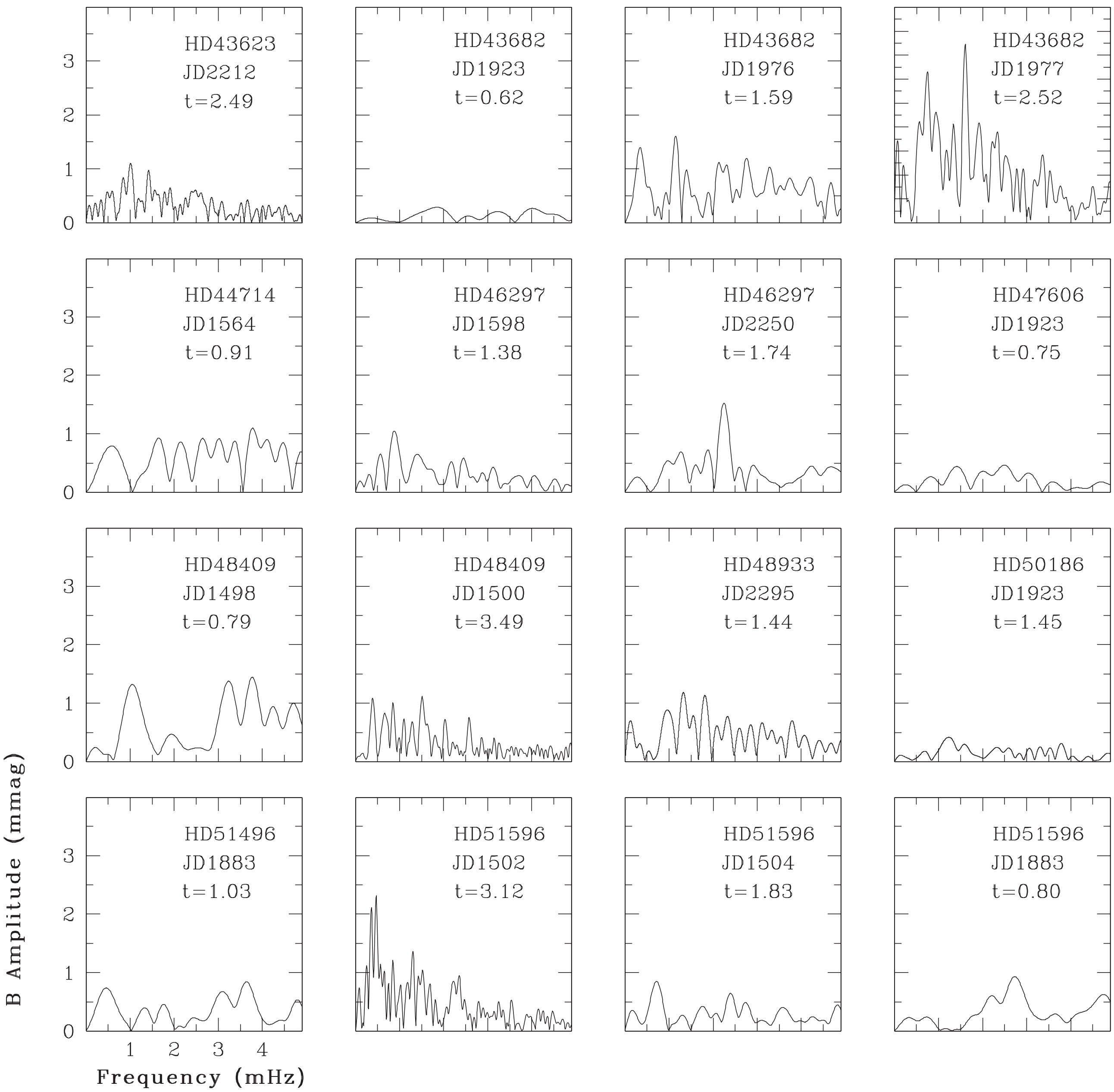

HD43623
JD2212
t=2.49
HD43682
JD1923
t=0.62
HD43682
JD1976
t=1.59
HD43682
JD1977
t=2.52
HD44714
JD1564
t=0.91
HD46297
JD1598
t=1.38
HD46297
JD2250
t=1.74
HD47606
JD1923
t=0.75
HD48409
JD1498
t=0.79
HD48409
JD1500
t=3.49
HD48933
JD2295
t=1.44
HD50186
JD1923
t=1.45
HD51496
JD1883
t=1.03
HD51596
JD1502
t=3.12
HD51596
JD1504
t=1.83
HD51596
JD1883
t=0.80
B Amplitude (mmag)
Frequency (mHz)
0
1
2
3
4

Fig. 10.

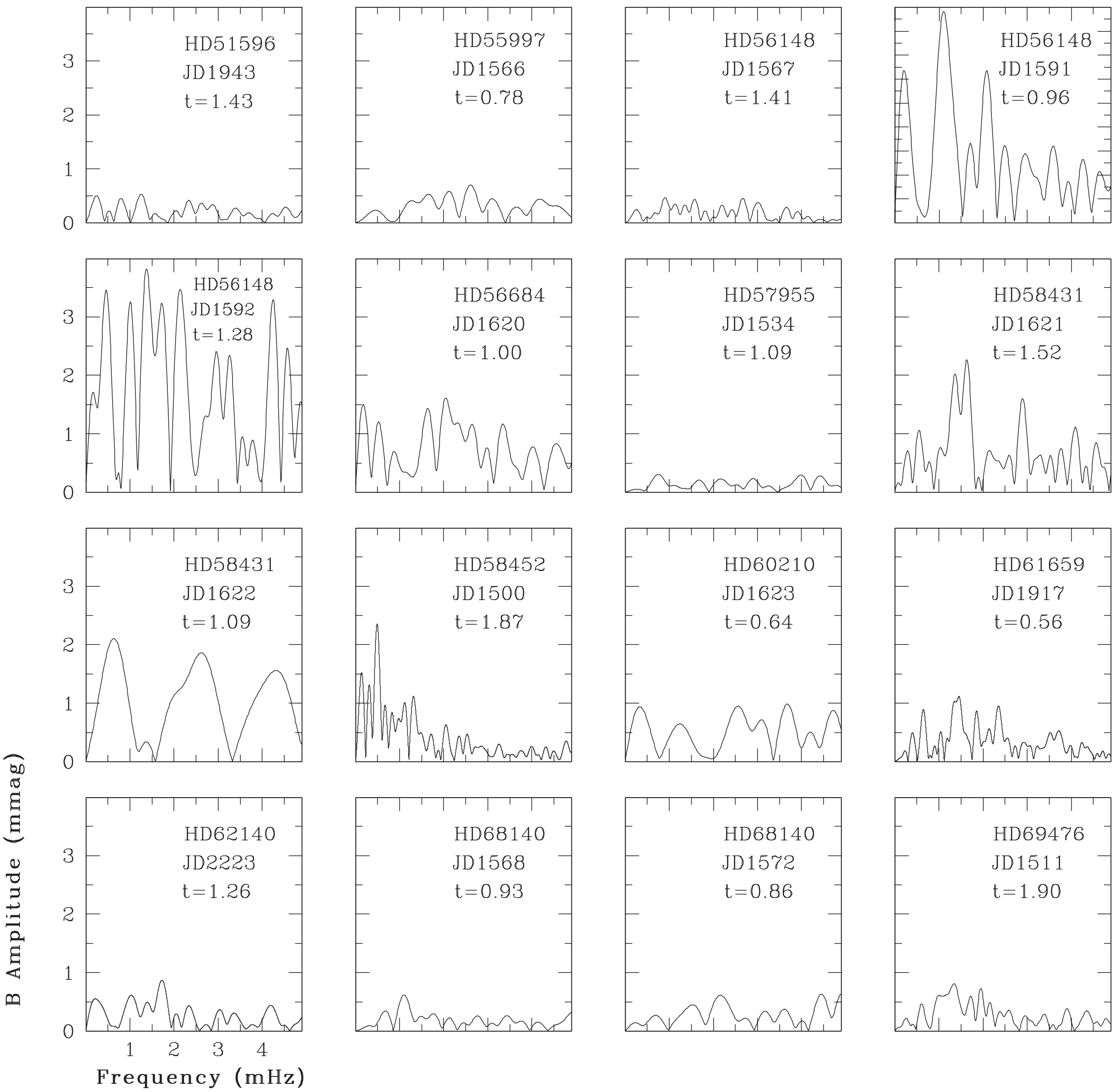
HD51596
JD1943
t=1.43
HD55997
JD1566
t=0.78
HD56148
JD1567
t=1.41
HD56148
JD1591
t=0.96
HD56148
JD1592
t=1.28
HD56684
JD1620
t=1.00
HD57955
JD1534
t=1.09
HD58431
JD1621
t=1.52
HD58431
JD1622
t=1.09
HD58452
JD1500
t=1.87
HD60210
JD1623
t=0.64
HD61659
JD1917
t=0.56
HD62140
JD2223
t=1.26
HD68140
JD1568
t=0.93
HD68140
JD1572
t=0.86
HD69476
JD1511
t=1.90
B Amplitude (mmag)
0
1
2
3
Frequency (mHz)
1
2
3
4

Fig. 10.

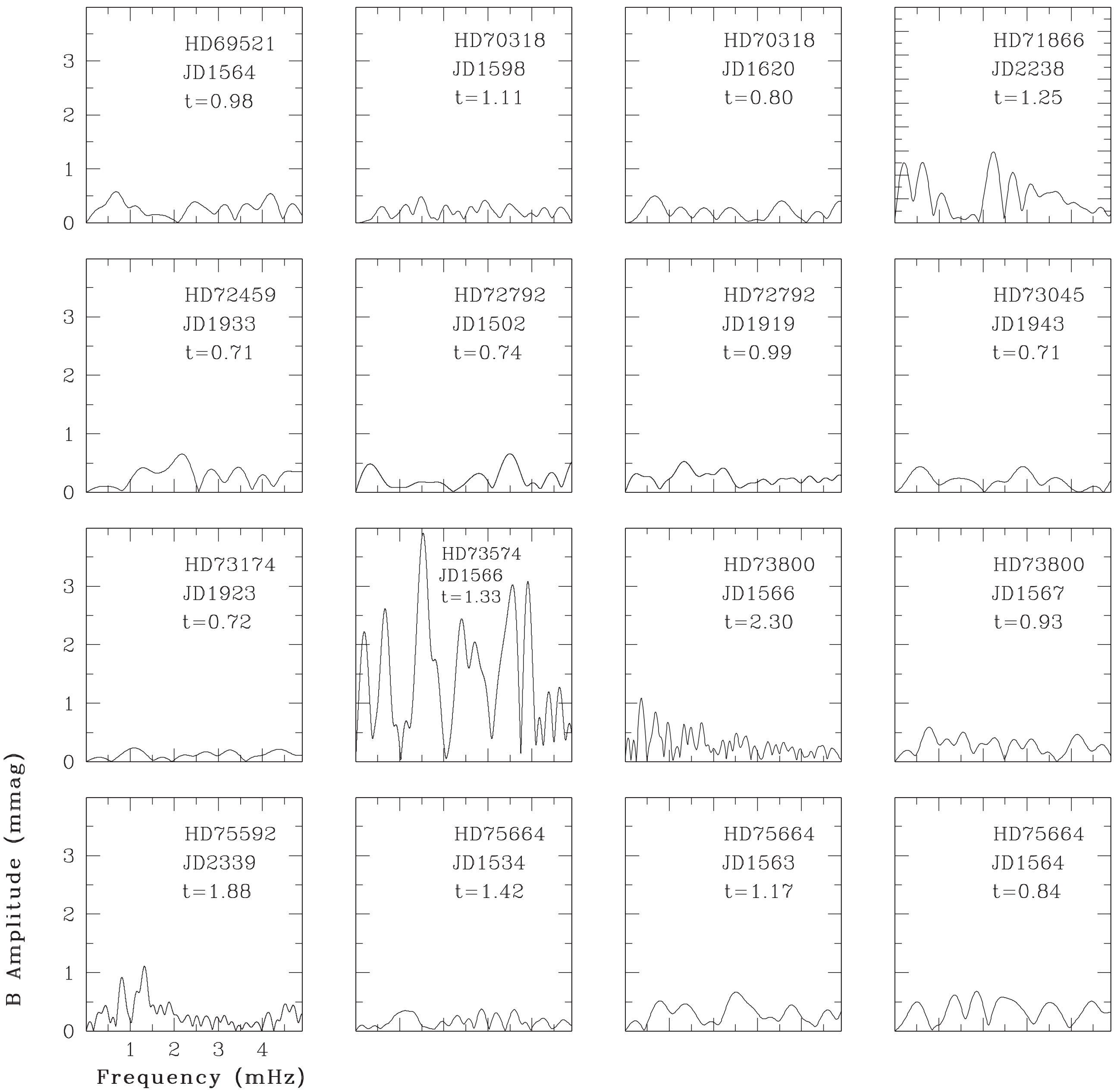
HD69521
JD1564
t=0.98
HD70318
JD1598
t=1.11
HD70318
JD1620
t=0.80
HD71866
JD2238
t=1.25
HD72459
JD1933
t=0.71
HD72792
JD1502
t=0.74
HD72792
JD1919
t=0.99
HD73045
JD1943
t=0.71
HD73174
JD1923
t=0.72
HD73574
JD1566
t=1.33
HD73800
JD1566
t=2.30
HD73800
JD1567
t=0.93
HD75592
JD2339
t=1.88
HD75664
JD1534
t=1.42
HD75664
JD1563
t=1.17
HD75664
JD1564
t=0.84
B Amplitude (mmag)
0
1
2
3
Frequency (mHz)
1
2
3
4

Fig. 10.

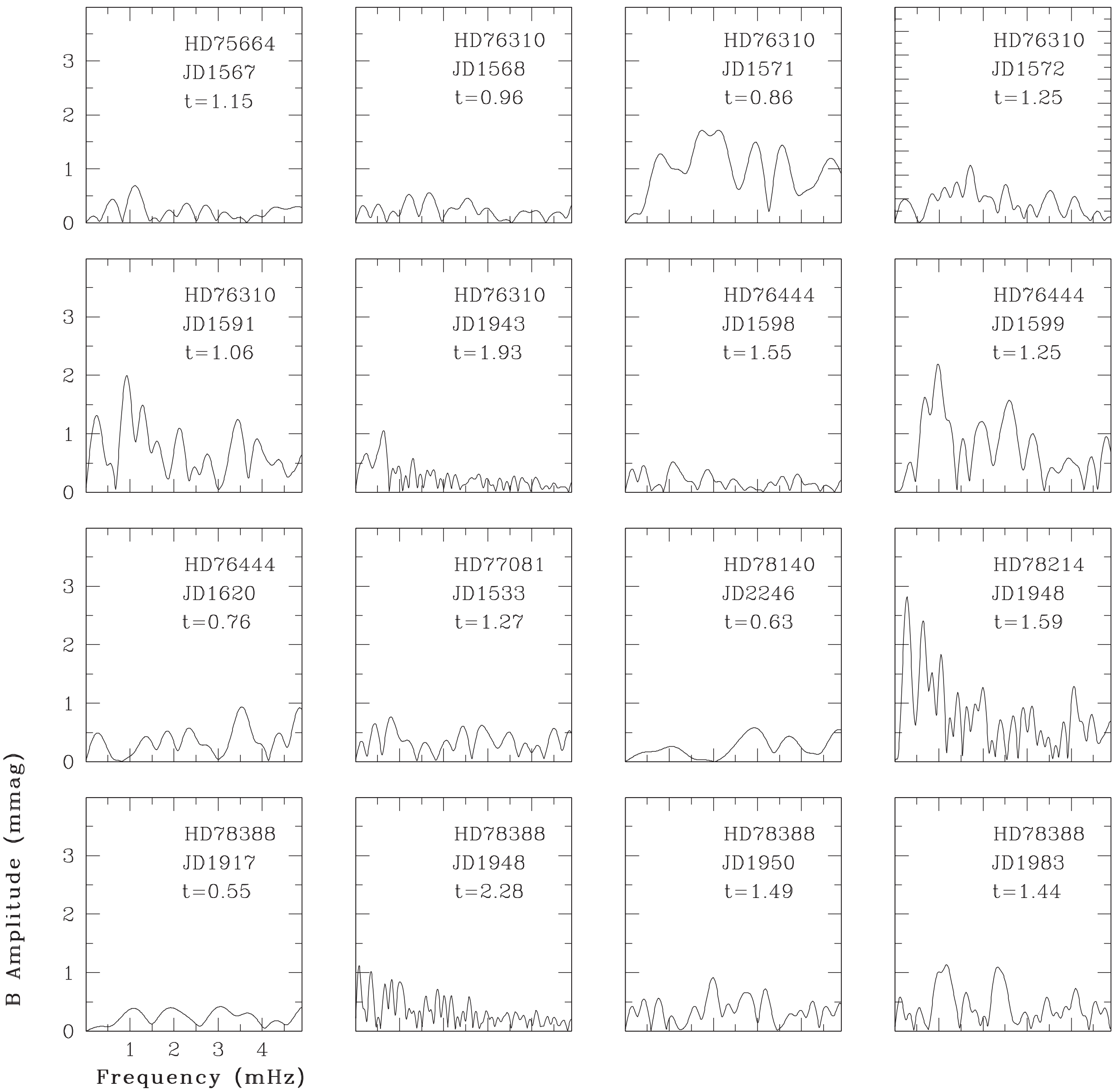
HD75664
JD1567
t=1.15
HD76310
JD1568
t=0.96
HD76310
JD1571
t=0.86
HD76310
JD1572
t=1.25
HD76310
JD1591
t=1.06
HD76310
JD1943
t=1.93
HD76444
JD1598
t=1.55
HD76444
JD1599
t=1.25
HD76444
JD1620
t=0.76
HD77081
JD1533
t=1.27
HD78140
JD2246
t=0.63
HD78214
JD1948
t=1.59
HD78388
JD1917
t=0.55
HD78388
JD1948
t=2.28
HD78388
JD1950
t=1.49
HD78388
JD1983
t=1.44
B Amplitude (mmag)
Frequency (mHz)

Fig. 10.

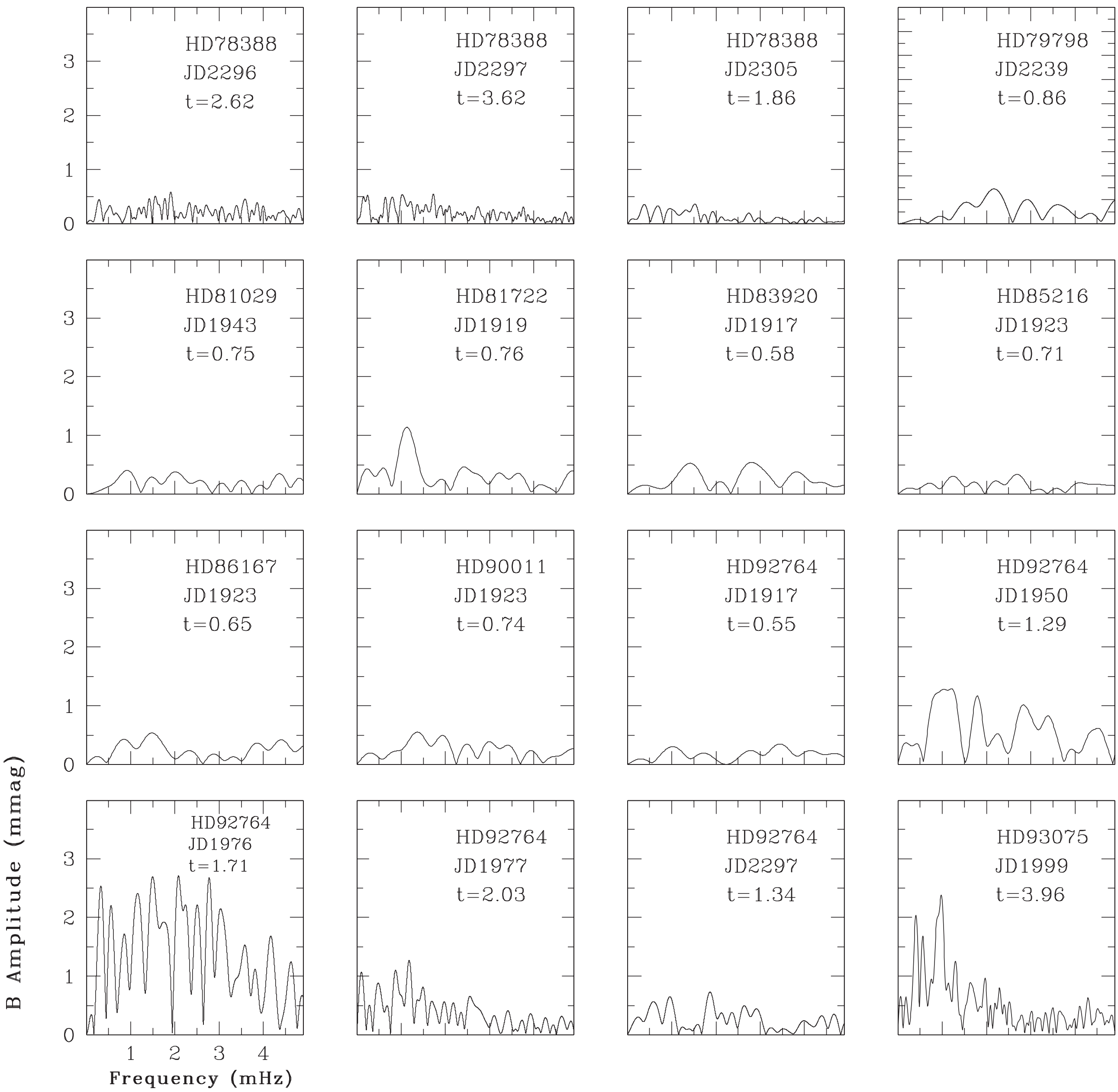
HD78388
JD2296
t=2.62
HD78388
JD2297
t=3.62
HD78388
JD2305
t=1.86
HD79798
JD2239
t=0.86
HD81029
JD1943
t=0.75
HD81722
JD1919
t=0.76
HD83920
JD1917
t=0.58
HD85216
JD1923
t=0.71
HD86167
JD1923
t=0.65
HD90011
JD1923
t=0.74
HD92764
JD1917
t=0.55
HD92764
JD1950
t=1.29
HD92764
JD1976
t=1.71
HD92764
JD1977
t=2.03
HD92764
JD2297
t=1.34
HD93075
JD1999
t=3.96
B Amplitude (mmag)
Frequency (mHz)
0
1
2
3
4

Fig. 10.

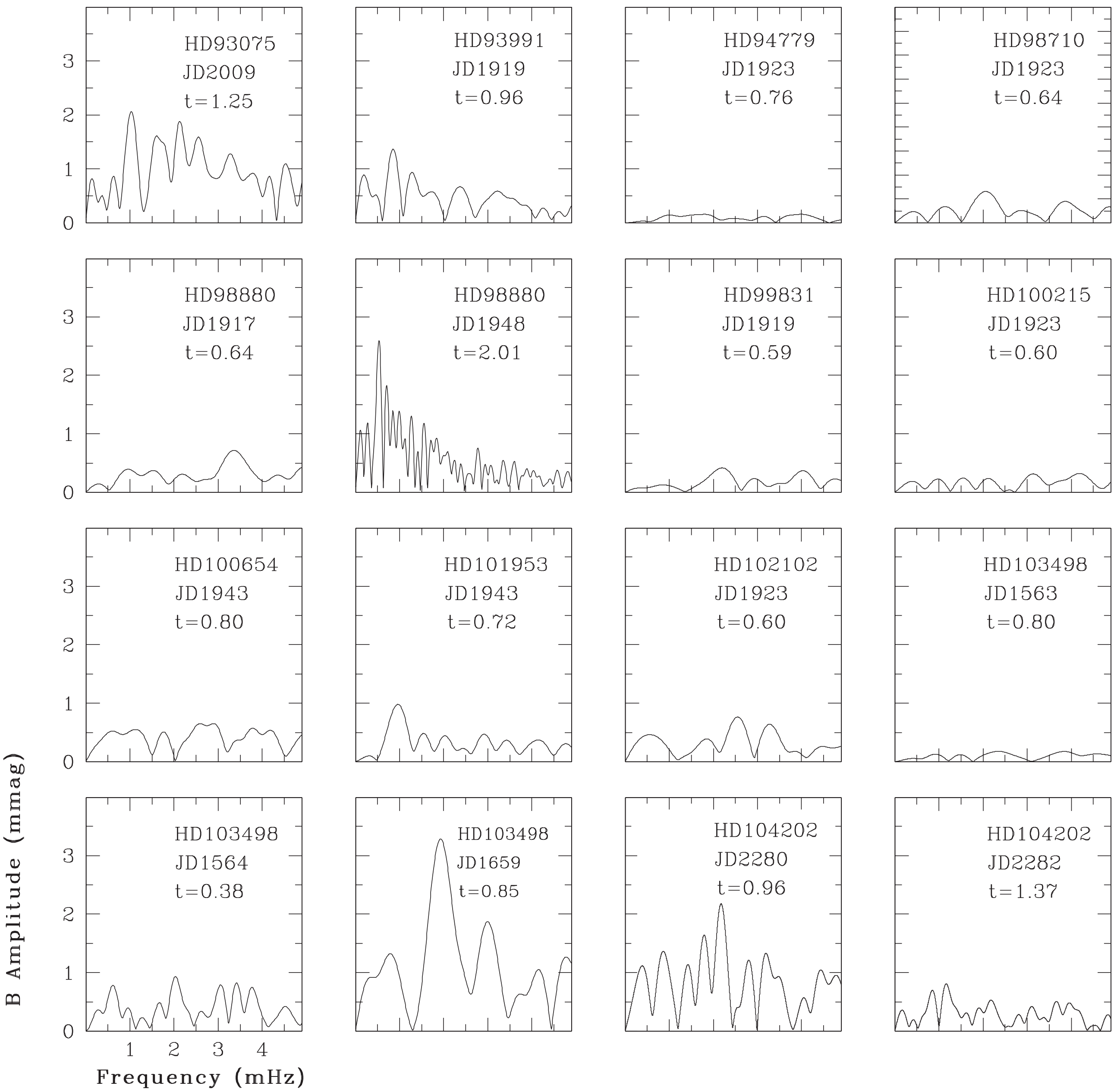
HD93075
JD2009
t=1.25
HD93991
JD1919
t=0.96
HD94779
JD1923
t=0.76
HD98710
JD1923
t=0.64
HD98880
JD1917
t=0.64
HD98880
JD1948
t=2.01
HD99831
JD1919
t=0.59
HD100215
JD1923
t=0.60
HD100654
JD1943
t=0.80
HD101953
JD1943
t=0.72
HD102102
JD1923
t=0.60
HD103498
JD1563
t=0.80
HD103498
JD1564
t=0.38
HD103498
JD1659
t=0.85
HD104202
JD2280
t=0.96
HD104202
JD2282
t=1.37
B Amplitude (mmag)
Frequency (mHz)
0
1
2
3
4

Fig. 10.

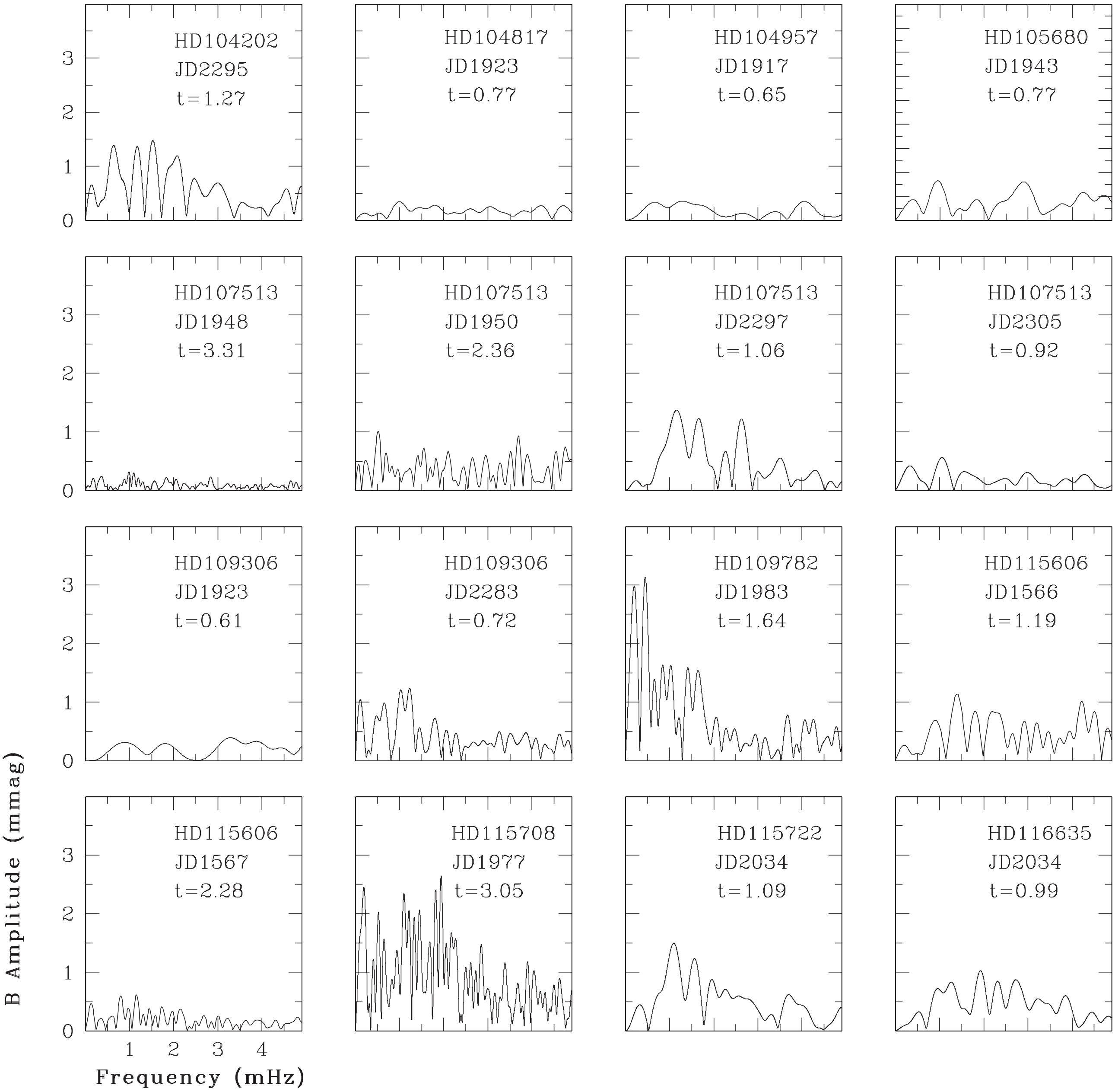
HD104202
JD2295
t=1.27
HD104817
JD1923
t=0.77
HD104957
JD1917
t=0.65
HD105680
JD1943
t=0.77
HD107513
JD1948
t=3.31
HD107513
JD1950
t=2.36
HD107513
JD2297
t=1.06
HD107513
JD2305
t=0.92
HD109306
JD1923
t=0.61
HD109306
JD2283
t=0.72
HD109782
JD1983
t=1.64
HD115606
JD1566
t=1.19
HD115606
JD1567
t=2.28
HD115708
JD1977
t=3.05
HD115722
JD2034
t=1.09
HD116635
JD2034
t=0.99
B Amplitude (mmag)
Frequency (mHz)
0
1
2
3
1
2
3
4

Fig. 10.

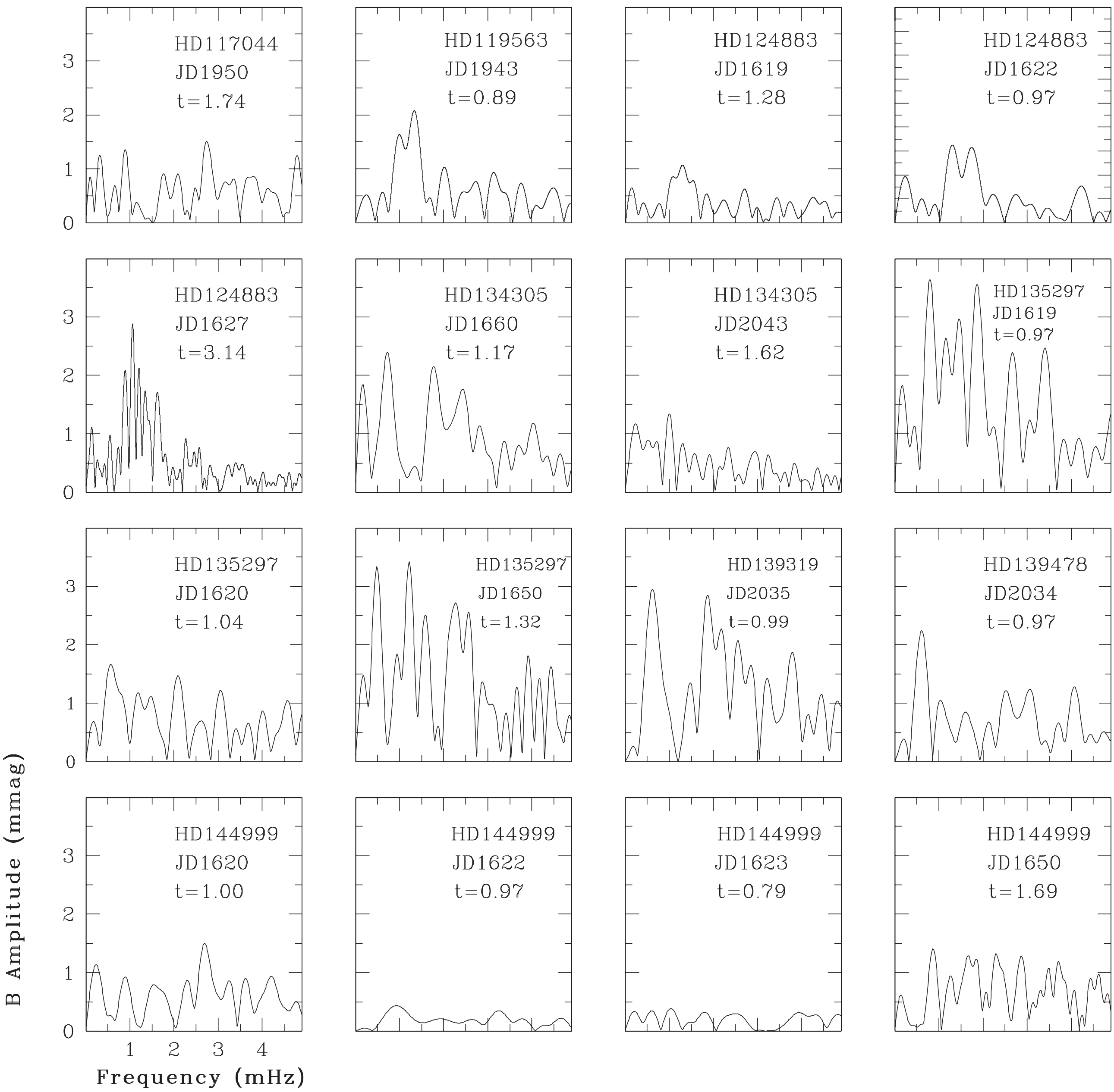
HD117044
JD1950
t=1.74
HD119563
JD1943
t=0.89
HD124883
JD1619
t=1.28
HD124883
JD1622
t=0.97
HD124883
JD1627
t=3.14
HD134305
JD1660
t=1.17
HD134305
JD2043
t=1.62
HD135297
JD1619
t=0.97
HD135297
JD1620
t=1.04
HD135297
JD1650
t=1.32
HD139319
JD2035
t=0.99
HD139478
JD2034
t=0.97
HD144999
JD1620
t=1.00
HD144999
JD1622
t=0.97
HD144999
JD1623
t=0.79
HD144999
JD1650
t=1.69
B Amplitude (mmag)
Frequency (mHz)
0
1
2
3
4

Fig. 10.

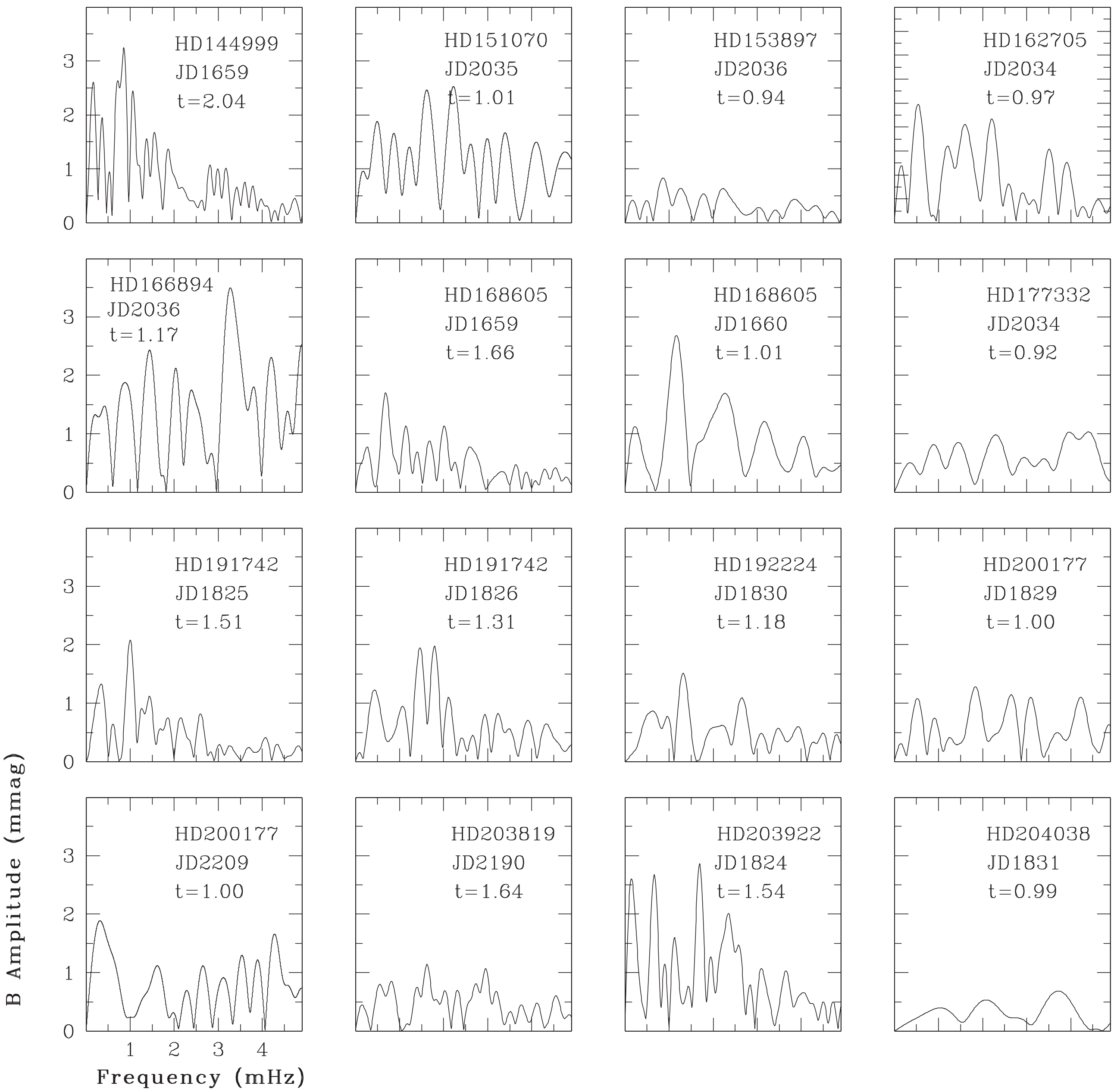
HD144999
JD1659
t=2.04
HD151070
JD2035
t=1.01
HD153897
JD2036
t=0.94
HD162705
JD2034
t=0.97
HD166894
JD2036
t=1.17
HD168605
JD1659
t=1.66
HD168605
JD1660
t=1.01
HD177332
JD2034
t=0.92
HD191742
JD1825
t=1.51
HD191742
JD1826
t=1.31
HD192224
JD1830
t=1.18
HD200177
JD1829
t=1.00
HD200177
JD2209
t=1.00
HD203819
JD2190
t=1.64
HD203922
JD1824
t=1.54
HD204038
JD1831
t=0.99
B Amplitude (mmag)
Frequency (mHz)

Fig. 10.

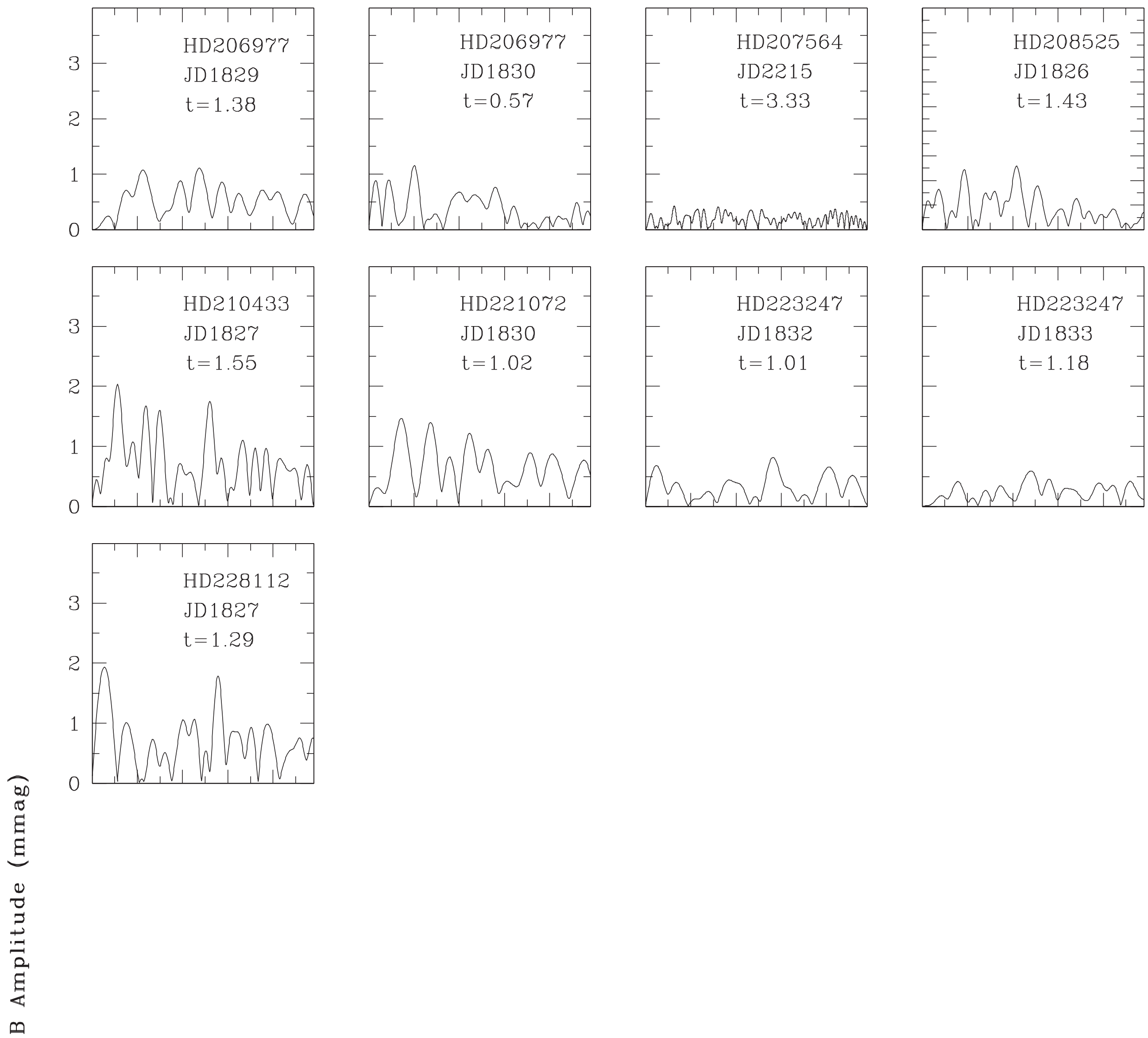
HD206977
JD1829
t=1.38
HD206977
JD1830
t=0.57
HD207564
JD2215
t=3.33
HD208525
JD1826
t=1.43
HD210433
JD1827
t=1.55
HD221072
JD1830
t=1.02
HD223247
JD1832
t=1.01
HD223247
JD1833
t=1.18
HD228112
JD1827
t=1.29
B Amplitude (mmag)
0
1
2
3

Fig. 10.